Development of Cathodic Electrocatalysts for Use in Low Temperature H_2/O_2 Fuel Cells with an Alkaline Electrolyte

Contract No. NASW-1233

Q-3

Third Quarterly Report
Covering January 1
Through March 31, 1966

for
National Aeronautics and Space Administration
Headquarters, Washington, D.C.

NOTICE

This report was prepared as an account of Government sponsored work. Neither the United States, nor the National Aeronautics and Space Administration (NASA), nor any person acting on behalf of NASA:

A.) Makes any warranty or representation, expressed or implied, with respect to the accuracy, completeness, or usefulness of the information contained in this report, or that the use of any information, apparatus, method, or process disclosed in this report may not infringe privately owned rights; or

B.) Assumes any liabilities with respect to the use of, or for damages resulting from the use of any information, apparatus, method or process disclosed in this report.

As used above, "person acting on behalf of NASA" includes any employee or contractor of NASA, or employee of such contractor, to the extent that such employee or contractor of NASA, or employee of such contractor prepared, disseminates, or provides access to, any information pursuant to his employment or contract with NASA or his employment with such contractor.

Requests for copies of this report should be referred to

National Aeronautics and Space Administration
Office of Scientific and Technical Information
Attn: AFSS-A
Washington, D. C. 20546

DEVELOPMENT OF CATHODIC ELECTROCATALYSTS FOR USE IN LOW TEMPERATURE H_2/O_2 FUEL CELLS WITH AN ALKALINE ELECTROLYTE

Contract No. NASW-1233

Q-3

Third Quarterly Report

Covering January 1

Through March 31, 1966

for

National Aeronautics and Space
Administration
Headquarters, Washington, D.C.

"DEVELOPMENT OF CATHODIC ELECTROCATALYSTS FOR USE IN LOW TEMPERATURE H_2/O_2 FUEL CELLS WITH AN ALKALINE ELECTROLYTE"

CONTRACT OBJECTIVES

The research under contract NASW-1233 is directed towards the development of an improved oxygen electrode for use in alkaline H_2/O_2 fuel cells. The work is being carried out for the National Aeronautics and Space Administration with Mr. E. Cohn as technical monitor. Principal Investigators are J. Giner, A. C. Makrides, and R. J. Jasinski.

CONTENTS

I. SUMMARY AND CONCLUSIONS

An additional forty-five materials have been tested this quarter for corrosion resistance and activity as oxygen electrodes in potassium hydroxide at 75°C. When the materials were available as one piece ingots, the technique used was to measure the current-potential curve with compact electrodes completely immersed in KOH solutions saturated either with nitrogen or oxygen.

Of the elements tested, manganese showed activity for the reduction of O_2 above + 800 mv. Apparently, this activity depends on the presence of a surface oxide (MnO_2), since it decreased in the potential region where the oxide is reduced. Alloys of manganese with nickel (2:1 and 1:1) showed less corrosion (surface reduction) and also lower activity for oxygen reduction in the 700-800 mv range. Ti_3Au showed activity at least comparable to that of gold. The activity of coprecipitated alloys of Au-Pt (3:2) and Au-Pd (3:2) was comparable to that of gold.

The "floating electrode" assembly was used to study materials available as dispersed powders. Replicate runs on commercially available Pt-Teflon electrodes established that the reproducibility of this measuring technique itself is within $\pm$ 10 mv. These variations have been attributed to minor instabilities in the "dynamic hydrogen reference electrode".

The performances of electrodes prepared directly from platinum blacks were somewhat inferior to commercial electrodes. A porous silver electrode was also constructed. At high potentials (925-975 mv) this electrode was superior in performance to the best of the commercial platinum electrodes.

A sample of Fe_2C - Fe_3C was Teflon-bonded to a nickel screen and studied in the "floating electrode" assembly. This material showed activity for O_2-reduction, e.g. 80 ma/cm^2 at + 775 mv. However, because of the high ohmic resistance of the electrode, it is questionable whether this measurement represents a true evaluation of the material.

Borides and silicides of the group IVB, VB, and VIB were also tested. Severe corrosion was observed in all cases.

TiN showed significant activity for the reduction of O_2, being more active and more corrosion resistant than titanium metal. TiC also showed activity for O_2 reduction; however, this activity was less and the corrosion was more than observed for TiN. The group VB nitrides also corroded over the voltage range studied; Cr_2N corroded above + 900 mv; ZrN and HfN were inert.

II. INTRODUCTION

In order to improve the over-all efficiency of hydrogen-oxygen fuel cells, improvements in the performance of the oxygen electrode are needed, since the high polarization of this electrode is the main source of inefficiency.

The approach followed in this work in order to obtain better O_2-electrodes is to investigate the catalytic properties for O_2-reduction and the corrosion resistance to the alkali electrolyte of a large number of compounds selected according to structural or atomic considerations. The criteria for catalyst selection according to structural factors have been discussed in detail in the first quarterly report. Selections are made from intermetallic compounds of the T - T - type (i.e. of two transition metals) with the objective of testing the possibility that the continuum properties (electronic properties) of the crystal may have decisive influence on its catalytic activity even if the elements (or one of them) are not catalytically active. Similarly, compounds of the T - B - type (i.e. one transition metal and an element on the right side of the periodic table) with special emphasis on interstitial/substitutional compounds such as borides, carbides, nitrides, oxides, and silicides are being tested.

Since, under the conditions of electrolyte and potential, the surface of the catalyst will usually be a mixed oxide, oxides are of especial interest, and attention will be given to them in a later phase of this work.

To select a catalyst according to atomistic considerations, elements with favorable catalytic activity and/or corrosion resistance, as established empirically in published research or during the course of the present work, will be combined in order to give a composite material of better over-all performance.

III. EXPERIMENTAL

A. Methods of Preparation

1. Metals, Alloys and Intermetallic Compounds

The following materials were prepared as solid ingots by arc melting the proper proportions of the elements (see second quarterly report): 1:1 Ni-Mn, 1:2 Ni-Mn, $TaNi_2$, HfCo, Ti_3Au. These samples were evaluated via the rotating disk technique, together with the metals: Pb, Cu, W, Mn and a commercial sample of Alnico.

2. Intermetallic/Substitutional Compounds of Refractory Elements

The compounds listed in Table 1 were obtained as hot-pressed cones of 95% density and were tested for corrosion and oxygen reduction activity using the rotating disk assembly previously described.

TABLE 1

Intermetallic and Substitutional Compounds of Refractory Elements

Borides:

TiB_2	NbB_2	CrB_2	WB
ZrB_2	TaB	Cr_5B_3	W_2B
VB_2	TaB_2	MoB	W_2B_5
NbB	CrB	MoB_2	

TABLE 1 (Cont.)

Intermetallic and Substitutional Compounds of Refractory Elements

Silicides:

$TiSi_2$	$NbSi_2$	Cr_3Si	WSi_2	$Si\text{-}B_6Si$
$ZrSi_2$	Ta_5Si_3	$CrSi_2$	$CoSi_2$	
VSi_2	$TaSi_2$	$MoSi_2$	$MnSi_2$	

Nitrides:

TiN	Cr_2N	VN
ZrN	NbN	
HfN	TaN	

Carbides:

TiC	80 WC - 20 Co
Cr_3C_2	

3. Preparation of Dispersed Carbides and Nitrides

Fe_2C - Prep. #1 — Pure Fe sponge was carburized with CO at 150° - 275°C for 27 hours. X-ray analysis - iron and iron oxide.

Fe_2C - Prep. #2 — Pure Fe sponge was reduced with H_2 at 325°C for 15 hours and carburized with CO at 170° - 300°C for 30 hours. X-ray analysis - iron, iron oxide, traces of Fe_2C, Fe_3C.

Fe_2C - Prep. #3 — Pure Fe sponge was reduced with hydrogen for 20 hours at 325°C and carburized with CO at 200 - 275°C for 96 hours. X-ray analysis - iron, iron oxide, traces of Fe_2C, Fe_3C.

Fe_2C - Prep. #4 — Pure Fe sponge was reduced with hydrogen at 350°C for 28 hours and carburized with CO at 200 - 250°C for 32 hours. X-ray analysis - Fe_2C - Fe_3C, B.E.T. surface area - 162 m^2/gm.

Fe_2C - Prep. #5 — Pure Fe sponge was reduced with H_2 at 500°C for 28 hours and carburized with CO 200 - 350°C for 56 hours. X-ray analysis, iron, iron oxide, trace Fe_2C, Fe_3C.

Fe_3C - Prep. #6 — Fe_2C - Fe_3C from prep. #4 was heated under N_2 to 475°C for 4 hours. X-ray analysis - Fe_3C, Fe. B.E.T. surface area - 143 m^2/gm

Fe_3C - Prep. #7 — Iron salt of mellitic acid was decomposed in vacuo at 450°C for 4 hours. X-ray analysis - Fe_3C, traces Fe_3O_4. B.E.T. surface area - 8.4 m^2/gm.

Ni_3C - Prep. #8 — Pure nickel powder was reduced with hydrogen at 200°C for 20 hours and carburized with CO at 350°C. This operation was interrupted by furnace failure after about 10 hours. X-ray analysis - Ni.

Fe_2N - Prep. #9	Pure Fe sponge was reduced with hydrogen at 300°C for 24 hours and nitrided with NH_3 at 300°C for 7 hours. X-ray analysis, Fe, oxides, γ' -Fe_4N, Fe_3N.
Co_2C - Prep. #10	Co_2O_3 obtained from thermal decomposition of $Co(NO_3)_2$ was reduced with H_2 at 230°C for 68 hours and carburized with CO at 230°C for 220 hours. X-ray analysis Co_2C traces of Co and Co_3O_4.
Fe_3N - Prep. #11	Pure Fe sponge was reduced with H_2 at 450°C for 24 hours and nitrided with NH_3 at 950°C for 48 hours. X-ray analysis - Fe_3N.
Ni_3C - Prep. #12	Pure Ni powder was reduced with H_2 at 300°C for 18 hours. The carburization with CO at 300°C was interrupted by furnace failure after 48 hours. X-ray analysis - Ni.
Ni_3C - Prep. #13	Nickel acetate was thermally decomposed at 350°C for 4 hours. X-ray analysis incomplete.
Ni_3N_2 - Prep. #14	Nickel powder was reduced with H_2 at 400°C for 21 hours and nitrided with NH_3 at 400°C for 48 hours. X-ray analysis incomplete.

B. Methods of Testing

The principles and equipment involved in both electrode test techniques were described in the previous reports on this contract. The rotating disk assembly is used to study materials in the form of one-piece ingots; the "floating electrode" technique is used to evaluate dispersed materials.

The performance and reproducibility of the floating electrode assembly was determined by replicate runs on a commercially available platinum black (9 mg/cm^2) Teflon electrode material. Four samples were cut from the same sheet of material; samples 2 and 3 were run in duplicate. The current-voltage curves, Fig. 1-6, Appendix 1, indicate only minor variations ($\pm$ 10 mv). Two other commercial electrodes were also tested. The performances are compared in Table 2.

TABLE 2

Voltage-Current Performance of Commercial Electrode

Test: Floating Electrode

Catalyst: Pt (9 mg/cm^2); sources A, B, C.

Conditions: 75°C, 35% KOH, O_2

Voltage (IR free) (mv vs. DHE)	Current (ma/cm^2) A	B	C
975	10	10	15
950	52	30	40
925	110	60	120
900	360	115	> 280

IV. RESULTS

The performances of materials studied by both the floating electrode and rotating electrode tests are placed into three broad categories:

1. Materials active for the reduction of O_2 (Table 3)
2. Materials indicating low activity (Table 4)
3. Materials exhibiting excessive corrosion or dissolution (Table 5).

The placement of materials within category 1 or category 2 is determined by whether significant cathodic current is observed above or below + 600 mv, i.e. $\eta \sim 600$ mv. The definition of the sublevels within each category is subjective. The materials included in Level 1, category 1 are those with activity above + 800 mv and with current-voltage profiles similar to that observed for platinum and silver. Level 2 contains those materials with activity above + 800 mv but whose performance is decreased by subsequent reduction of the surface. Mn and Co-Ni are examples of this class.

Level 3 contains those materials which do not yet exhibit substantial activity above + 800 mv and which do not exhibit a limiting current above + 500 mv.

TABLE 3

Materials Active for the Reduction of O_2 (η < 600 mv)

Level of Activity	Material
1	Ti_3Au (Fig. 16); 3:2 Au-Pt (Fig. 62); 3:2 Au-Pd (Fig. 63)
2	Mn (Fig. 10)
3	1:1 Mn-Ni (Fig. 11); 2:1 Mn-Ni (Fig. 12) Fe_2C (Figs. 64-67); TiN (Fig. 53)

TABLE 4

Materials Indicating Low Activity ($\eta \geq 600$ mv)

Alnico	(Fig. 13)
$TaNi_2$	(Fig. 15)
ZrN*	(Fig. 47)
HfN*	(Fig. 48)
Ni_3B	(Fig. 17)
Hf_2Co*	(Fig. 14)

*Inert

TABLE 5

Materials Exhibiting Excessive Corrosion or Dissolution

Borides	Silicides	Miscellaneous
TiB_2	$TiSi_2$	Cr_2N
ZrB_2	$ZrSi_2$	Cr_3C_2*
VB_2	VSi_2	TiC*
NbB	$NbSi_2$	WC-Co
TaB	Ta_5Si_3	W
TaB_2	$TaSi_2$	Pb
CrB	Cr_3Si	Fe_3C*
CrB_2	$CrSi_2$	Co_2C
Cr_5B_3	$MoSi_2$	
MoB	WSi_2	
MoB_2	$CoSi_2$	
WB	$MnSi_2$	
W_2B	$Si-B_6Si$	
W_2B_5		

* Activity plus corrosion - dissolution

V. DISCUSSION

A. Metals, Alloys, Intermetallics

The specific materials listed in Table 6 were studied.

TABLE 6

Materials Tested

Metals	Alloys	Intermetallics
W		$TaNi_2$
Pb	Ni-Mn (1:1)	Ti_3Au
Cu	Ni-Mn (1:2)	Hf_2Co
Mn	Alnico	Ni_3B

Tungsten corrodes above + 300 mv (Fig. 7) with the eventual formation of soluble $WO_4^=$

$$WO_4^= + 4\,H_2O + 6\,e^- = W + 8\,OH^- \qquad (E^\circ = -1.05\text{ v vs. NHE})$$

Similar behavior is observed for lead above + 300 mv (Fig. 8). The probable reactions involved are:

$$HPbO_2^- + H_2O + 2\,e^- = Pb + 3\,OH^- \qquad (E^\circ = -.54\text{ v vs. NHE or } +.25\text{ v vs. DHE})$$

The solubility of PbO as $HPbO_2^-$ is approximately 10^{-1} moles/lit at pH 14 (25°C).

A current-voltage scan of copper in 35% KOH (Fig. 9) indicates corrosion and cathodic reduction, apparently associated with the reactions:

$$2\,CuO + H_2O + 2\,e^- = Cu_2O + 2\,OH^- \qquad (E^\circ = -0.08\text{ v vs. NHE or } +0.74\text{ v vs. DHE})$$

$$Cu_2O + H_2O + 2\,e^- = 2\,Cu + 2\,OH^- \qquad (E^\circ = -.358\text{ v vs. NHE or } +0.46\text{ v vs. DHE})$$

The solubility of CuO at pH 14 (25°C) is 10^{-4} moles/liter as $HCuO_2^-$.

Manganese will also "corrode" in the voltage range of interest (Fig. 10). As this potential is reduced from + 1200 mv, anodic current is observed until approximately + 650 mv. In this region MnO_2 is reduced; it is this reaction which accounts for the activity of MnO_2 in alkaline batteries. At approximately + 550 mv an anodic oxidation reaction(s) takes place. The identification of the specie involved has not been made.

Apparently MnO_2 will catalyze the reduction of O_2 since activity is observed between + 900 and + 750 mv. Below this potential region MnO_2 is reduced and the activity falls off.

Two alloys (2:1 and 1:1) were formed with manganese and nickel. The "corrosion" reactions were suppressed; some oxygen activity was observed although it was also suppressed. (Figs. 11, 12) The electrodes appeared to be more active after being taken to 0.0 mv (vs. DHE). The 2:1 alloy generated anodic current in the potential region 0 - 400 mv which was somewhat greater in the absence of oxygen. It has not yet been established whether this reaction is due to the oxidation of cathodically formed H_2 or the catalyst itself.

A sample of Alnico was also tested; this material showed low corrosion and low O_2 electrode activity. (Fig. 13). Hf_2Co was essentially inert over the voltage range studied (Fig. 14).

$TaNi_2$ had little activity for the reduction of O_2. The activity observed was enhanced by taking the catalyst to 0 mv. Apparently some surface oxide was reduced in the process since the corrosion current also increased (Fig. 15).

The intermetallic Ti_3Au was active for the reduction of O_2 (Fig. 16); cathodic current was observed below + 900 mv. The limiting current density is approximately the same as observed for gold itself. In the case of gold, silver and platinum, cathodic current is first observed at + 950 mv.

The performance of Ni_3B was rechecked; there is negligible activity above + 300 mv (Fig. 17).

B. Refractory Metal Compounds

Borides: Borides of groups IVB, VB, VIB, were tested by the rotating disk technique. The specific compounds are listed in Table 1; the performance curves are Figs. 18 through 32, Appendix 1.

All samples tested indicated severe corrosion within the voltage range of interest which prohibits consideration as possible catalysts for the reduction of oxygen.

Silicides: Some silicides of the group IVB, VB, VIB, and VIIB metals were also tested by the rotating disk method. The specific compounds tested are listed in Table 1; the performance curves are Figs. 33 through 46, Appendix 1.

As with the borides, severe corrosion was observed in all cases. Except for Cr_3Si and Ta_5Si_3, the major component was always silicon. There were only minor differences in corrosion behavior between Cr_3Si and $CrSi_2$; the latter compound showed a somewhat higher cathodic current at low voltages. A greater difference was observed between Ta_5Si_3 and $TaSi_2$. Although both compounds corroded, the former compound was somewhat more stable at low potentials.

Nitrides: The nitrides of Ti, Zr, Hf, Cr, Nb, Ta, V, were evaluated. (Figs. 47-53, Appendix 1). The group VB nitrides corroded over the entire voltage range studied; Cr_2N corroded above + 900 mv. ZrN and HfN were essentially stable over the voltage range studied and showed no activity as oxygen electrode catalysts.

Titanium nitride (Fig. 53) did show significant activity for the reduction of O_2, being more active and more corrosion resistant than titanium metal (see Fig. 54). It can be argued from the double layer capacity data (540 $\mu f/cm^2$ for TiN vs. 100 $\mu f/cm^2$ for Ti) that the activity is due to the increased real surface. However this argument does not explain the lower corrosion rate. This experiment was repeated with a graphite counter electrode to avoid possible contamination from soluble platinum; the results were identical.

Carbides: The carbides of the group VIII elements are discussed elsewhere in this report. TiC , Cr_3C_2 and a 4:1 mixture of WC and Co were also run (Figs. 55-57, Appendix 1).

TiC showed slight activity for O_2 reduction below + 850 mv, and significant corrosion above + 850 mv.

Cr_3C_2 showed activity for O_2 reduction and corrosion over the voltage range studied. Severe corrosion was noted for the WC - Co sample.

C. Dispersed Metals, Alloys

1. Platinum

The reproducibility of the measuring system was discussed in section III-B of this report, in terms of commercial electrodes. A number of Pt-Teflon bonded electrodes were prepared from commercially available platinum black. The performance curves, (Figs. 58-61) showing some scatter, are also included in Appendix 1. The best data is given in Table 7.

TABLE 7

Voltage-Current Performance of Experimental Electrode

Test: Floating Electrode

Catalyst: Pt (29 mg/ cm^2)

Conditions: 75°C , 35% KOH , O_2 , 25% TFE

Voltage (IR free) (mv vs. DHE)	Current (ma/ cm^2)
975	20
950	45
925	90
900	160

Silver: Porous silver electrodes were prepared by mixing Ag_2O powder and Teflon, spreading the mixture on Ni screen, and sintering. The Teflon content was varied between 20% (Electrode A) and 15% (Electrode B); sintering temperatures of 250° (Electrodes A, B) and 350°C (Electrode C) were used. The Teflon content of electrode C was 15%. The performance data is summarized in Table 8.

TABLE 8

Voltage-Current Performance of Experimental Electrodes

Test: Floating Electrode

Catalyst: Silver (19 mg/cm^2)

Conditions: 75°C , 35% KOH , O_2

Voltage (IR free) (mv vs. DHE)	Current (ma/cm^2) A	B	C
975	45	30	10
950	65	45	20
925	105	60	25
900	150	80	35
850	250	125	60

Too low a Teflon content and a high sintering temperature are detrimental to electrode performance. It is expected that an optimum Teflon content exists for a given cell configuration and that poorer performance will be obtained with more or less Teflon. Note that, at high potentials the silver electrode is more than comparable to the best of the commercial platinum electrodes when tested in the "floating" electrode assembly.

Gold Alloys. "Alloys" of platinum-gold (60%) and palladium-gold (60%) were prepared by coprecipitation with $NaBH_4$. The performances of these materials as oxygen electrodes are shown in Figs. 62-63

and are summarized in Table 9. The BET surface area of the Pt-Au powder was 26.9 m^2/gm and that of the Pd-Au powder was 25.3 m^2/gm.

TABLE 9

Voltage-Current Performance of Experimental Electrodes

Test: Floating Electrode

Catalyst: Pt-Au (60%)-Electrode A (29 mg/cm^2)
Pd-Au (60%)-Electrode B (20 mg/cm^2)

Conditions: 75°C , 35% KOH , O_2

Voltage (IR free) (mv vs. DHE)	Current (ma/cm^2) A	B
975	20	15
950	45	30
925	90	75
900	160	140

D. Dispersed Carbides

A number of iron carbides were prepared according to the techniques described in section III-A. All electrodes were prepared directly from the powders, i.e. without a conductive binder. As a result the electrodes all involved high ohmic losses. It is possible to correct the measurements for the IR drop, but it is not possible to alter the effect of IR drop on the discharge kinetics of the porous electrode. In effect then a high IR drop will limit the utilization of the catalyst and provide a higher activation polarization for a given current density. Thus the data resulting from this configuration represents a lower limit to the activity possible from the material studied.

Fe_2C - Fe_3C Prep. #4. This material shows some activity for O_2 reduction (80 ma/cm^2 at 775 mv vs. DHE), but also exhibits a high ohmic resistance (Figs. 64-67).

Fe_3C Prep. #6. Some activity was also observed (80 ma/ cm^2 at 700 mv vs. DHE); this electrode also involved a high IR loss (Figs. 68-69).

Fe_3C Prep. #7. This material shows approximately no O_2 activity (~ 2 ma/ cm^2 at 676 mv) and appears to dissolve in KOH. The electrode also involved a high ohmic resistance.

Note that the voltage-current curves obtained for iron carbide in these experiments compare quite well, in form, to the data obtained previously with the rotating disk assembly (Fig. 52, second quarterly report).

Co_2C Prep. #10. This material showed little activity for O_2 reduction (4 ma/ cm^2 at 670 mv). Furthermore the catalyst dissolved in KOH.

VI. FUTURE WORK

1. Development of an electrode composition suitable for materials of low electrical conductivity.

2. Continued preparation and testing of carbides, nitrides, and carbonitrides of Fe , Co , Ni , both as dispersed materials and as compact materials (surface layers on pure metals).

3. Testing "floating electrodes" obtained from highly dispersed catalysts (carbides, carbonitrides, etc.; Pd-Au "blacks", etc.)

4. Testing of compact samples of Pt-Au , Pd-Au , Ag-Au and other noble metals.

5. Testing of oxides and spinels, e.g. NiO doped with Li , Ni-Co spinel, Fe_3O_4 .

6. Testing of manganese alloys and interstitials.

VII. APPENDIX 1 - SCANNING CURVES

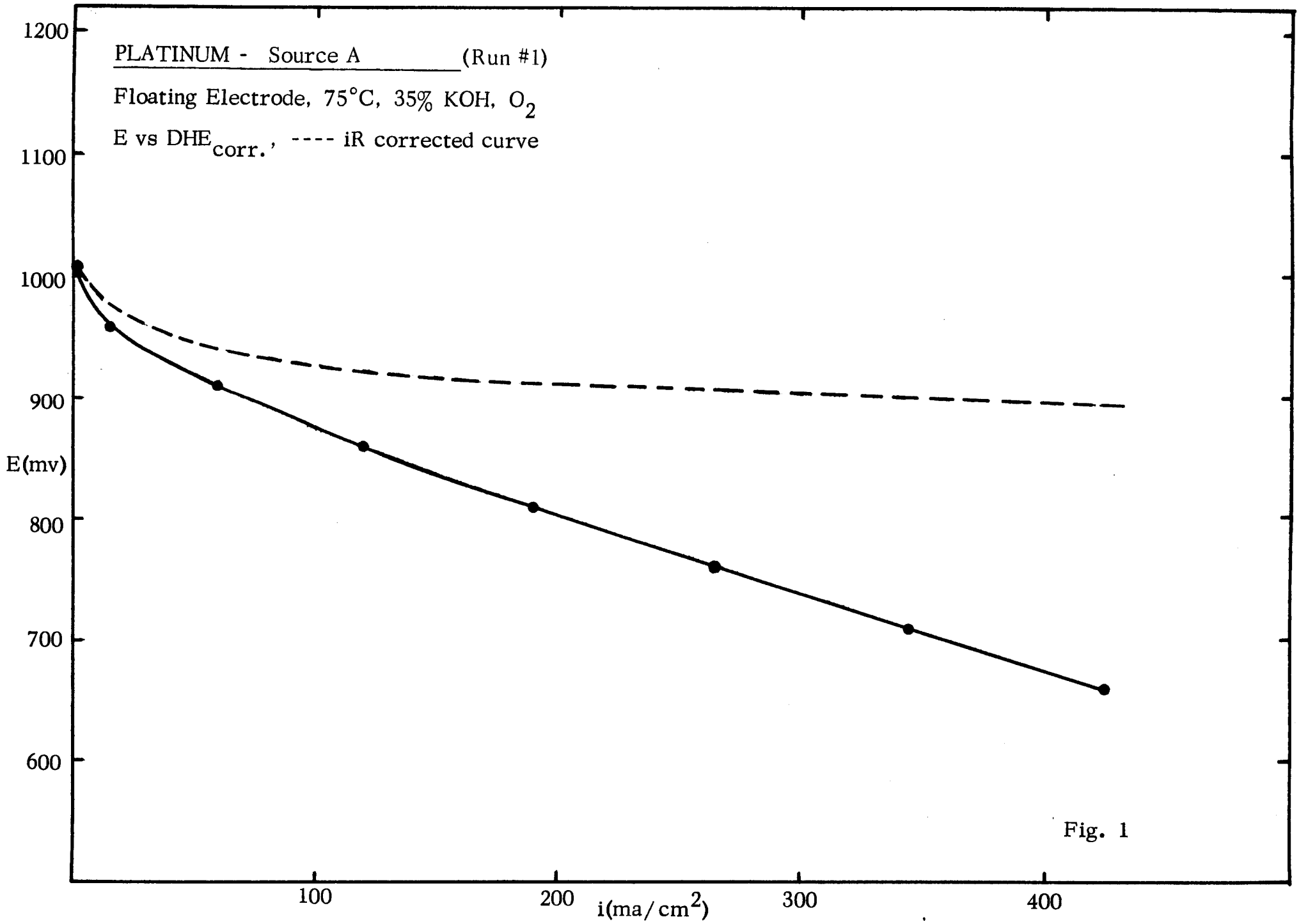
PLATINUM - Source A (Run #1)
Floating Electrode, 75°C, 35% KOH, O_2
E vs $DHE_{corr.}$, ---- iR corrected curve
1200
1100
1000
900
800
700
600
E(mv)
100
200
300
400
i(ma/cm^2)

Fig. 1

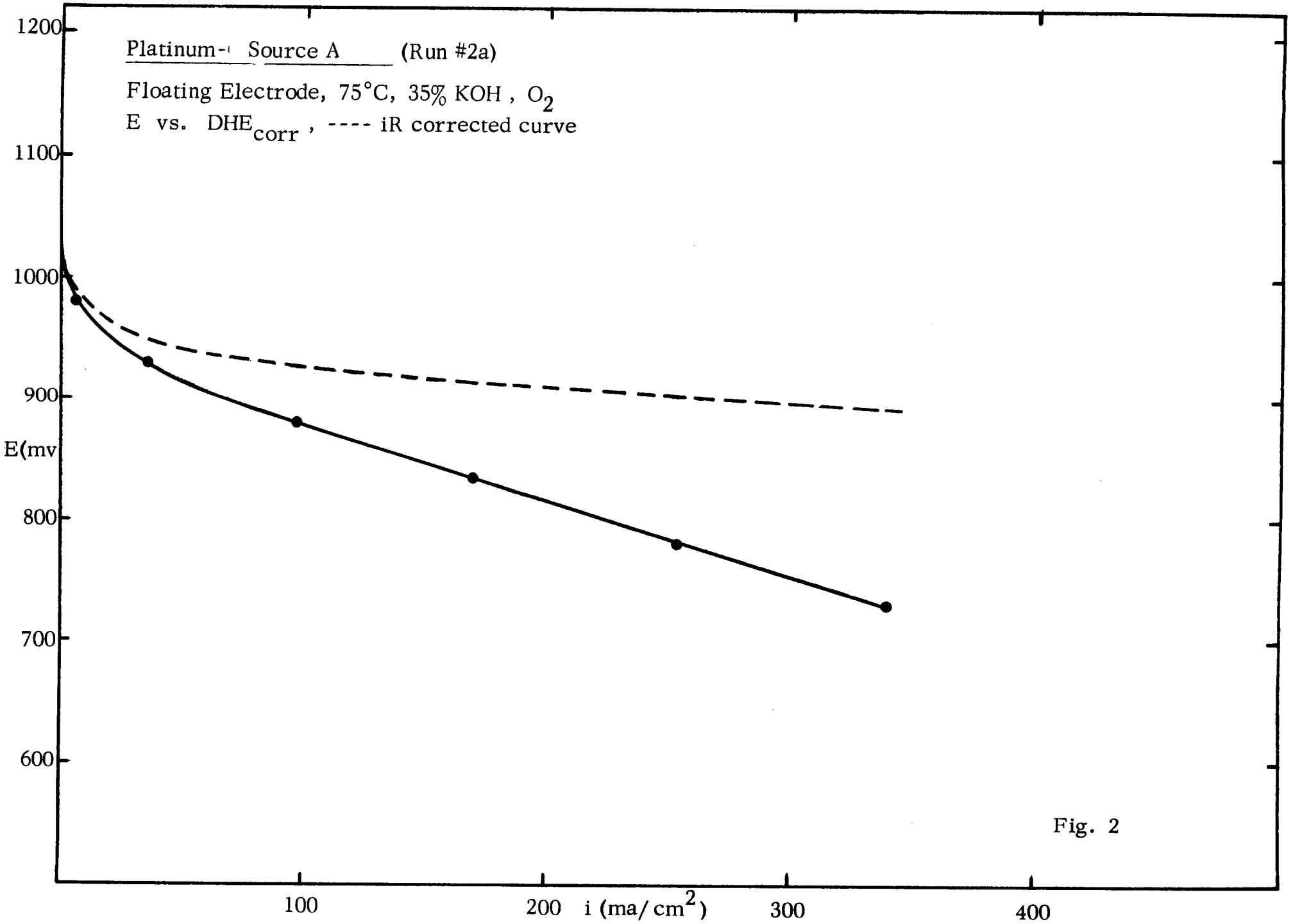
Platinum-Source A (Run #2a)
Floating Electrode, 75°C, 35% KOH , O_2
E vs. DHE_{corr} , ---- iR corrected curve
1200
1100
1000
900
800
700
600
E(mv
100
200
i (ma/ cm^2)
300
400

Fig. 2

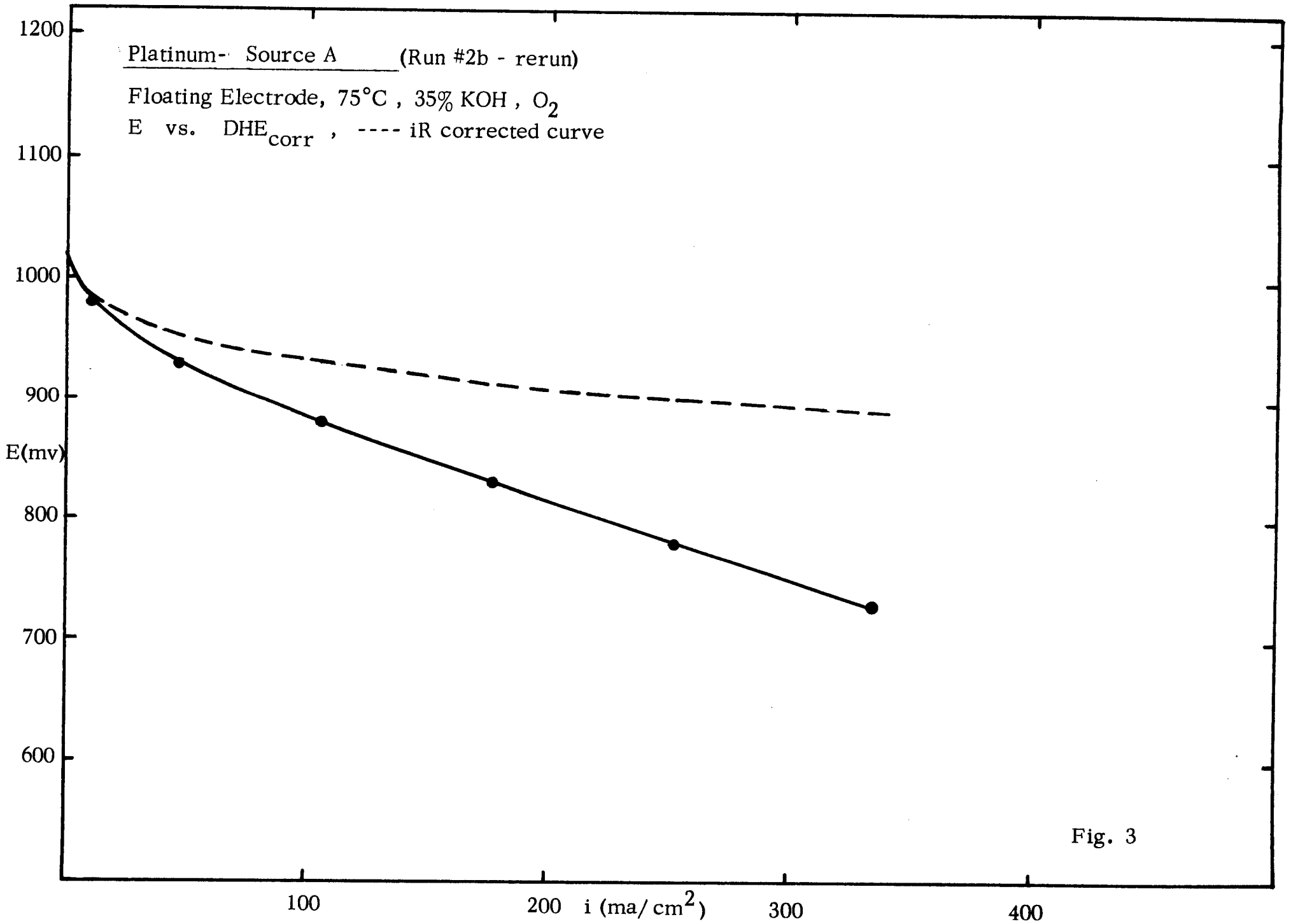
Platinum- Source A (Run #2b - rerun)
Floating Electrode, 75°C , 35% KOH , O_2
E vs. DHE_{corr} , ---- iR corrected curve
1200
1100
1000
900
800
700
600
E(mv)
100
200
i (ma/ cm^2)
300
400

Fig. 3

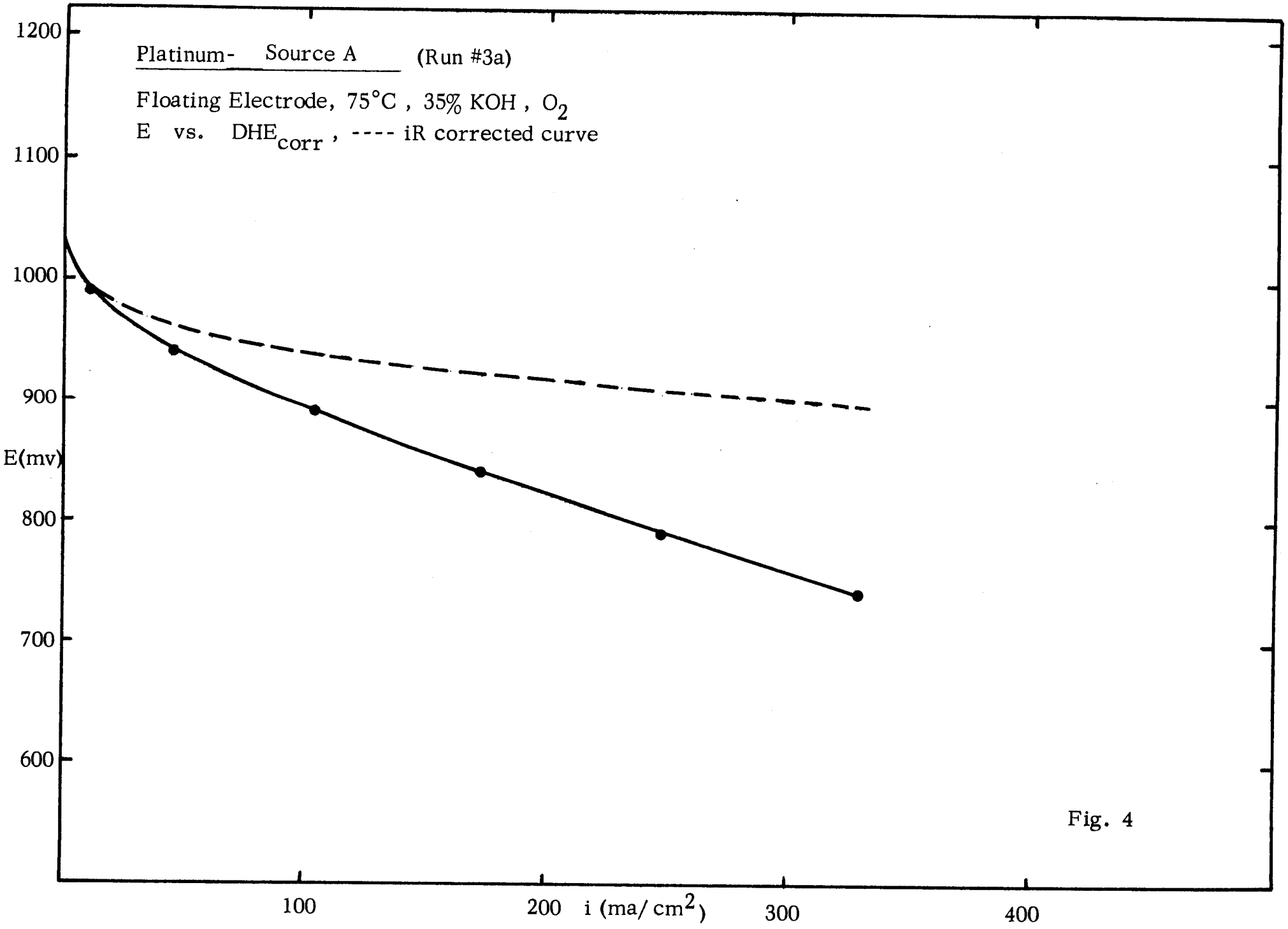
Platinum- Source A (Run #3a)
Floating Electrode, 75°C , 35% KOH , O_2
E vs. DHE_{corr} , ---- iR corrected curve
1200
1100
1000
900
800
700
600
E(mv)
100
200
300
400
i (ma/ cm^2)

Fig. 4

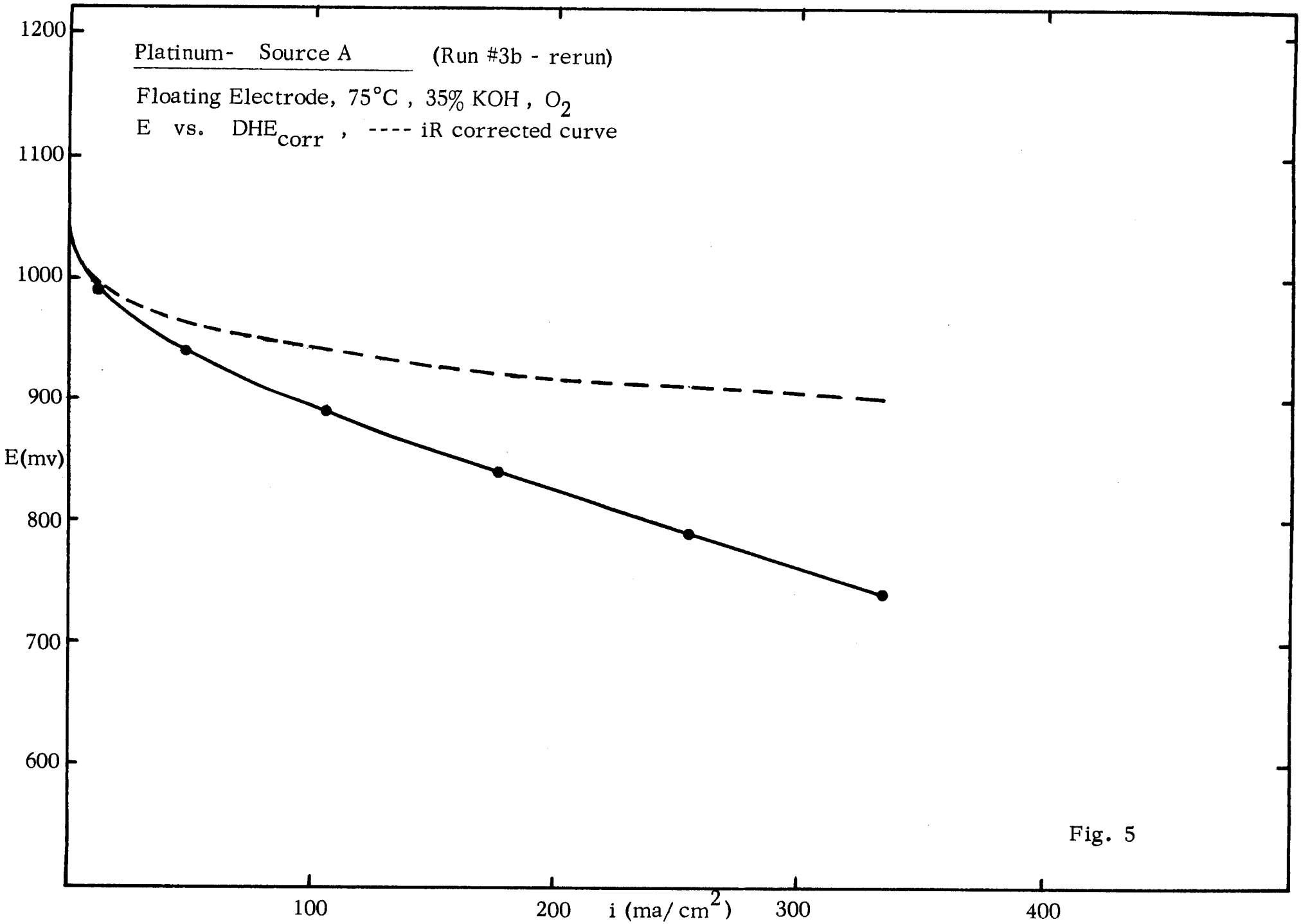
Platinum- Source A (Run #3b - rerun)
Floating Electrode, 75°C , 35% KOH , O_2
E vs. DHE_{corr} , ---- iR corrected curve
1200
1100
1000
900
800
700
600
E(mv)
100
200
i (ma/ cm^2)
300
400

Fig. 5

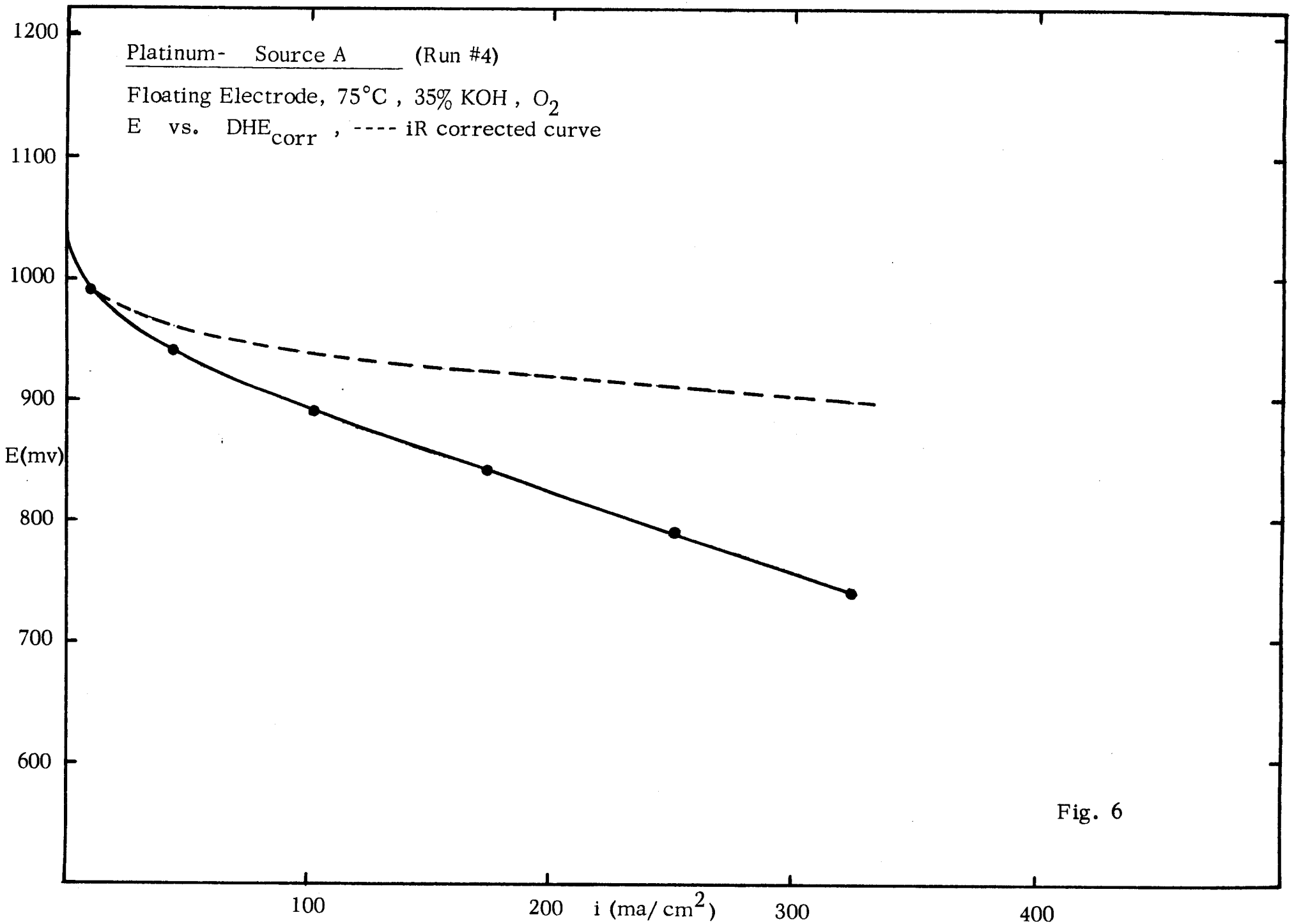
Platinum- Source A (Run #4)
Floating Electrode, 75°C , 35% KOH , O_2
E vs. DHE_{corr} , ---- iR corrected curve
1200
1100
1000
900
800
700
600
E(mv)
100
200
i (ma/ cm^2)
300
400

Fig. 6

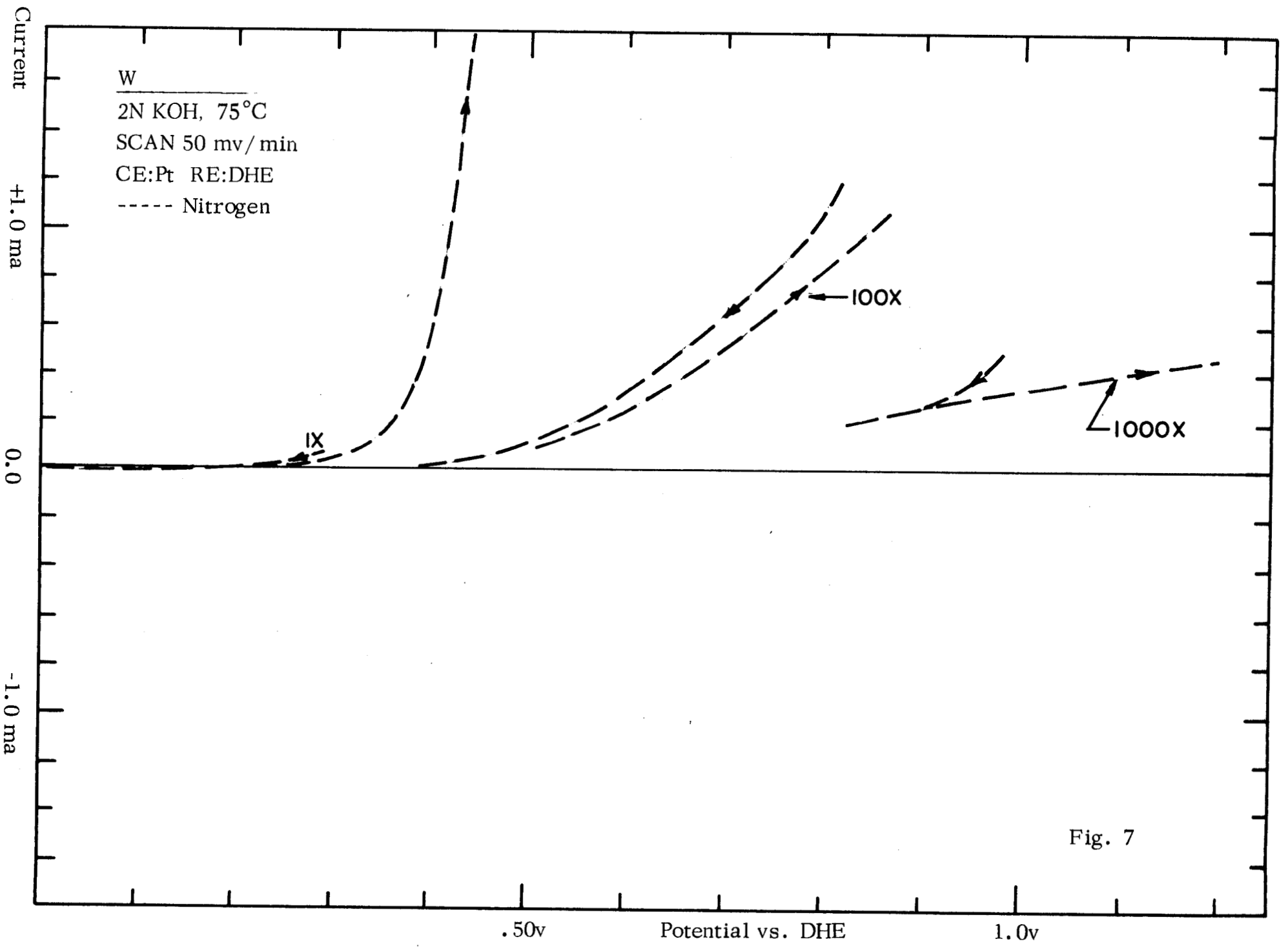
Current
+1.0 ma
0.0
-1.0 ma
W
2N KOH, 75°C
SCAN 50 mv/min
CE:Pt RE:DHE
----- Nitrogen
1X
100X
1000X
.50v
Potential vs. DHE
1.0v

Fig. 7

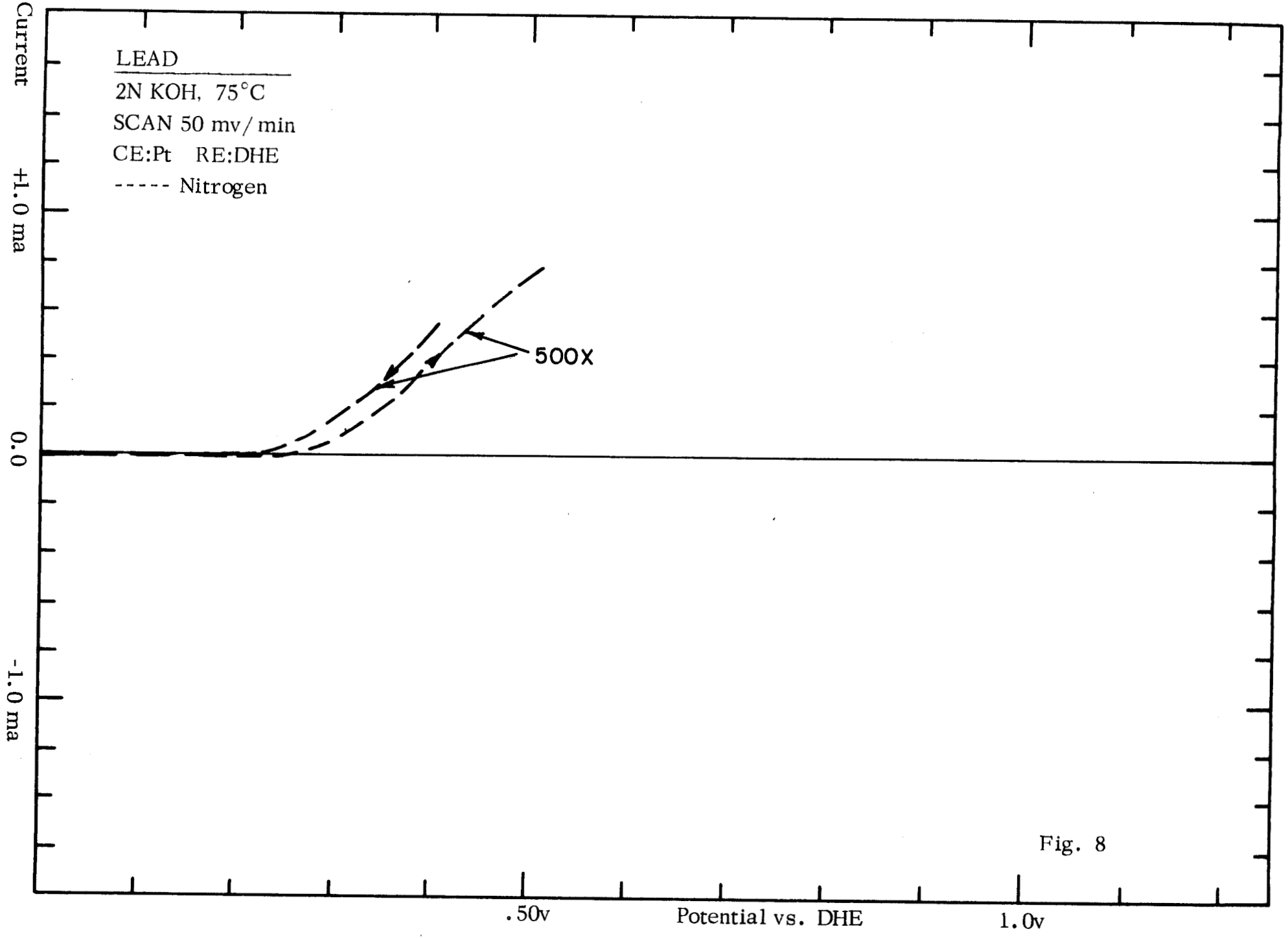
LEAD
2N KOH, 75°C
SCAN 50 mv/min
CE:Pt RE:DHE
----- Nitrogen
500X
Current
+1.0 ma
0.0
-1.0 ma
.50v
Potential vs. DHE
1.0v

Fig. 8

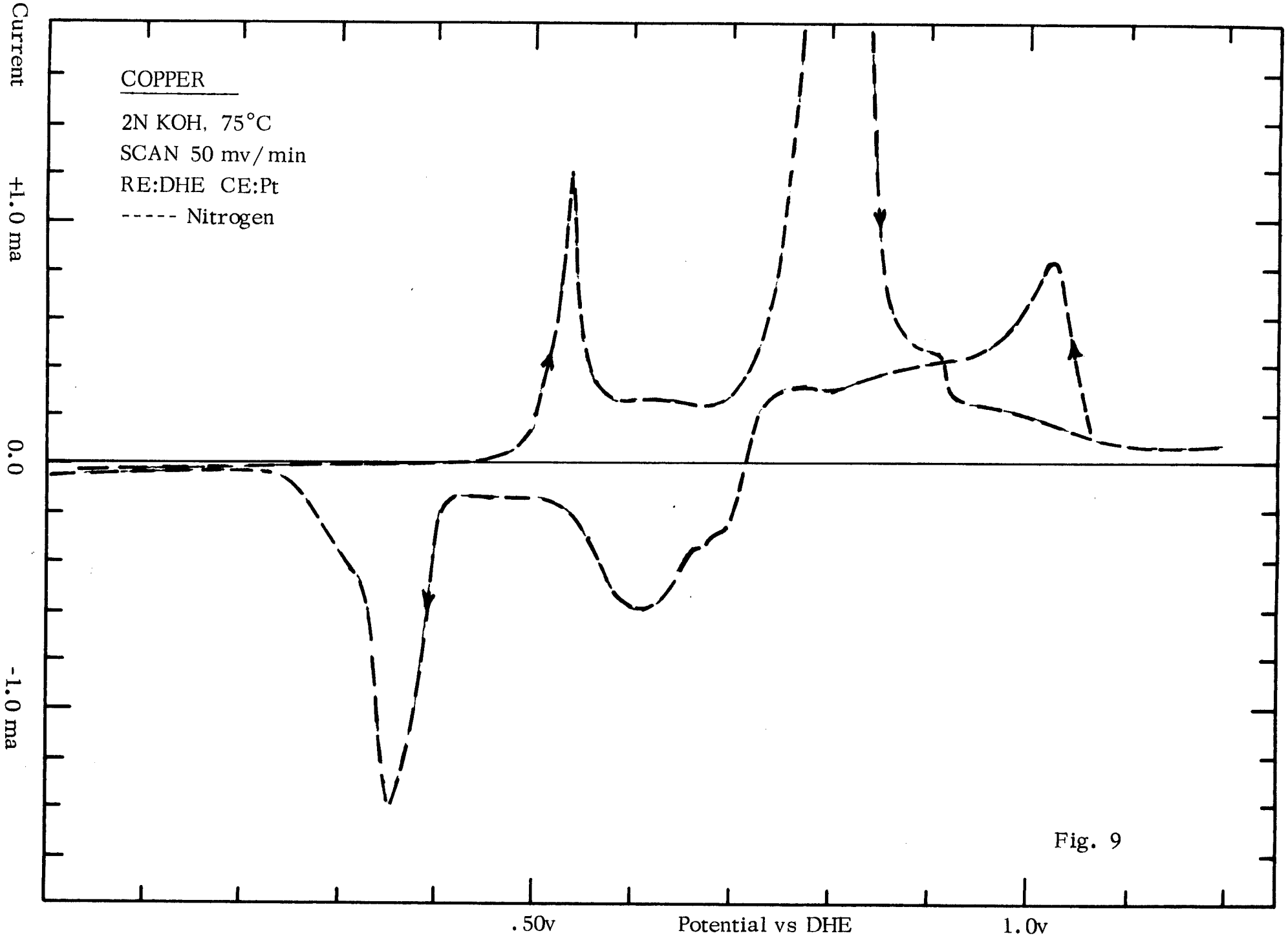
COPPER
2N KOH, 75°C
SCAN 50 mv/min
RE:DHE CE:Pt
----- Nitrogen
Current
+1.0 ma
0.0
-1.0 ma
.50v
Potential vs DHE
1.0v

Fig. 9

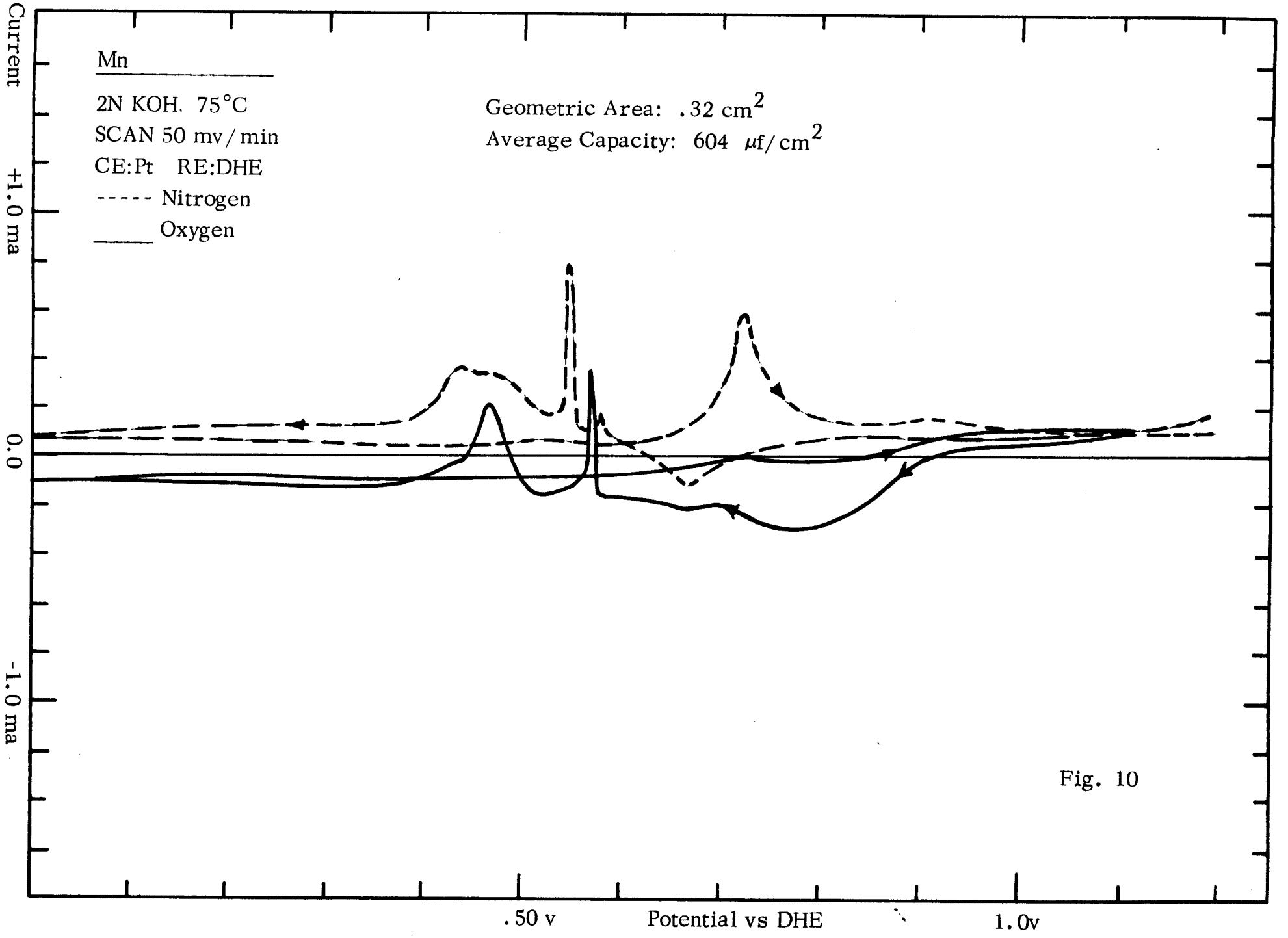
Current
+1.0 ma
0.0
-1.0 ma
Mn
2N KOH. 75°C
SCAN 50 mv/min
CE:Pt RE:DHE
----- Nitrogen
_____ Oxygen
Geometric Area: .32 cm2
Average Capacity: 604 μf/cm2
.50 v
Potential vs DHE
1.0v

Fig. 10

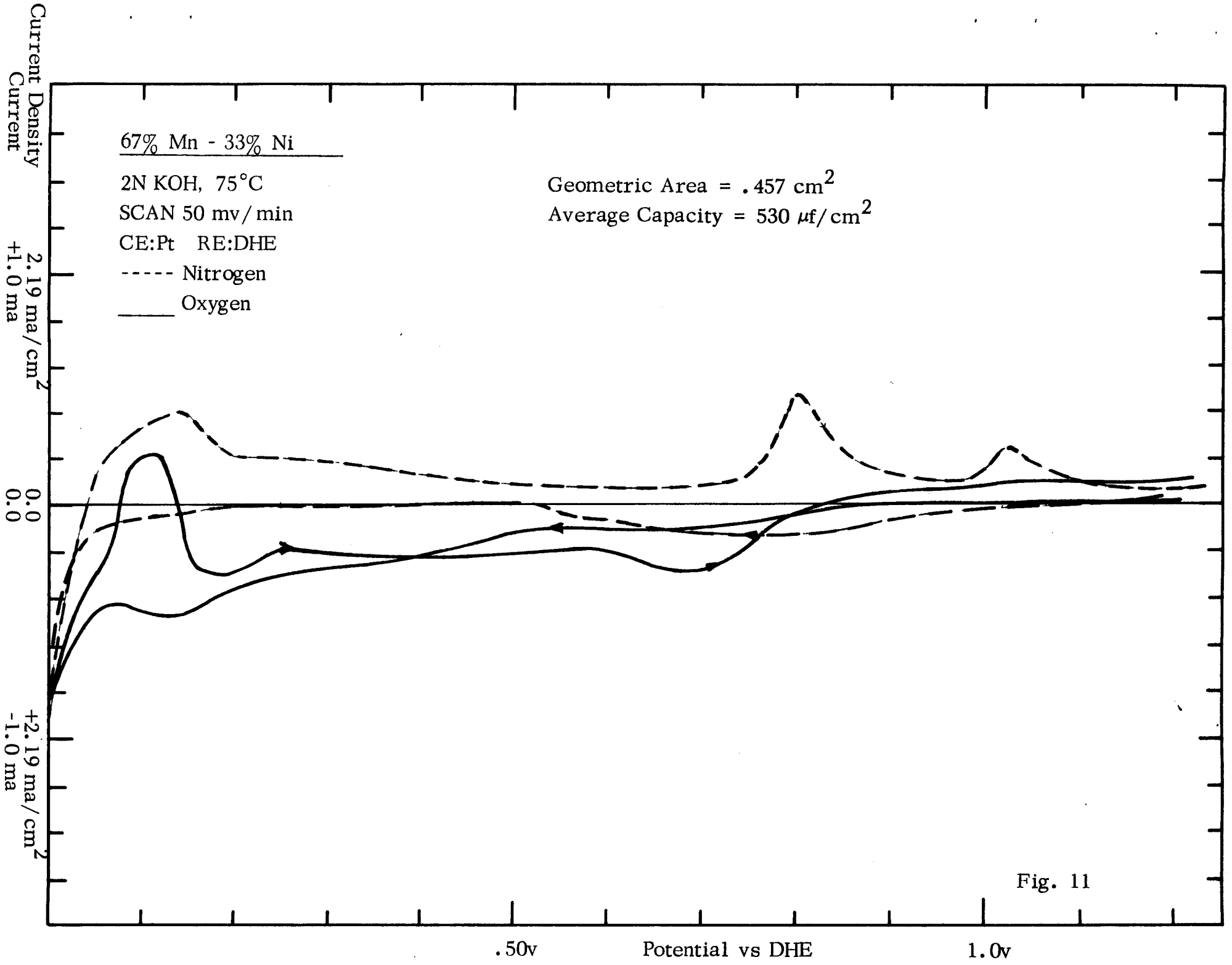
Current Density
Current
67% Mn - 33% Ni
2N KOH, 75°C
SCAN 50 mv/min
CE:Pt RE:DHE
----- Nitrogen
_____ Oxygen
Geometric Area = .457 cm2
Average Capacity = 530 μf/cm2
+2.19 ma/cm2
+1.0 ma
0.0
0.0
+2.19 ma/cm2
-1.0 ma
.50v
Potential vs DHE
1.0v

Fig. 11

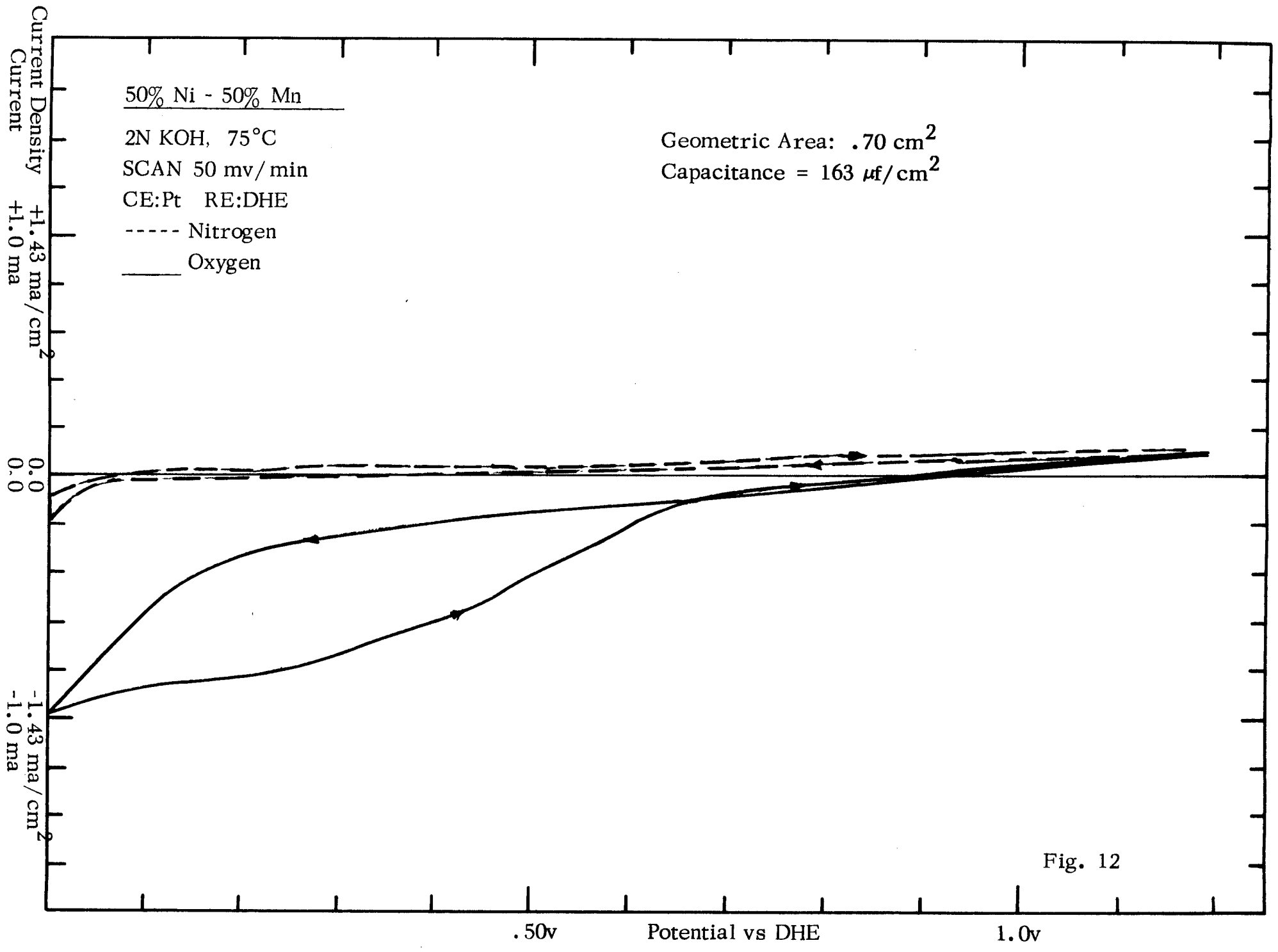
50% Ni - 50% Mn
2N KOH, 75°C
SCAN 50 mv/min
CE:Pt RE:DHE
----- Nitrogen
_____ Oxygen
Geometric Area: .70 cm2
Capacitance = 163 μf/cm2
Current Density Current
+1.43 ma/cm2
+1.0 ma
0.0
0.0
-1.43 ma/cm2
-1.0 ma
.50v
Potential vs DHE
1.0v

Fig. 12

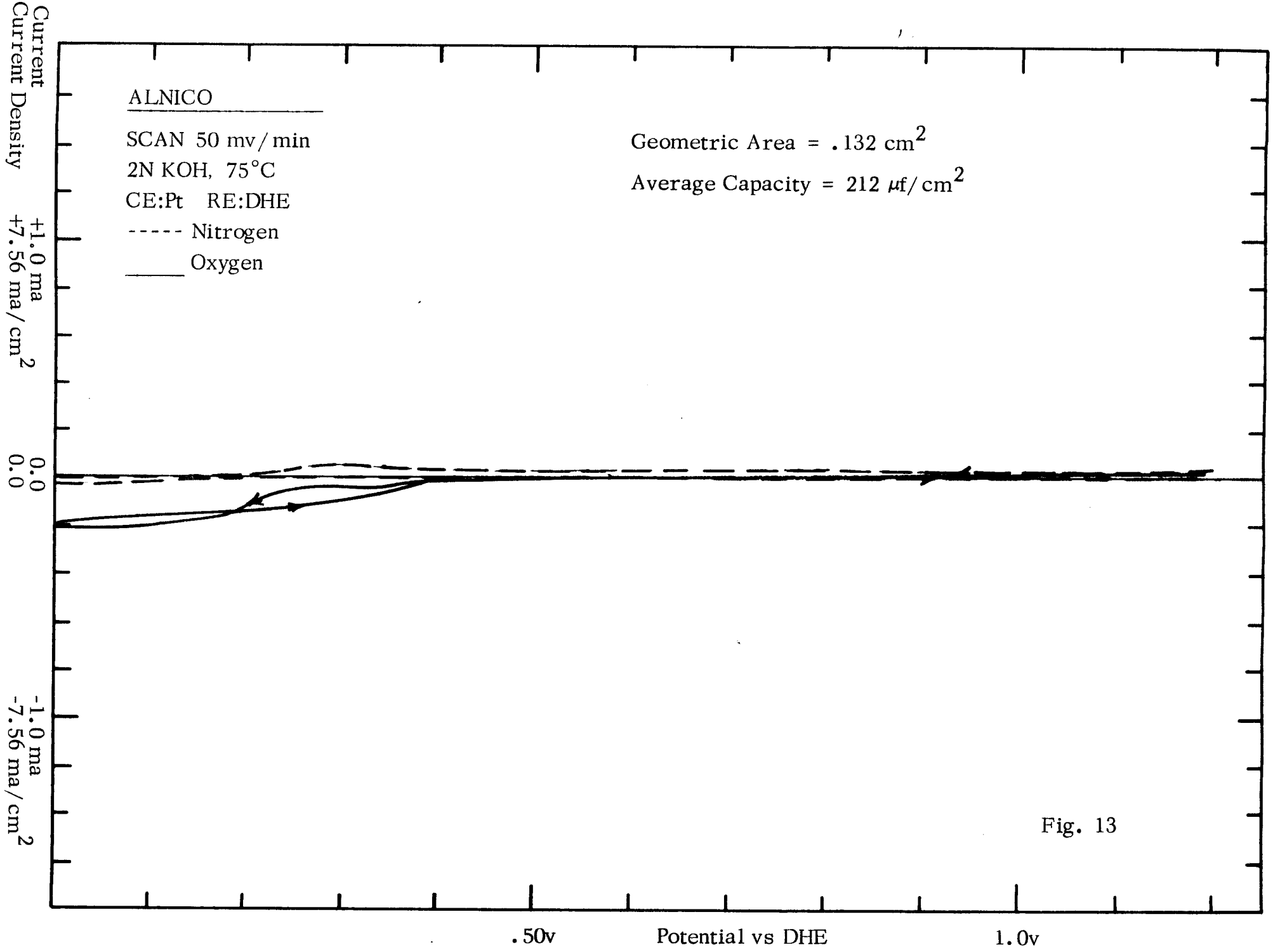
ALNICO
SCAN 50 mv/min
2N KOH, 75°C
CE:Pt RE:DHE
----- Nitrogen
_____ Oxygen
Geometric Area = .132 cm²
Average Capacity = 212 μf/cm²
Current
Current Density
+1.0 ma
+7.56 ma/cm²
0.0
0.0
-1.0 ma
-7.56 ma/cm²
.50v
Potential vs DHE
1.0v

Fig. 13

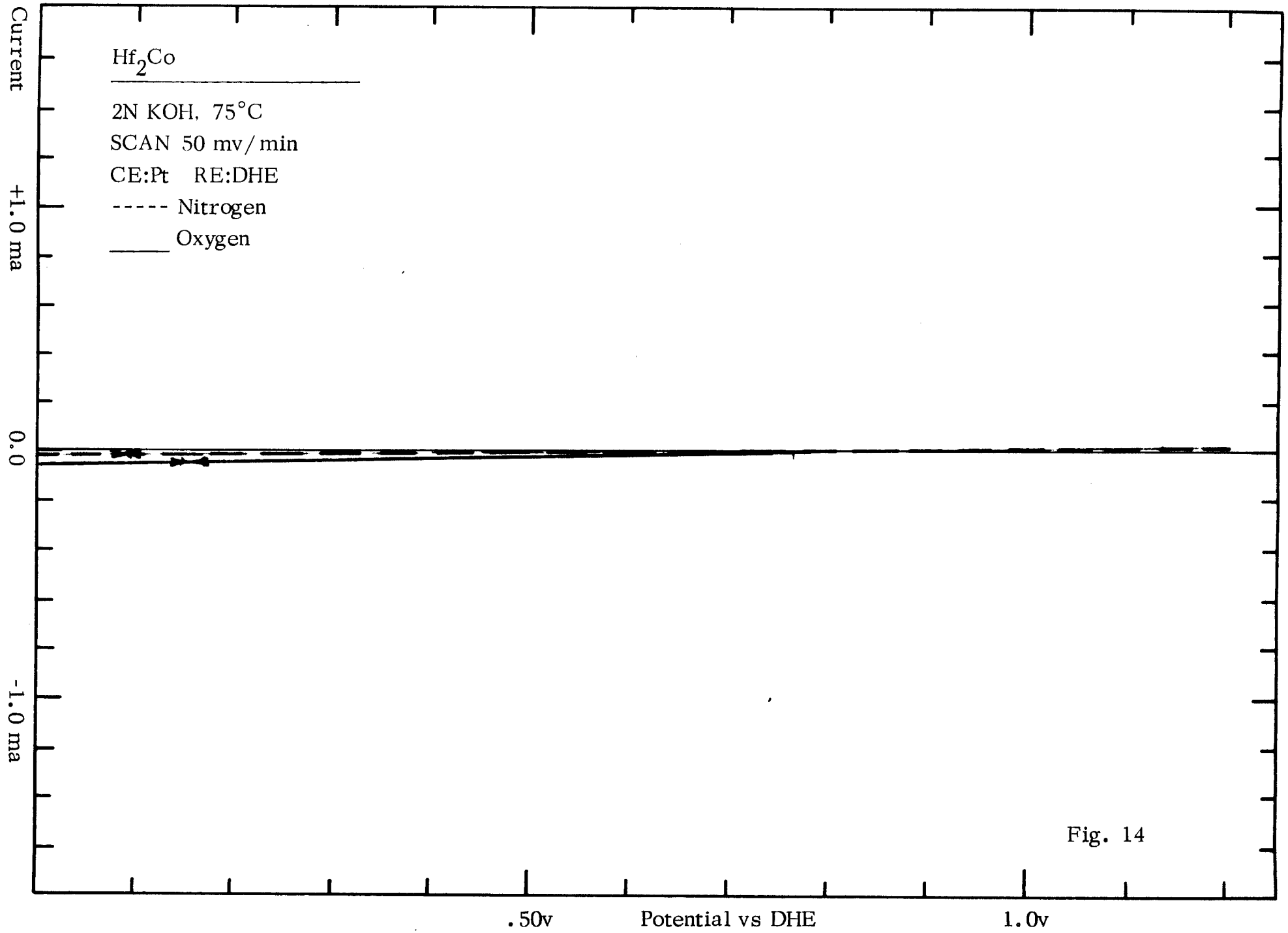
Current
+1.0 ma
0.0
-1.0 ma
Hf_2Co
2N KOH, 75°C
SCAN 50 mv/min
CE:Pt RE:DHE
----- Nitrogen
_____ Oxygen
.50v
Potential vs DHE
1.0v

Fig. 14

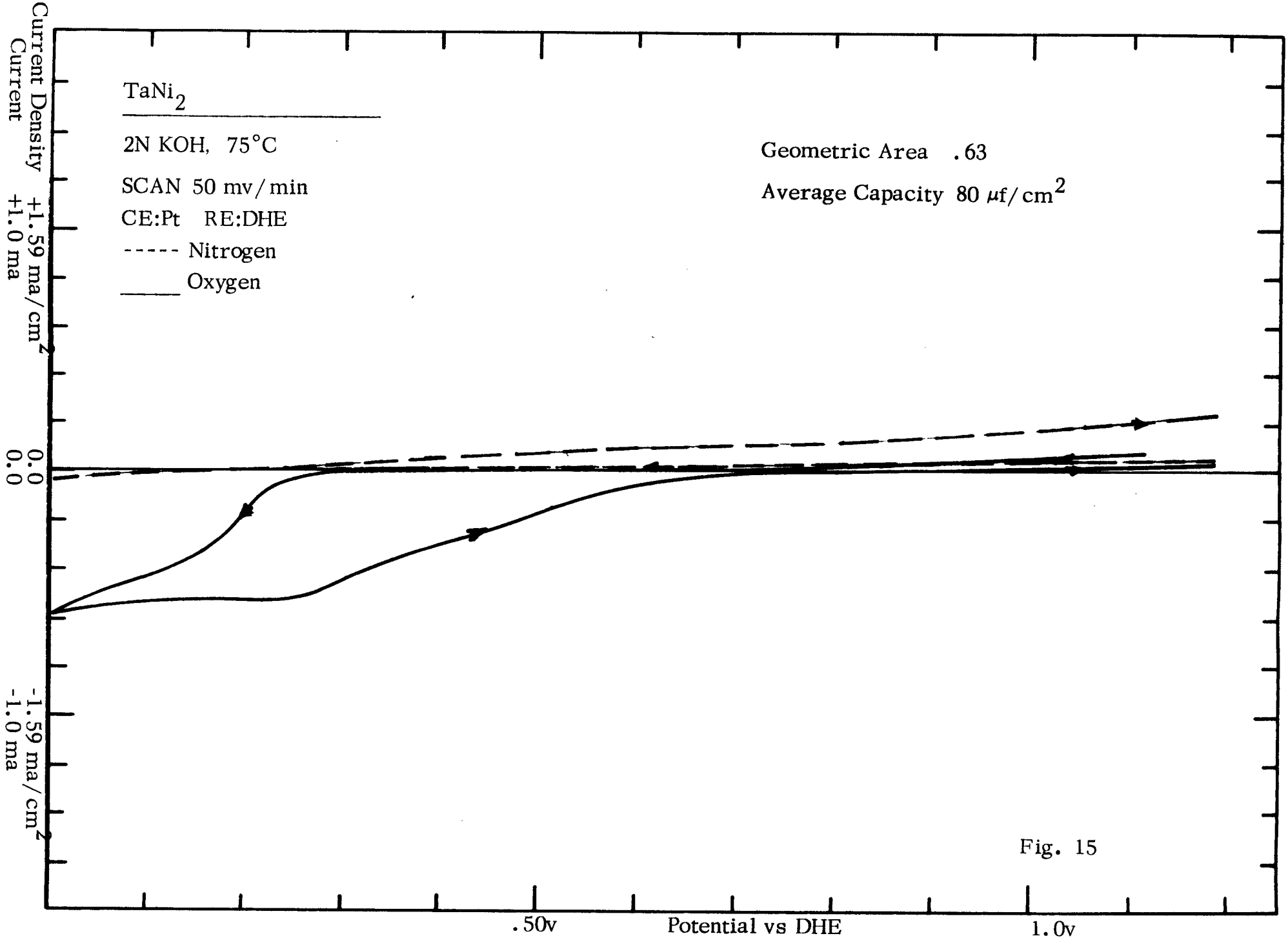
Current Density
Current
TaNi2
2N KOH, 75°C
SCAN 50 mv/min
CE:Pt RE:DHE
----- Nitrogen
_____ Oxygen
Geometric Area .63
Average Capacity 80 μf/cm2
+1.59 ma/cm2
+1.0 ma
0.0
0.0
-1.59 ma/cm2
-1.0 ma
.50v
Potential vs DHE
1.0v

Fig. 15

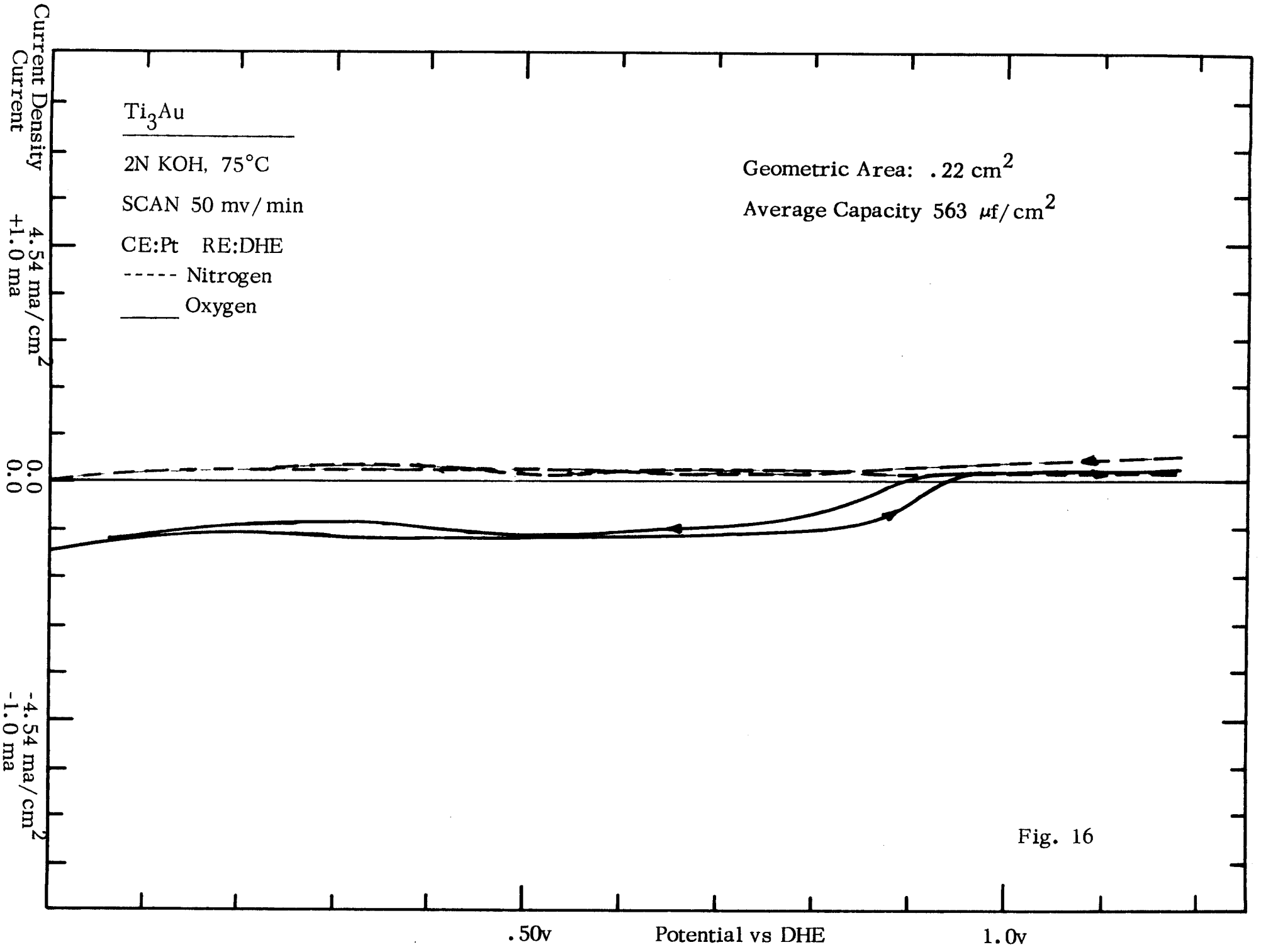
Current Density
Current
Ti_3Au
2N KOH, 75°C
SCAN 50 mv/min
CE:Pt RE:DHE
----- Nitrogen
_____ Oxygen
Geometric Area: .22 cm^2
Average Capacity 563 $\mu f/cm^2$
4.54 ma/cm^2
+1.0 ma
0.0
0.0
-4.54 ma/cm^2
-1.0 ma
.50v
Potential vs DHE
1.0v

Fig. 16

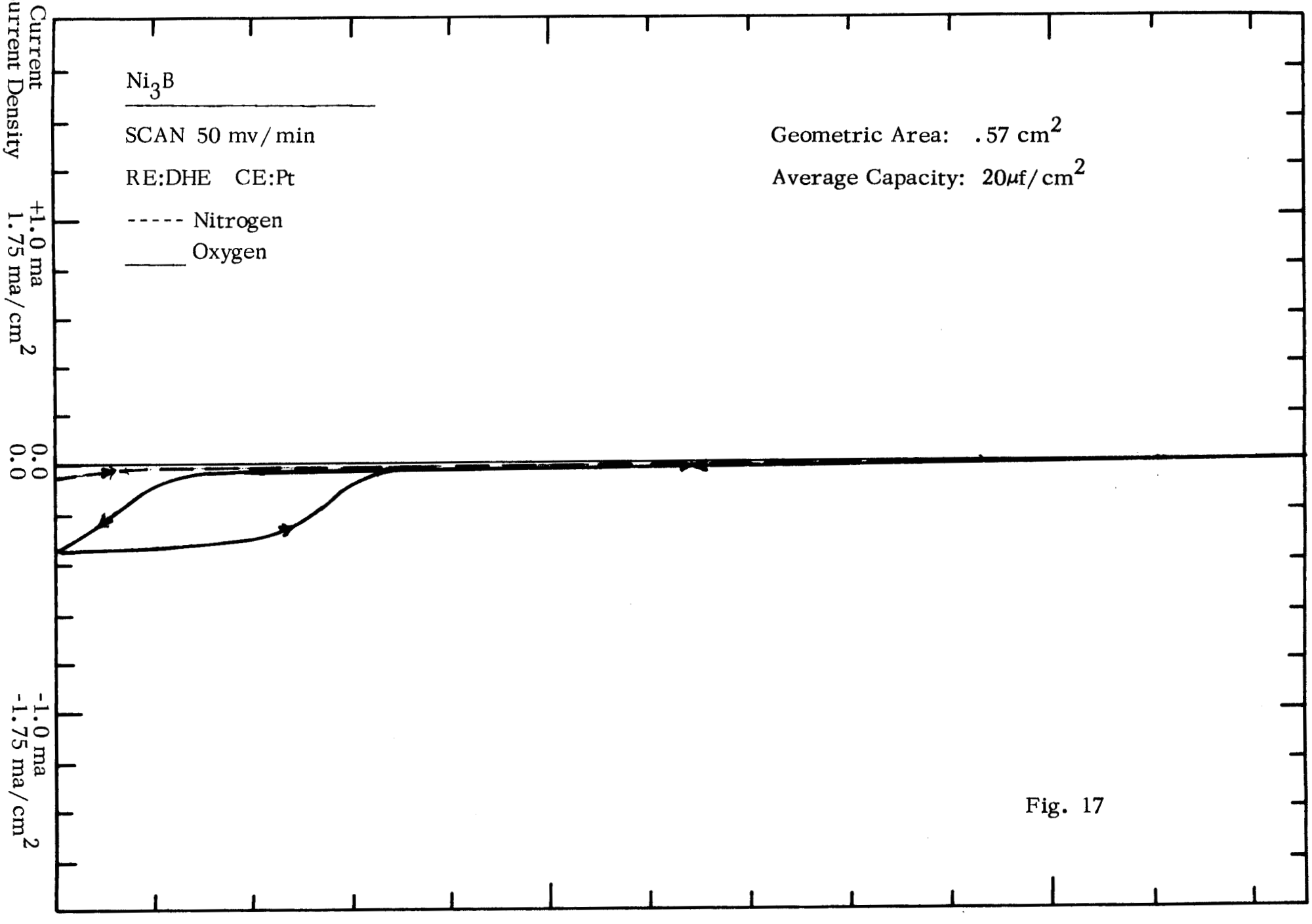
Current Density
Current
+1.0 ma
1.75 ma/cm2
0.0
0.0
-1.0 ma
-1.75 ma/cm2
Ni3B
SCAN 50 mv/min
RE:DHE CE:Pt
----- Nitrogen
_____ Oxygen
Geometric Area: .57 cm2
Average Capacity: 20μf/cm2

Fig. 17

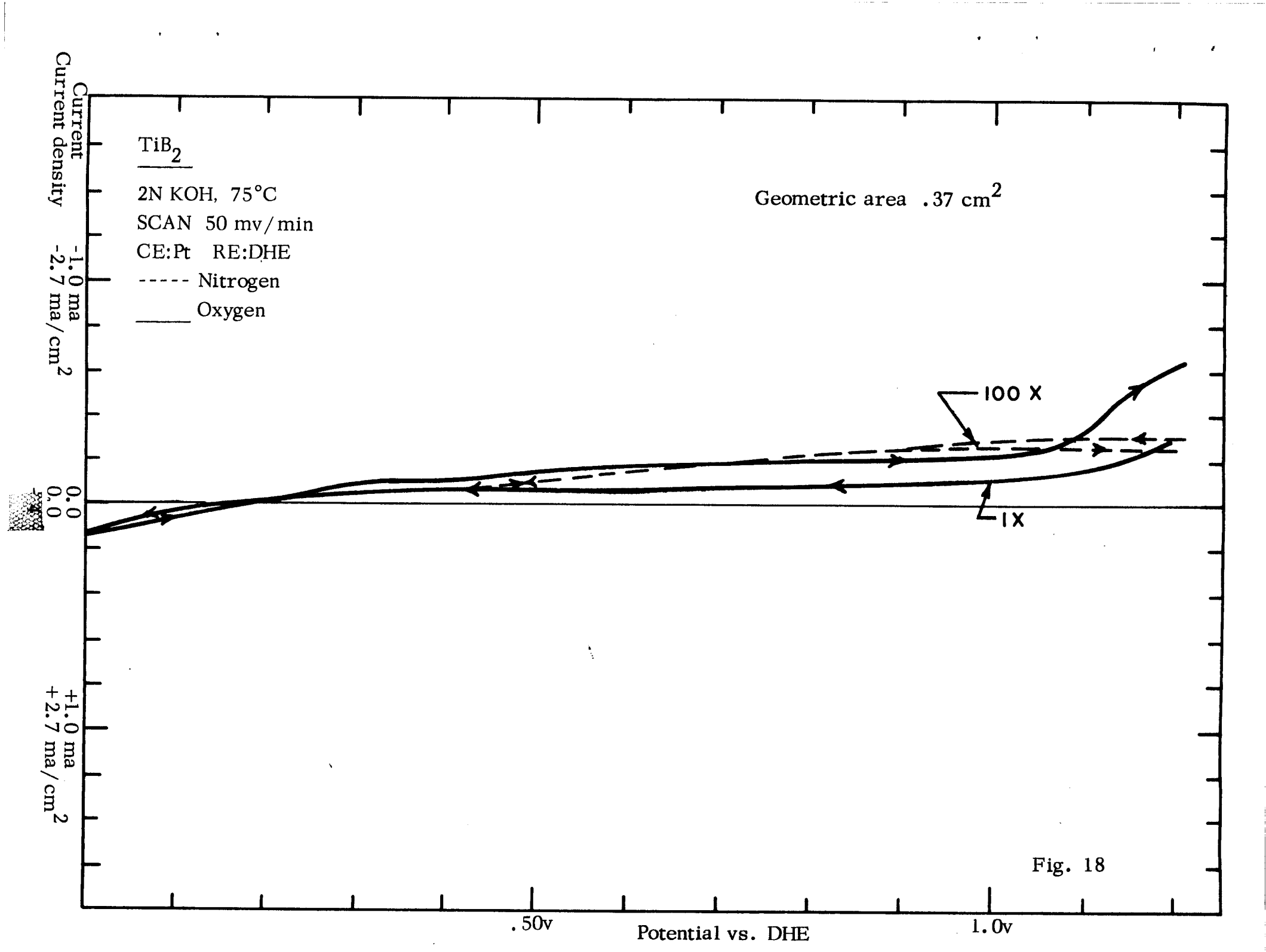
Current density
Current
TiB_2
2N KOH, 75°C
SCAN 50 mv/min
CE:Pt RE:DHE
----- Nitrogen
_____ Oxygen
Geometric area .37 cm^2
100 X
1 X
-1.0 ma
-2.7 ma/cm^2
0.0
0.0
+1.0 ma
+2.7 ma/cm^2
.50v
Potential vs. DHE
1.0v

Fig. 18

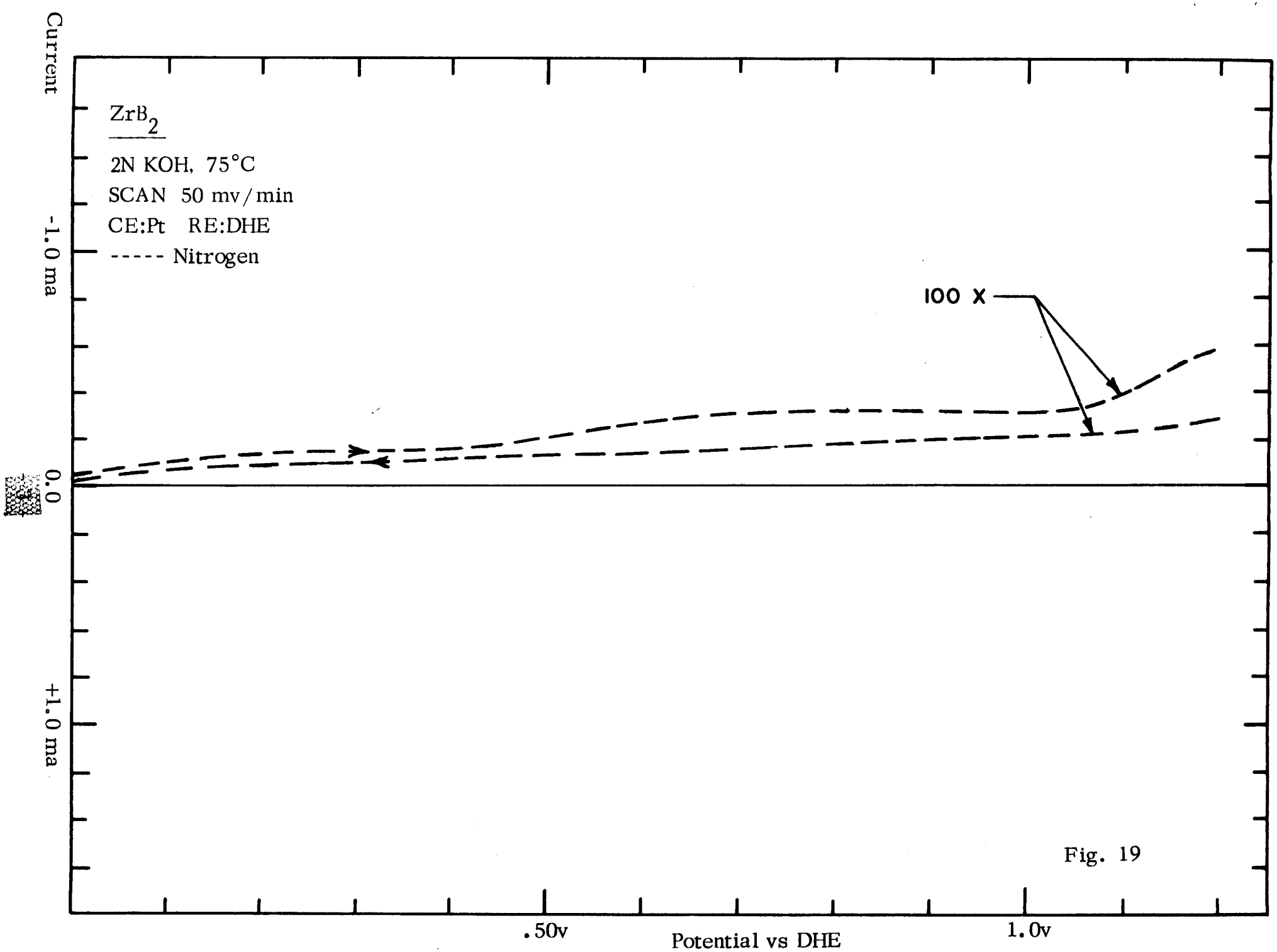
Current
-1.0 ma
0.0
+1.0 ma
ZrB_2
2N KOH, 75°C
SCAN 50 mv/min
CE:Pt RE:DHE
----- Nitrogen
100 X
.50v
Potential vs DHE
1.0v

Fig. 19

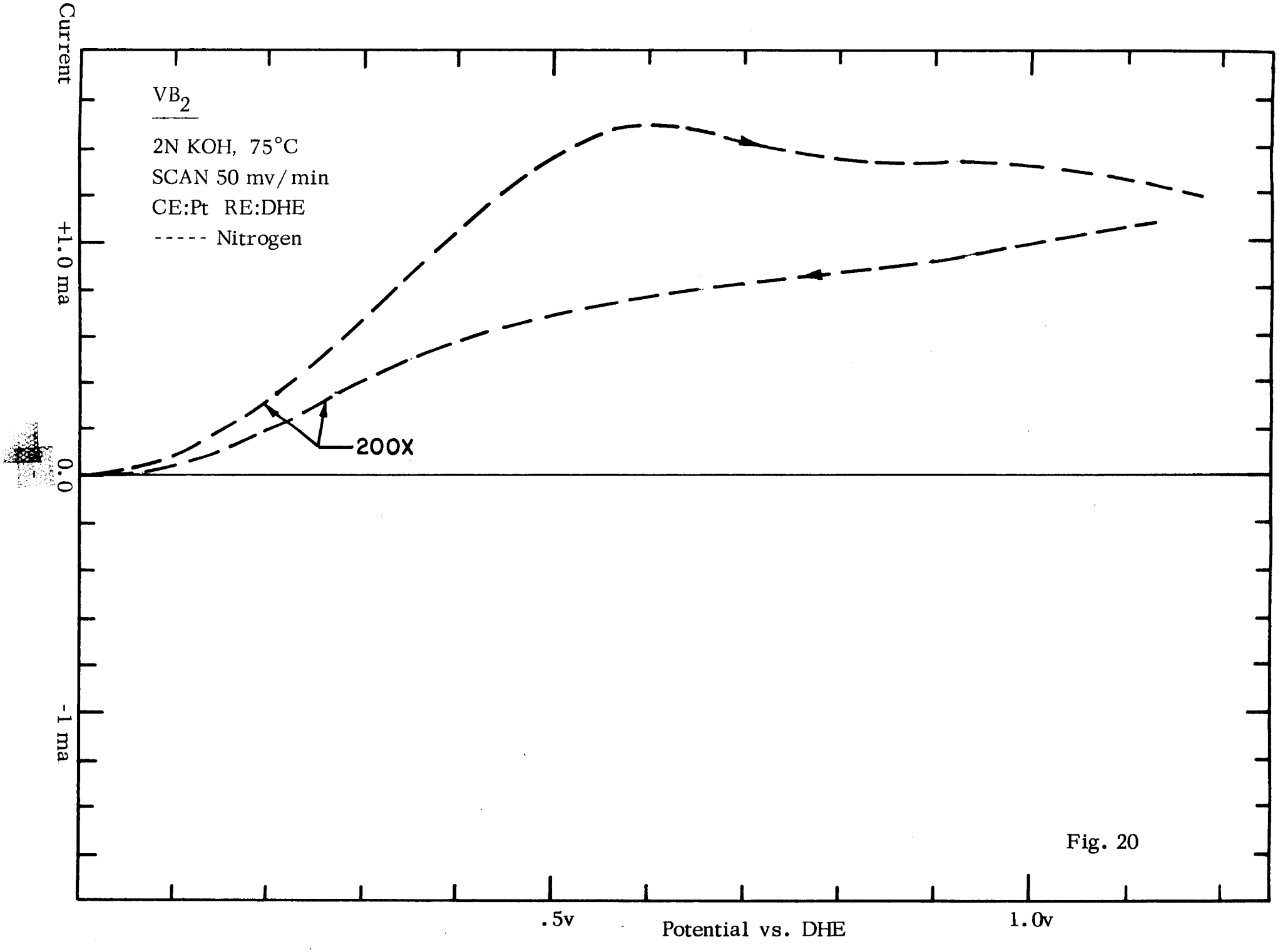
Current
+1.0 ma
0.0
-1 ma
VB_2
2N KOH, 75°C
SCAN 50 mv/min
CE:Pt RE:DHE
----- Nitrogen
200X
.5v
Potential vs. DHE
1.0v

Fig. 20

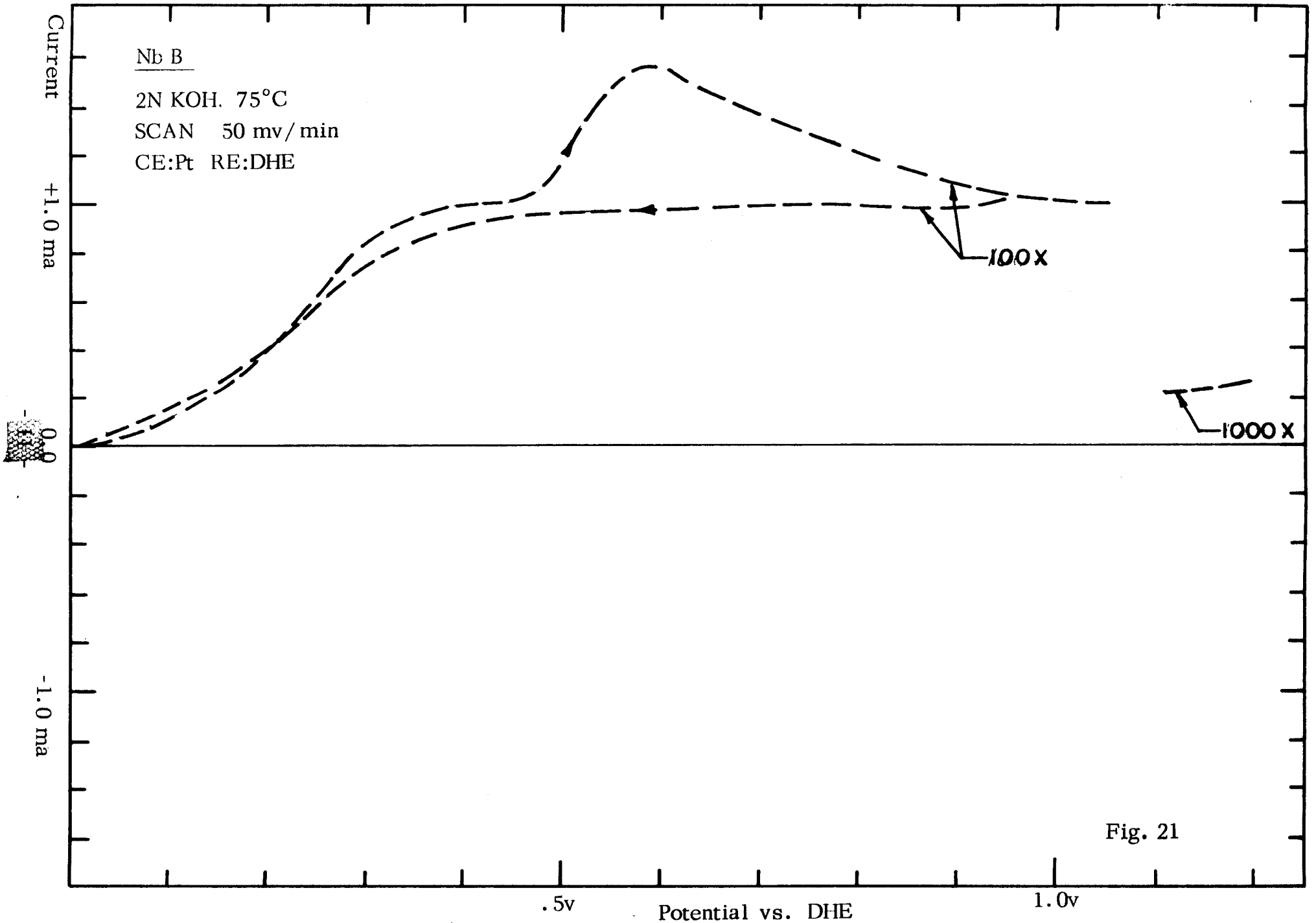
Nb B
2N KOH. 75°C
SCAN 50 mv/min
CE:Pt RE:DHE
Current
+1.0 ma
0.0
-1.0 ma
100 X
1000 X
.5v
Potential vs. DHE
1.0v

Fig. 21

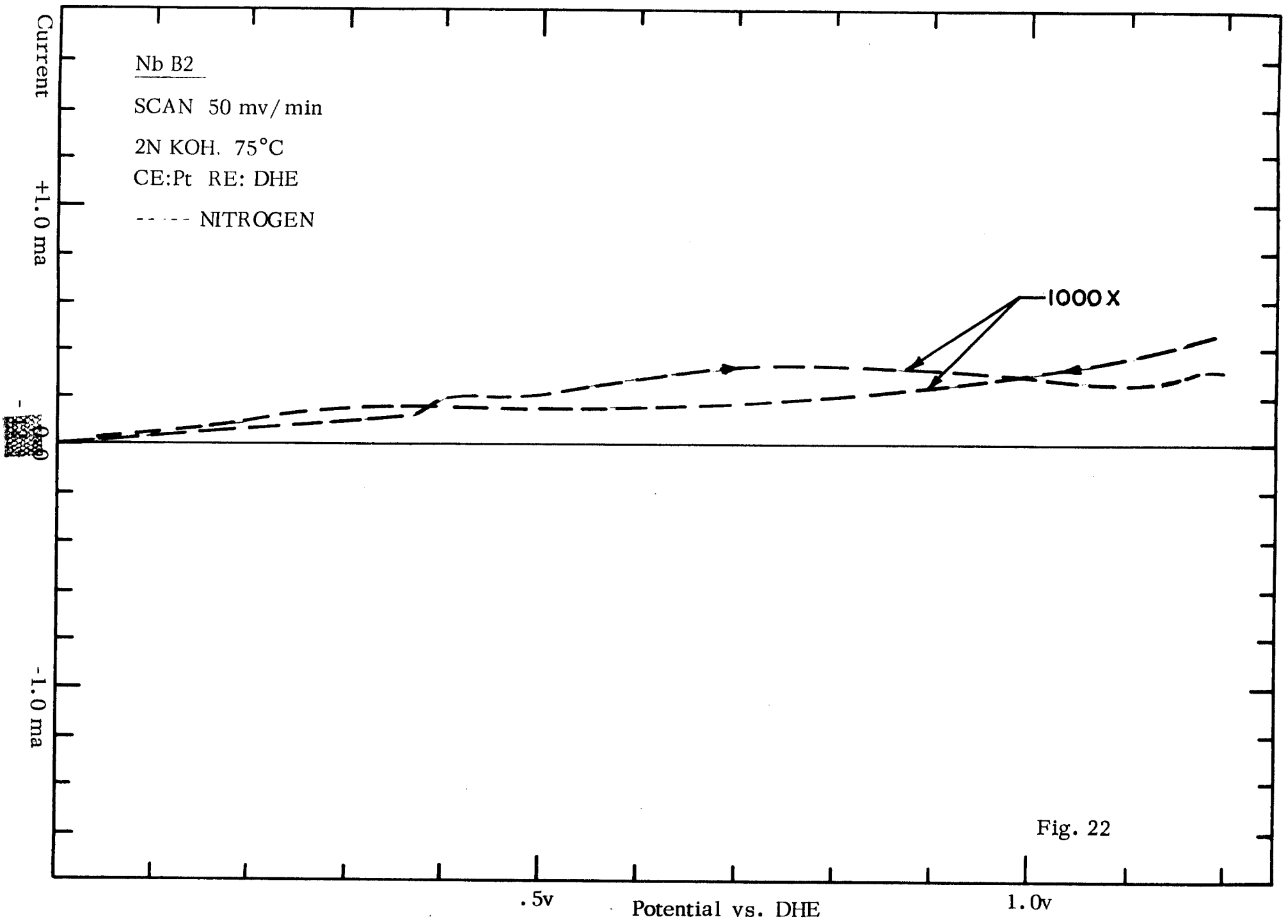
Nb B2
SCAN 50 mv/min
2N KOH. 75°C
CE:Pt RE: DHE
----- NITROGEN
1000 X
Current
+1.0 ma
-1.0 ma
.5v
Potential vs. DHE
1.0v

Fig. 22

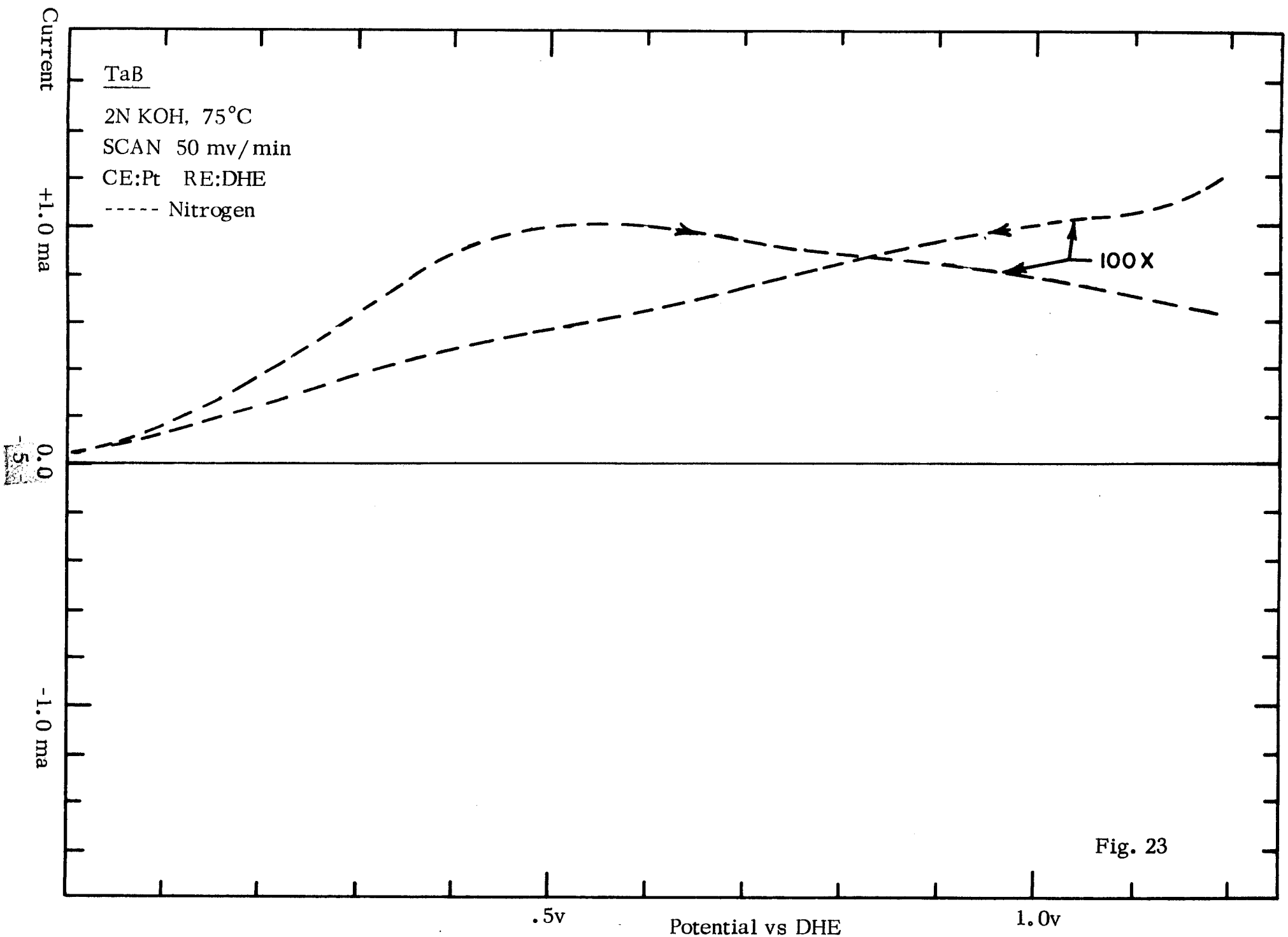
Current
+1.0 ma
0.0
-1.0 ma
TaB
2N KOH, 75°C
SCAN 50 mv/min
CE:Pt RE:DHE
----- Nitrogen
100 X
.5v
Potential vs DHE
1.0v

Fig. 23

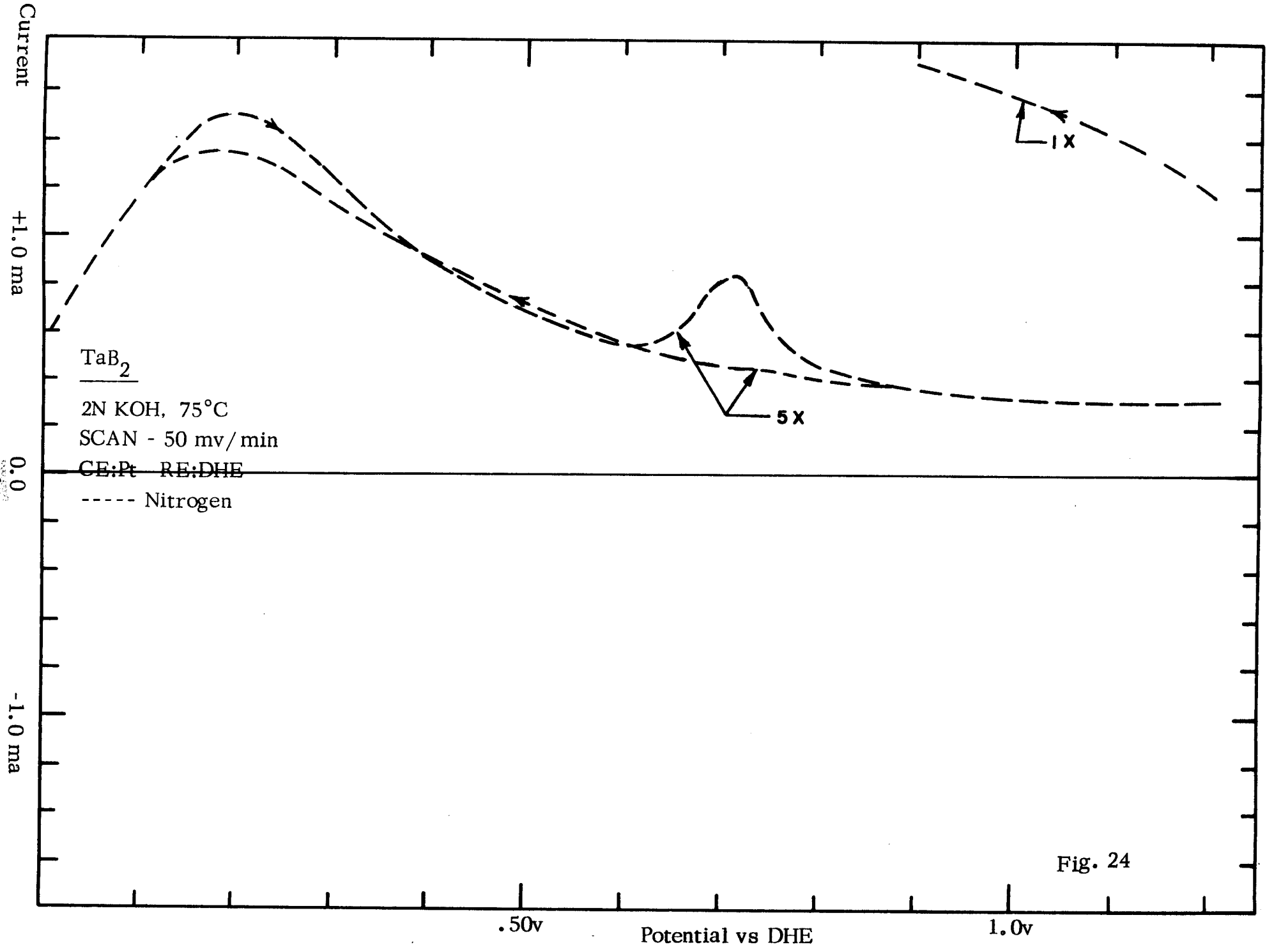
Current
+1.0 ma
0.0
-1.0 ma
TaB2
2N KOH, 75°C
SCAN - 50 mv/min
CE:Pt RE:DHE
----- Nitrogen
1X
5X
.50v
Potential vs DHE
1.0v

Fig. 24

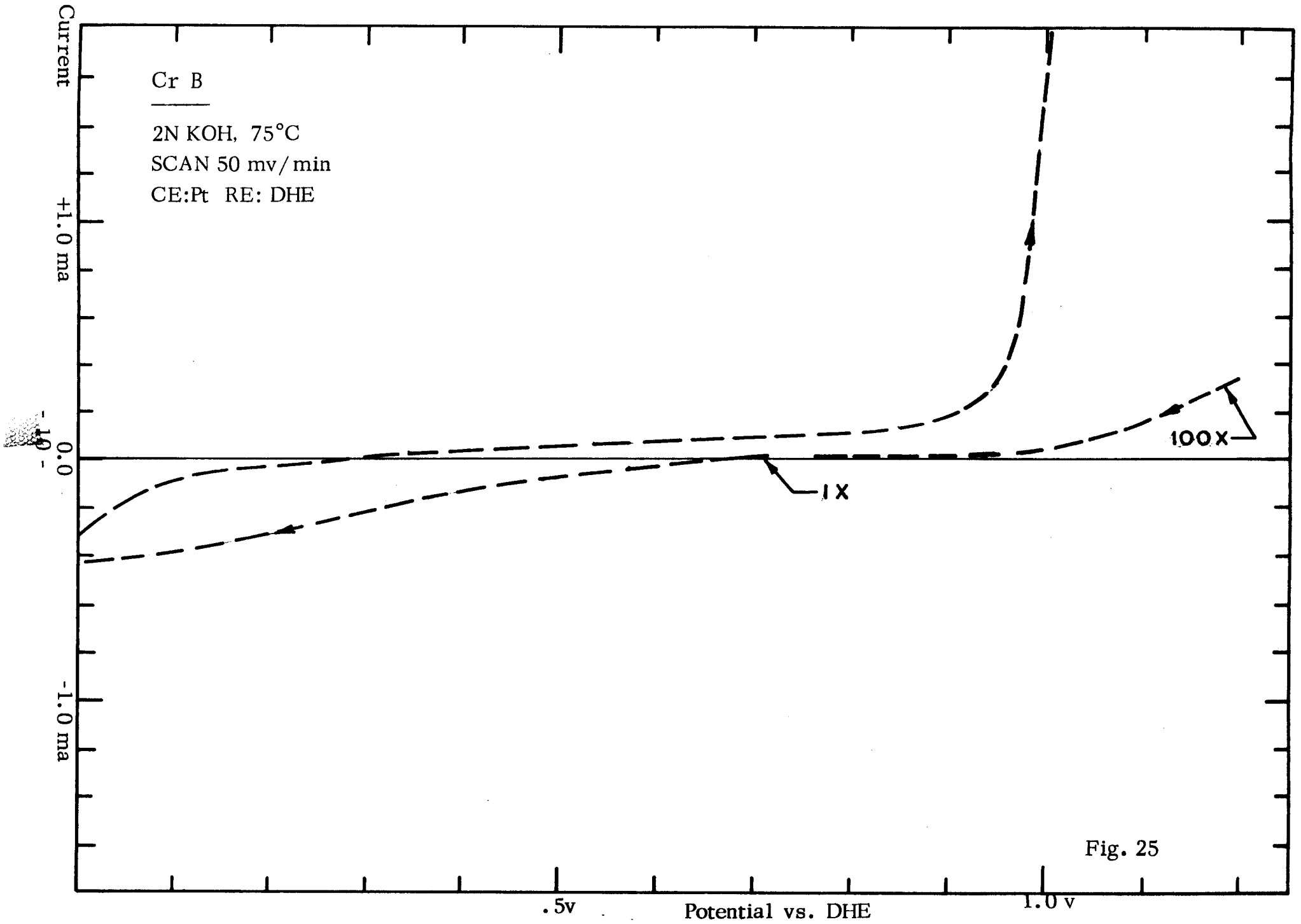
Current
+1.0 ma
0.0
-10 -
-1.0 ma
Cr B
2N KOH, 75°C
SCAN 50 mv/min
CE:Pt RE: DHE
100X
1X
.5v
Potential vs. DHE
1.0 v

Fig. 25

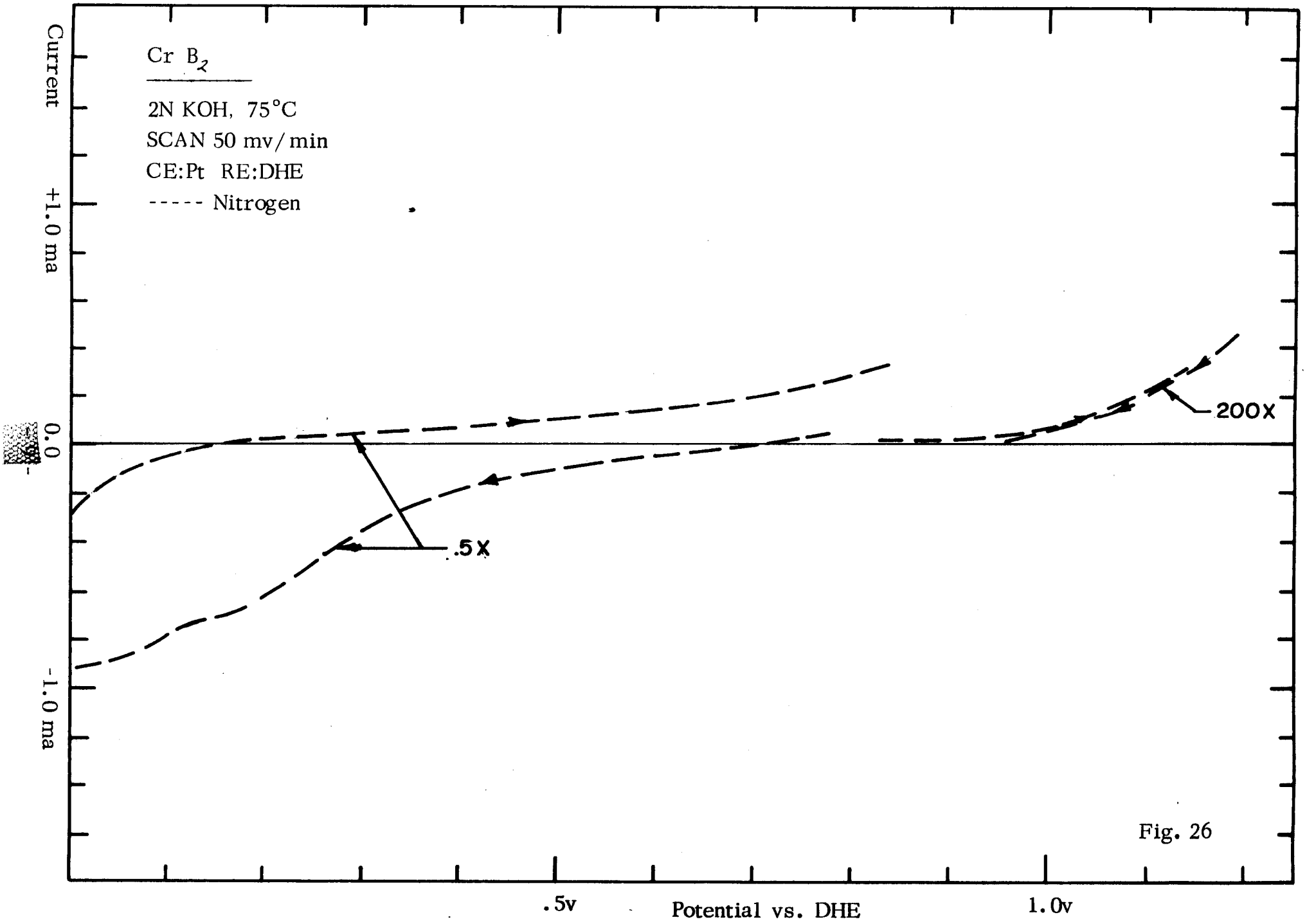
Cr B_2
2N KOH, 75°C
SCAN 50 mv/min
CE:Pt RE:DHE
----- Nitrogen
Current
+1.0 ma
0.0
-1.0 ma
200X
.5X
.5v
Potential vs. DHE
1.0v

Fig. 26

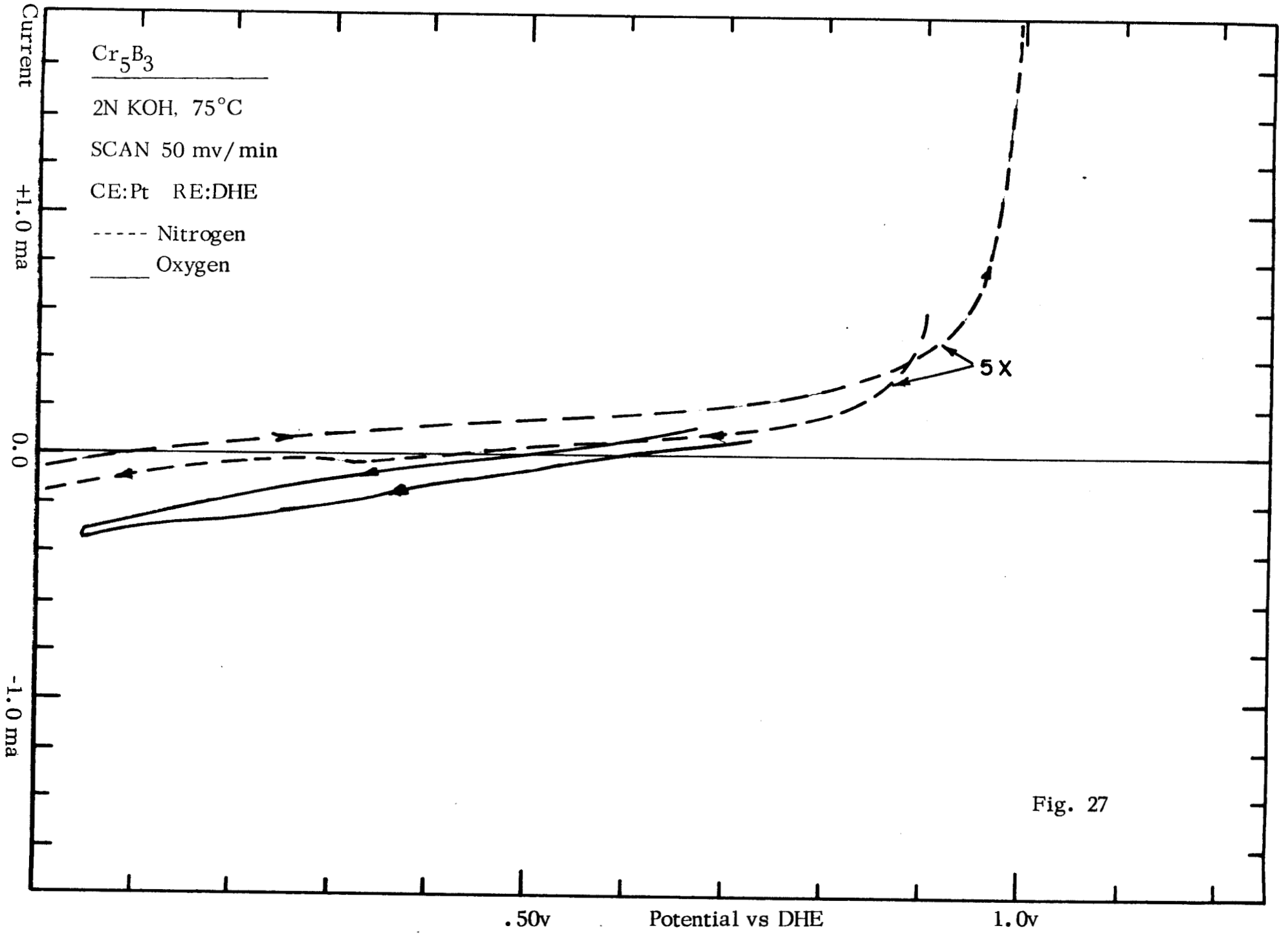
Current
+1.0 ma
0.0
-1.0 ma
Cr_5B_3
2N KOH, 75°C
SCAN 50 mv/min
CE:Pt RE:DHE
----- Nitrogen
_____ Oxygen
5X
.50v
Potential vs DHE
1.0v

Fig. 27

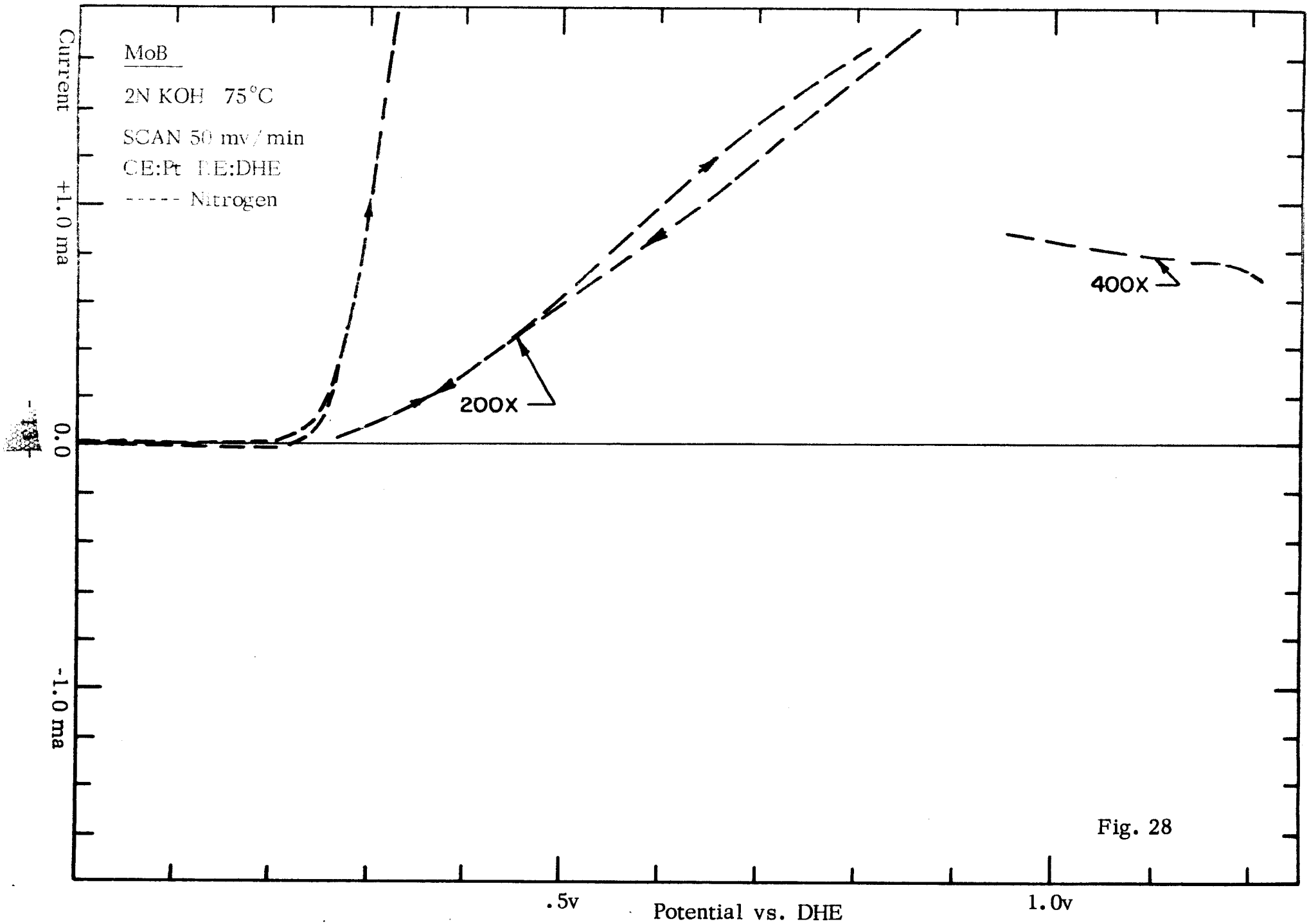
MoB
2N KOH 75°C
SCAN 50 mv/min
CE:Pt RE:DHE
----- Nitrogen
Current
+1.0 ma
0.0
-1.0 ma
200X
400X
.5v
Potential vs. DHE
1.0v

Fig. 28

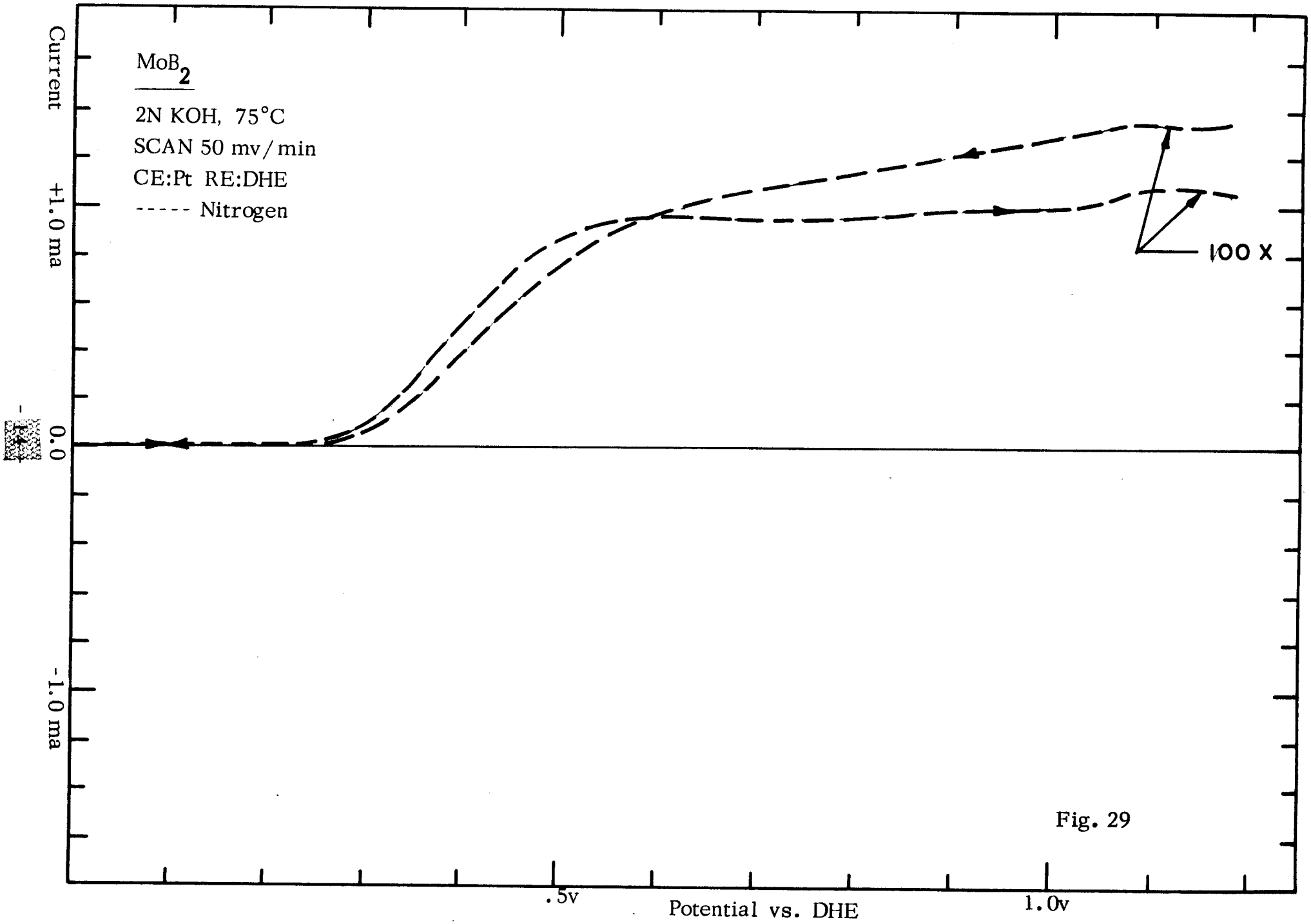
MoB2
2N KOH, 75°C
SCAN 50 mv/min
CE:Pt RE:DHE
----- Nitrogen
100 X
Current
+1.0 ma
0.0
-1.0 ma
.5v
Potential vs. DHE
1.0v

Fig. 29

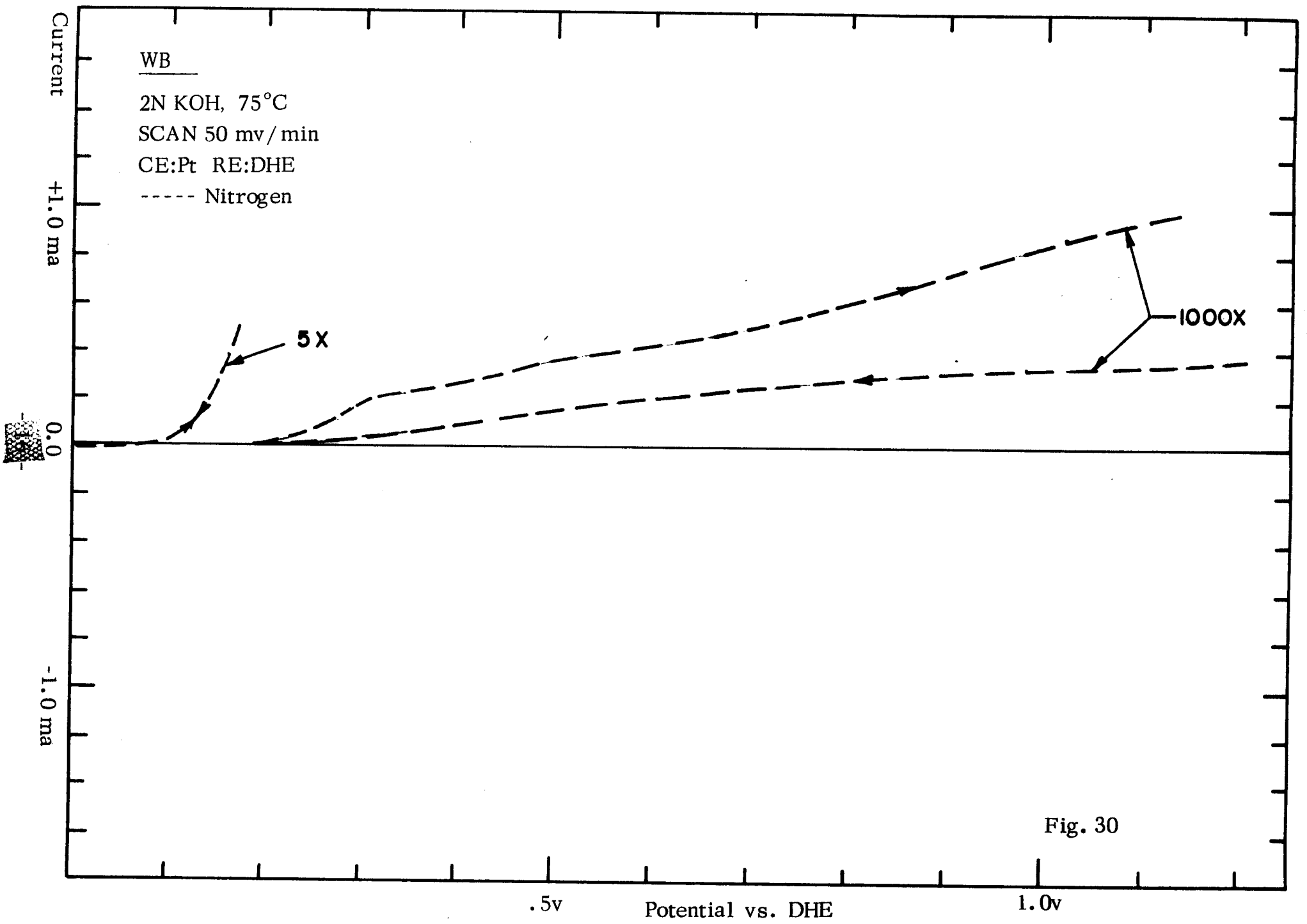
WB
2N KOH, 75°C
SCAN 50 mv/min
CE:Pt RE:DHE
----- Nitrogen
5X
1000X
Current
+1.0 ma
0.0
-1.0 ma
.5v
Potential vs. DHE
1.0v

Fig. 30

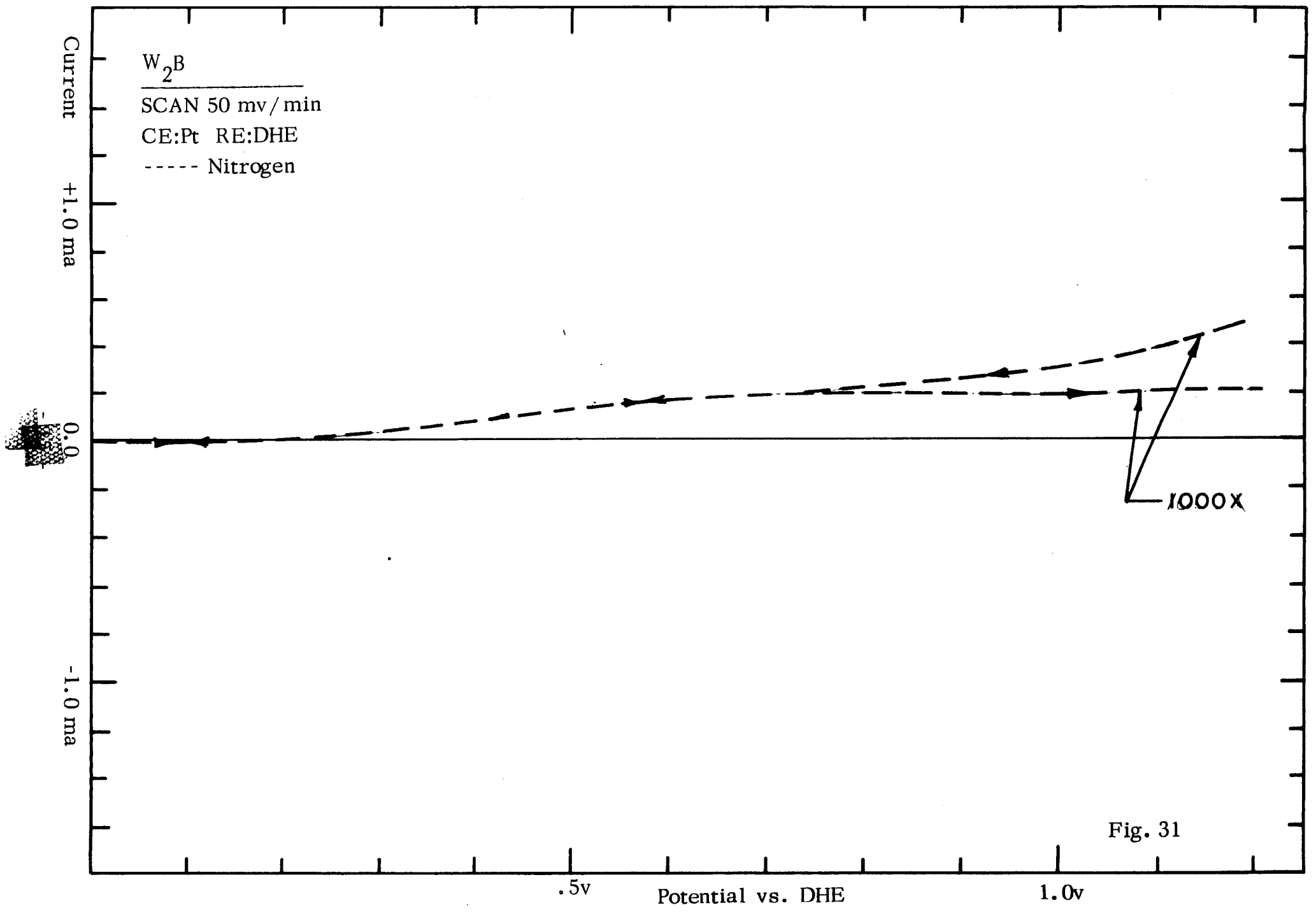
W_2B
SCAN 50 mv/min
CE:Pt RE:DHE
----- Nitrogen
Current
+1.0 ma
0.0
-1.0 ma
1000X
.5v
Potential vs. DHE
1.0v

Fig. 31

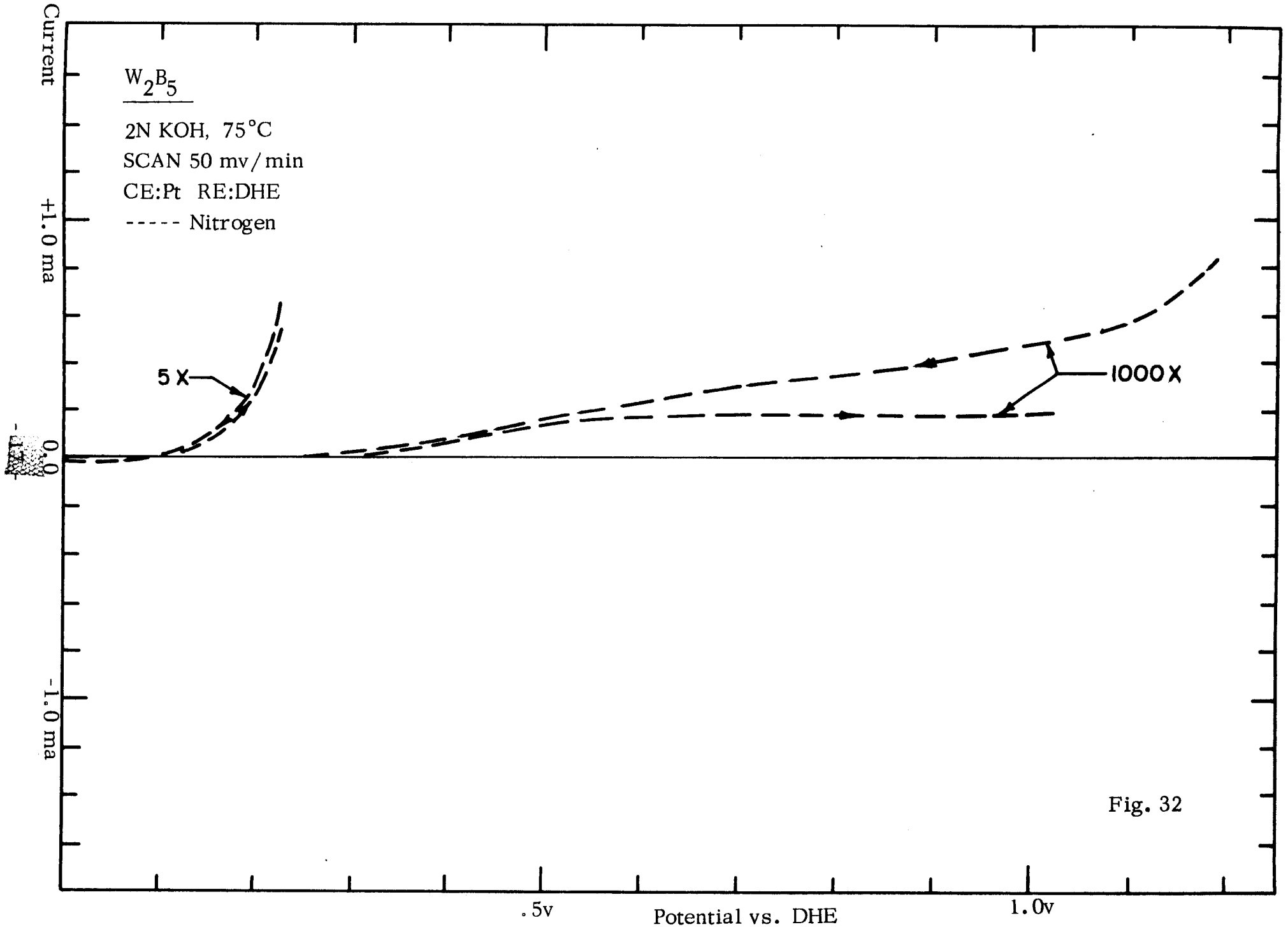
Current
W_2B_5
2N KOH, 75°C
SCAN 50 mv/min
CE:Pt RE:DHE
----- Nitrogen
+1.0 ma
0.0
-1.0 ma
5X
1000X
.5v
Potential vs. DHE
1.0v

Fig. 32

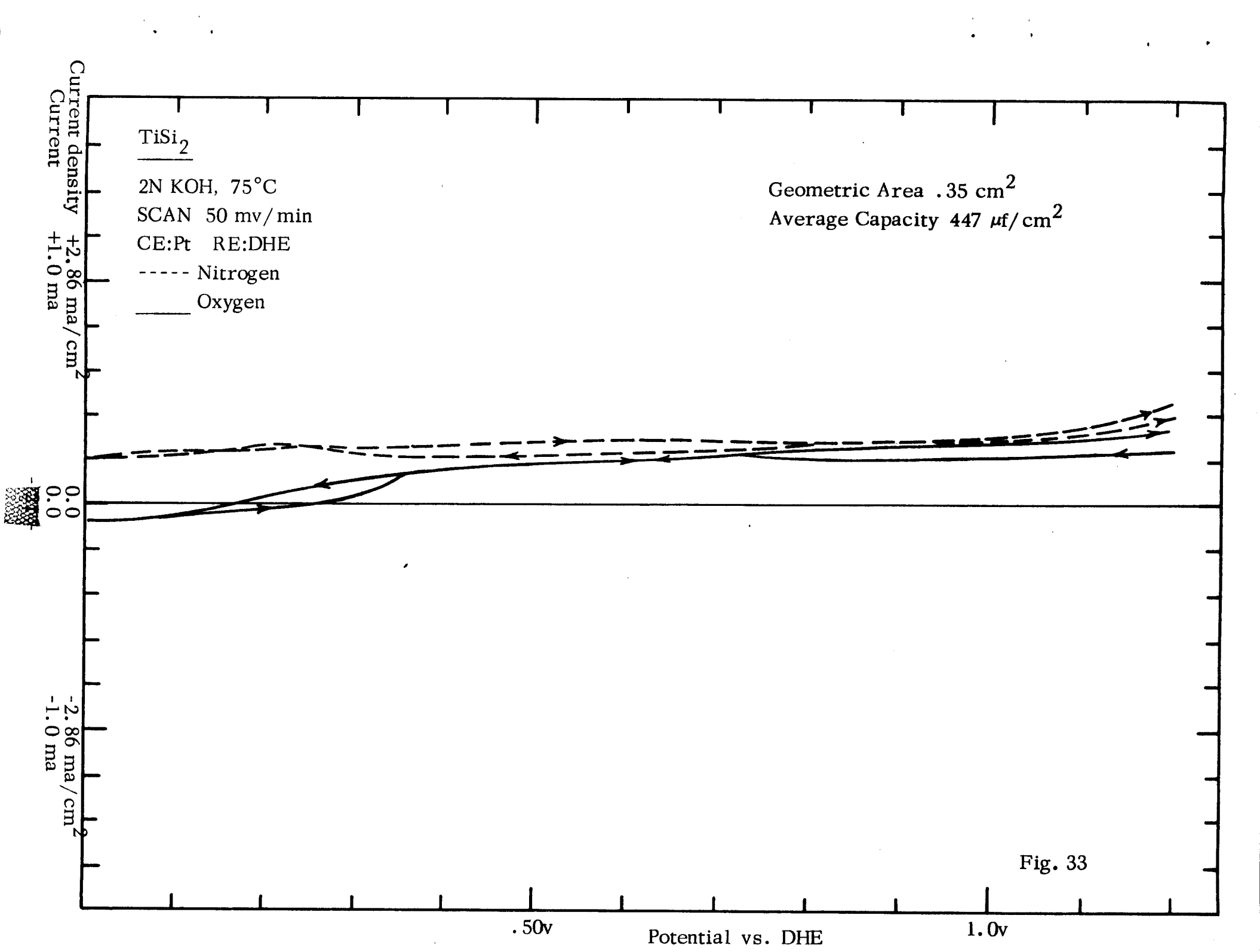
Current density
Current
+2.86 ma/cm²
+1.0 ma
0.0
0.0
-2.86 ma/cm²
-1.0 ma
TiSi2
2N KOH, 75°C
SCAN 50 mv/min
CE:Pt RE:DHE
----- Nitrogen
_____ Oxygen
Geometric Area .35 cm²
Average Capacity 447 μf/cm²
.50v
Potential vs. DHE
1.0v

Fig. 33

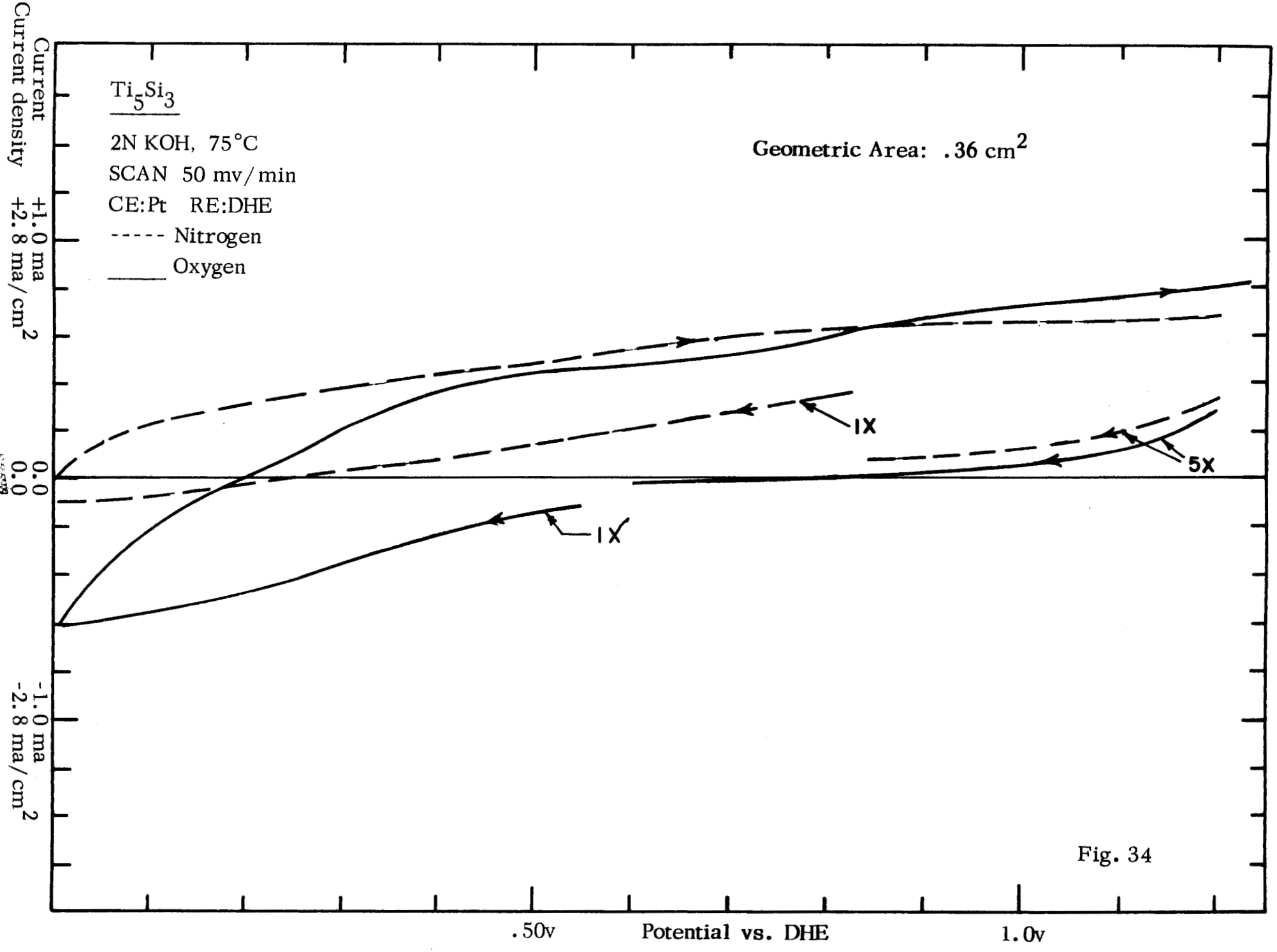
Current density
Current
+1.0 ma
+2.8 ma/cm2
0.0
0.0
-1.0 ma
-2.8 ma/cm2
Ti5Si3
2N KOH, 75°C
SCAN 50 mv/min
CE:Pt RE:DHE
----- Nitrogen
_____ Oxygen
Geometric Area: .36 cm2
1X
5X
1X
.50v
Potential vs. DHE
1.0v

Fig. 34

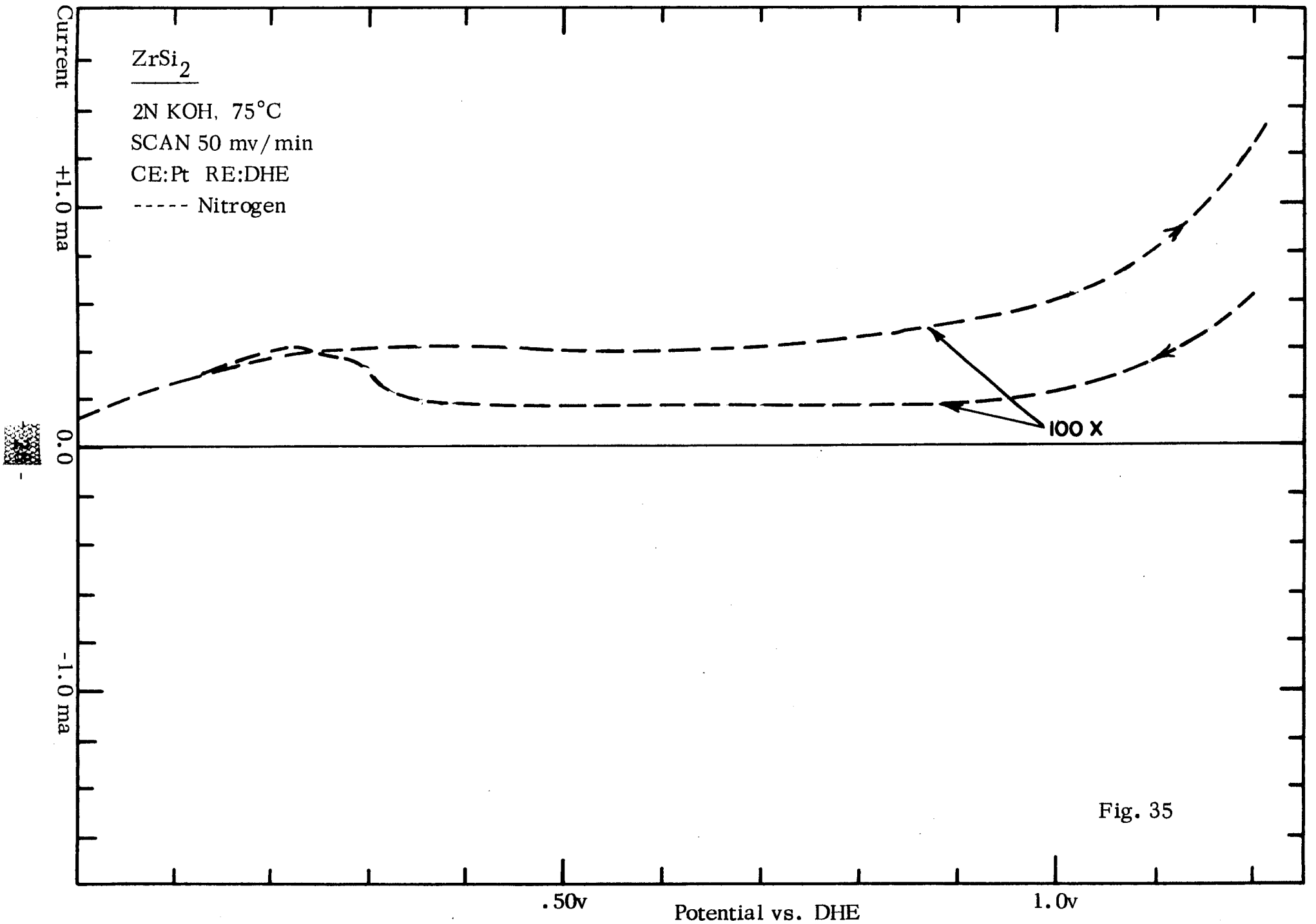
Current
$ZrSi_2$
2N KOH, 75°C
SCAN 50 mv/min
CE:Pt RE:DHE
----- Nitrogen
+1.0 ma
0.0
-1.0 ma
100 X
.50v
Potential vs. DHE
1.0v

Fig. 35

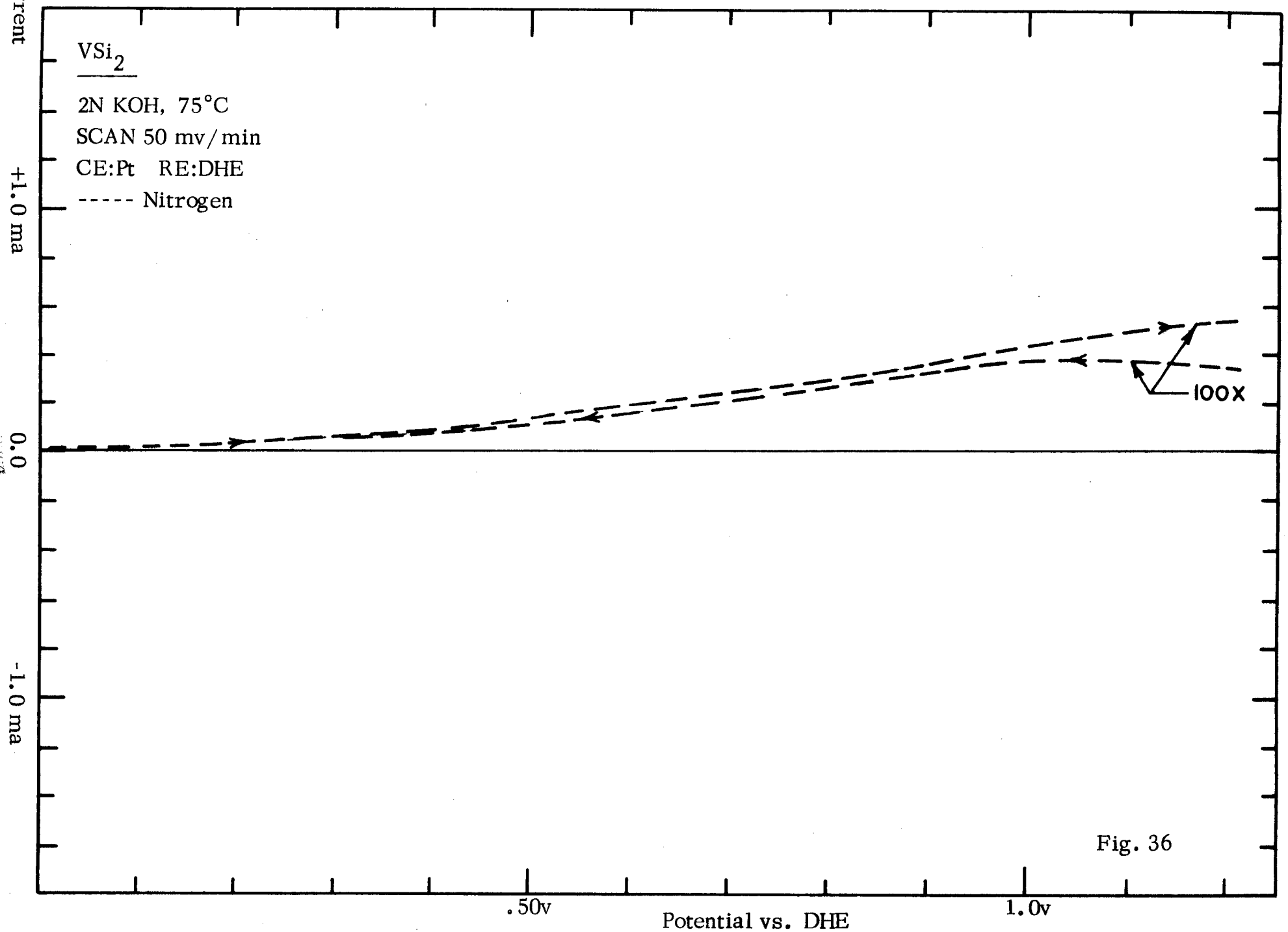
Current
+1.0 ma
0.0
-1.0 ma
VSi2
2N KOH, 75°C
SCAN 50 mv/min
CE:Pt RE:DHE
----- Nitrogen
100X
.50v
1.0v
Potential vs. DHE

Fig. 36

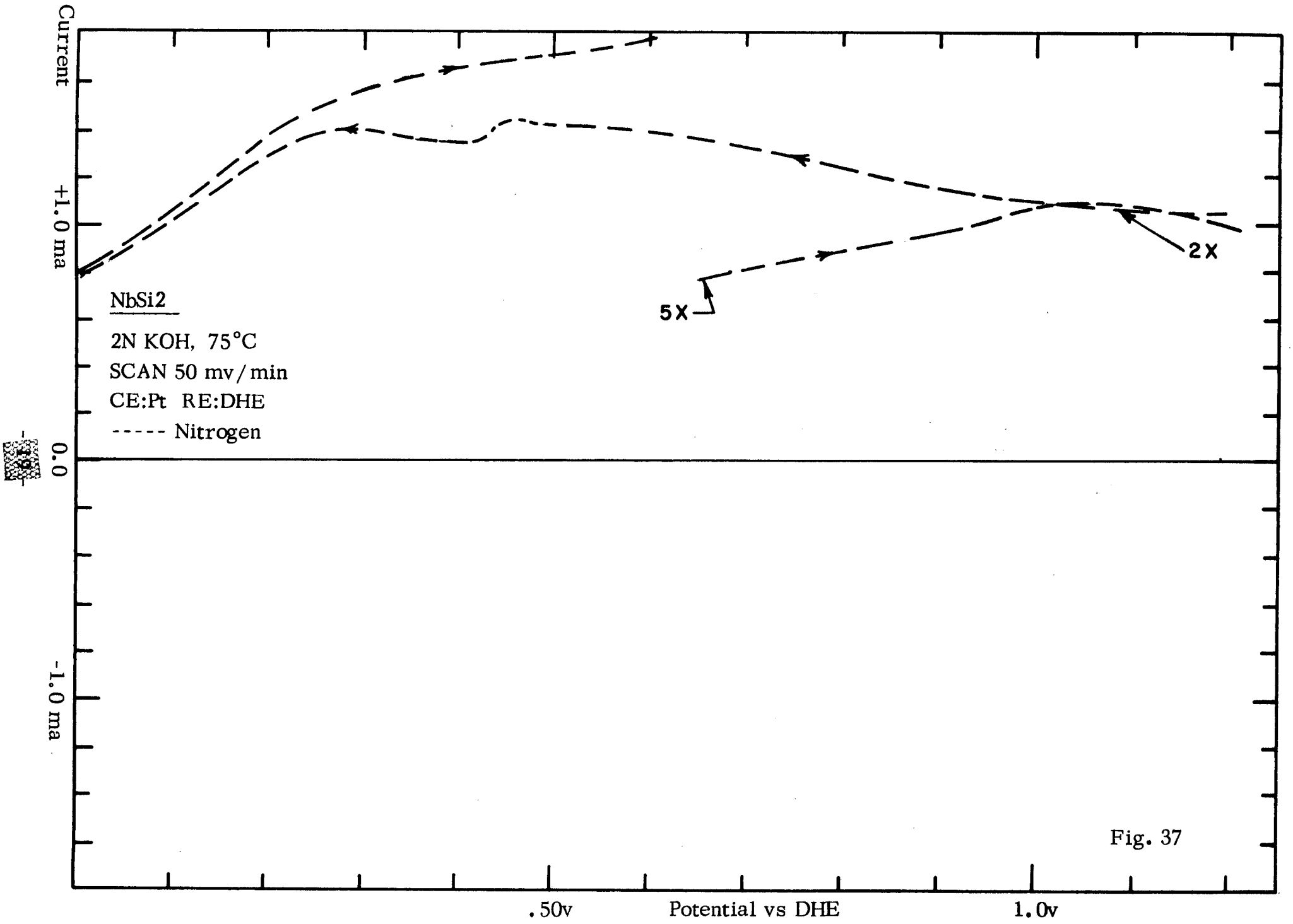
Current
+1.0 ma
0.0
-1.0 ma
NbSi2
2N KOH, 75°C
SCAN 50 mv/min
CE:Pt RE:DHE
----- Nitrogen
5X
2X
.50v
Potential vs DHE
1.0v

Fig. 37

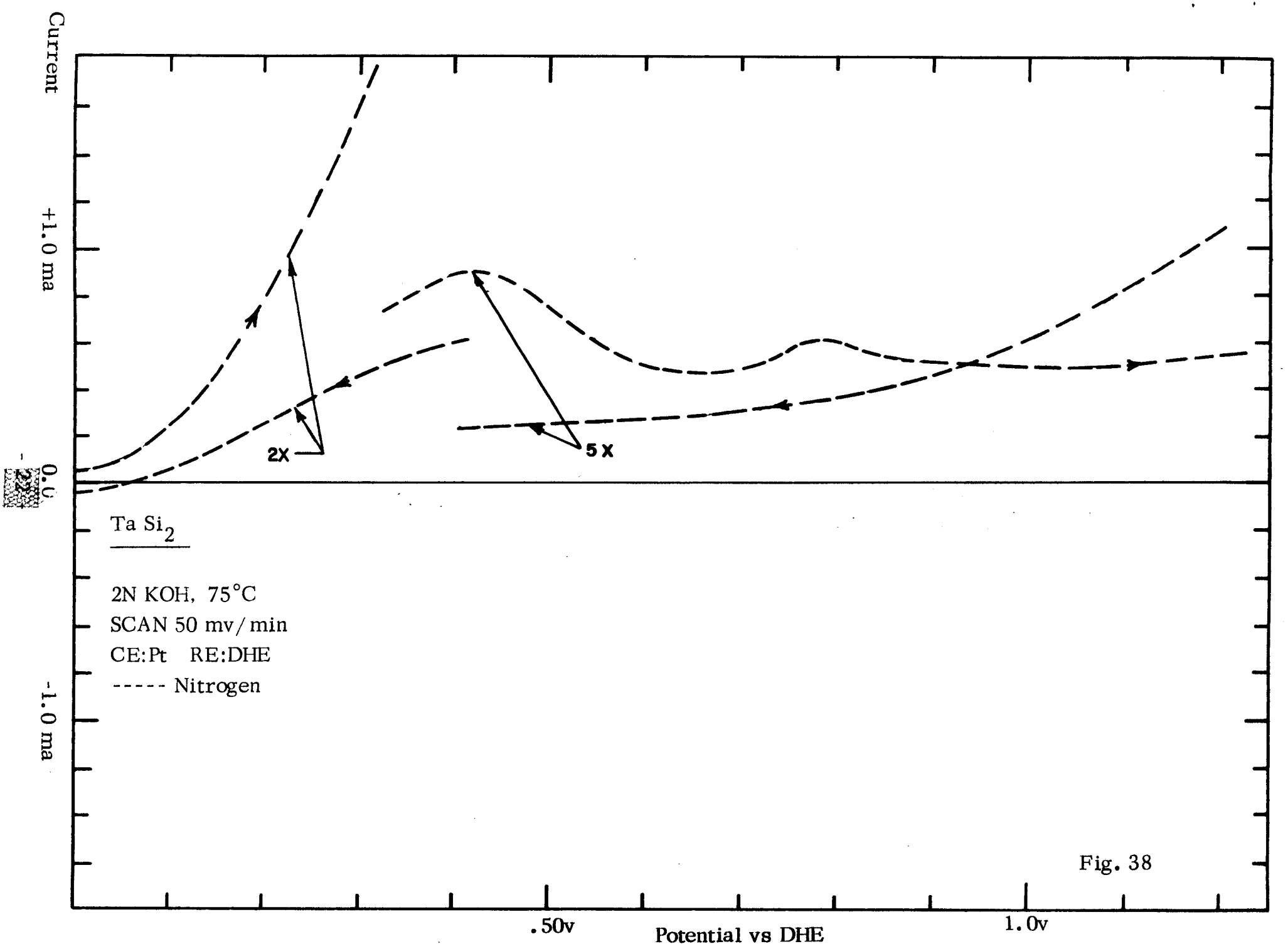
Current
+1.0 ma
0.0
-1.0 ma
2X
5 X
Ta Si2
2N KOH, 75°C
SCAN 50 mv/min
CE:Pt RE:DHE
----- Nitrogen
.50v
Potential vs DHE
1.0v

Fig. 38

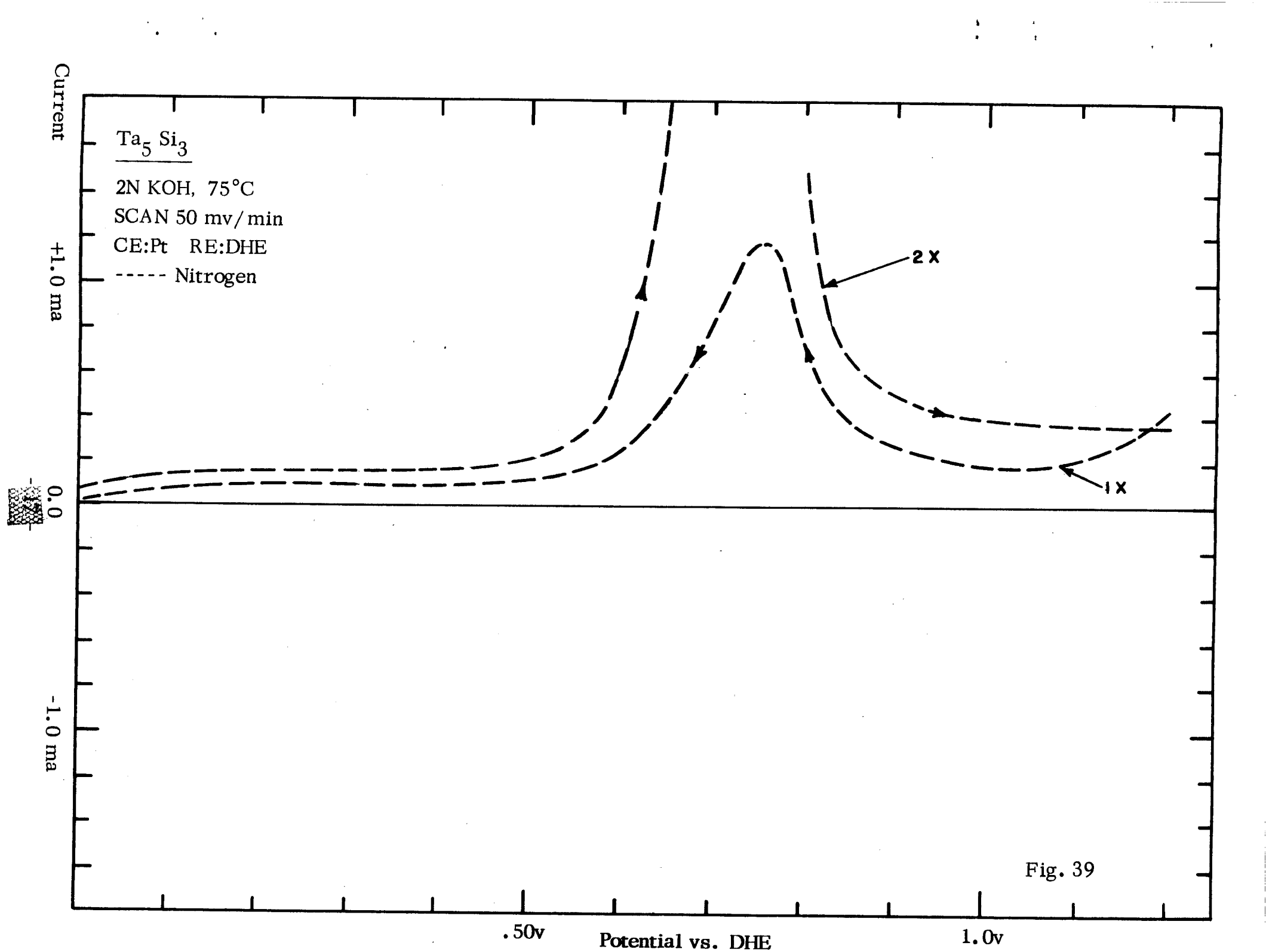
Current
+1.0 ma
0.0
-1.0 ma
$Ta_5 Si_3$
2N KOH, 75°C
SCAN 50 mv/min
CE:Pt RE:DHE
----- Nitrogen
2 X
1 X
.50v
Potential vs. DHE
1.0v

Fig. 39

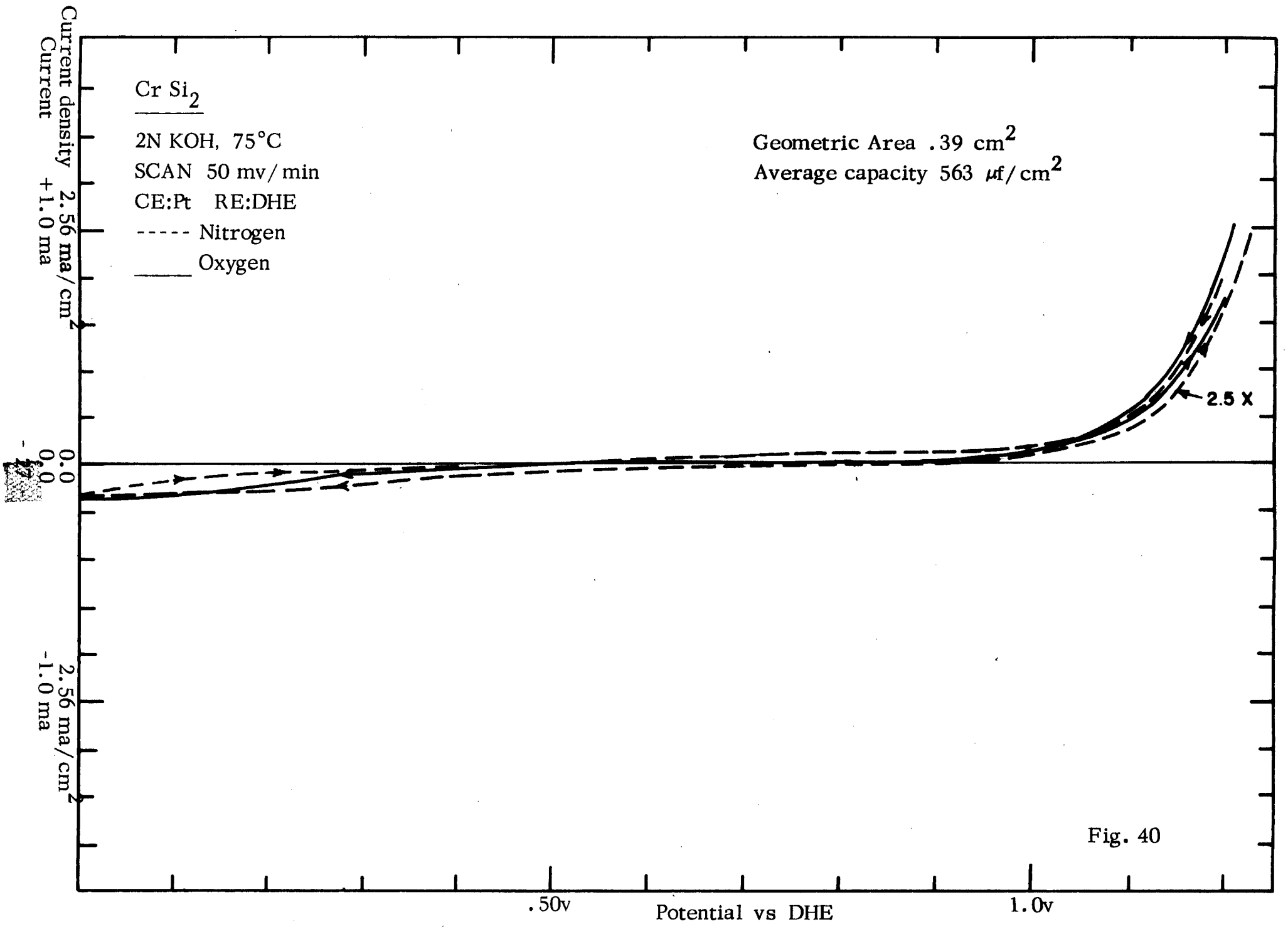
Cr Si_2
2N KOH, 75°C
SCAN 50 mv/min
CE:Pt RE:DHE
----- Nitrogen
_____ Oxygen
Geometric Area .39 cm^2
Average capacity 563 $\mu f/cm^2$
2.5 X
Current density
Current
+1.0 ma
2.56 ma/cm^2
0.0
0.0
-1.0 ma
2.56 ma/cm^2
.50v
Potential vs DHE
1.0v

Fig. 40

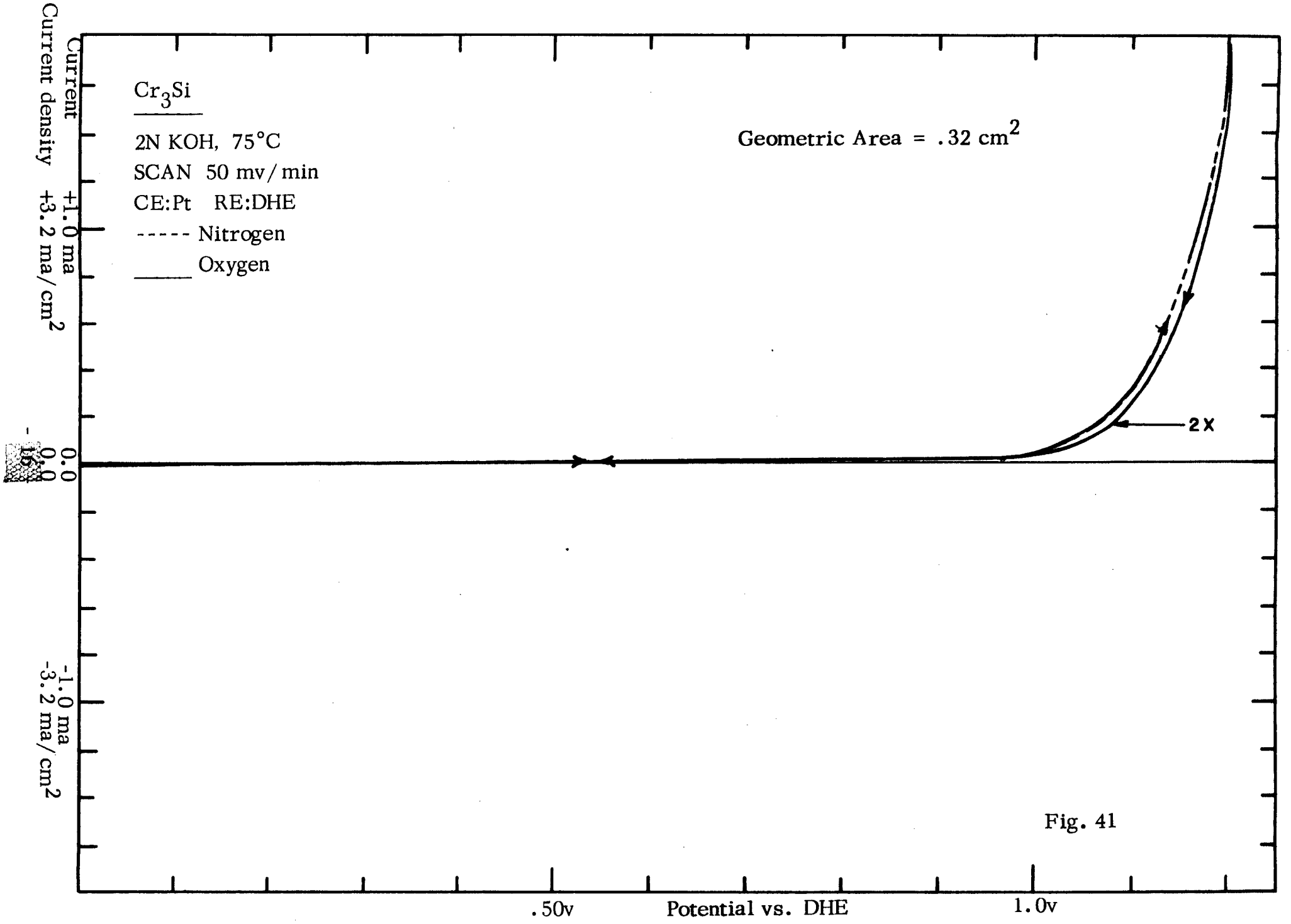
Current density
Current
+1.0 ma
+3.2 ma/cm2
0.0
0.0
-1.0 ma
-3.2 ma/cm2
Cr3Si
2N KOH, 75°C
SCAN 50 mv/min
CE:Pt RE:DHE
----- Nitrogen
_____ Oxygen
Geometric Area = .32 cm2
2X
.50v
Potential vs. DHE
1.0v

Fig. 41

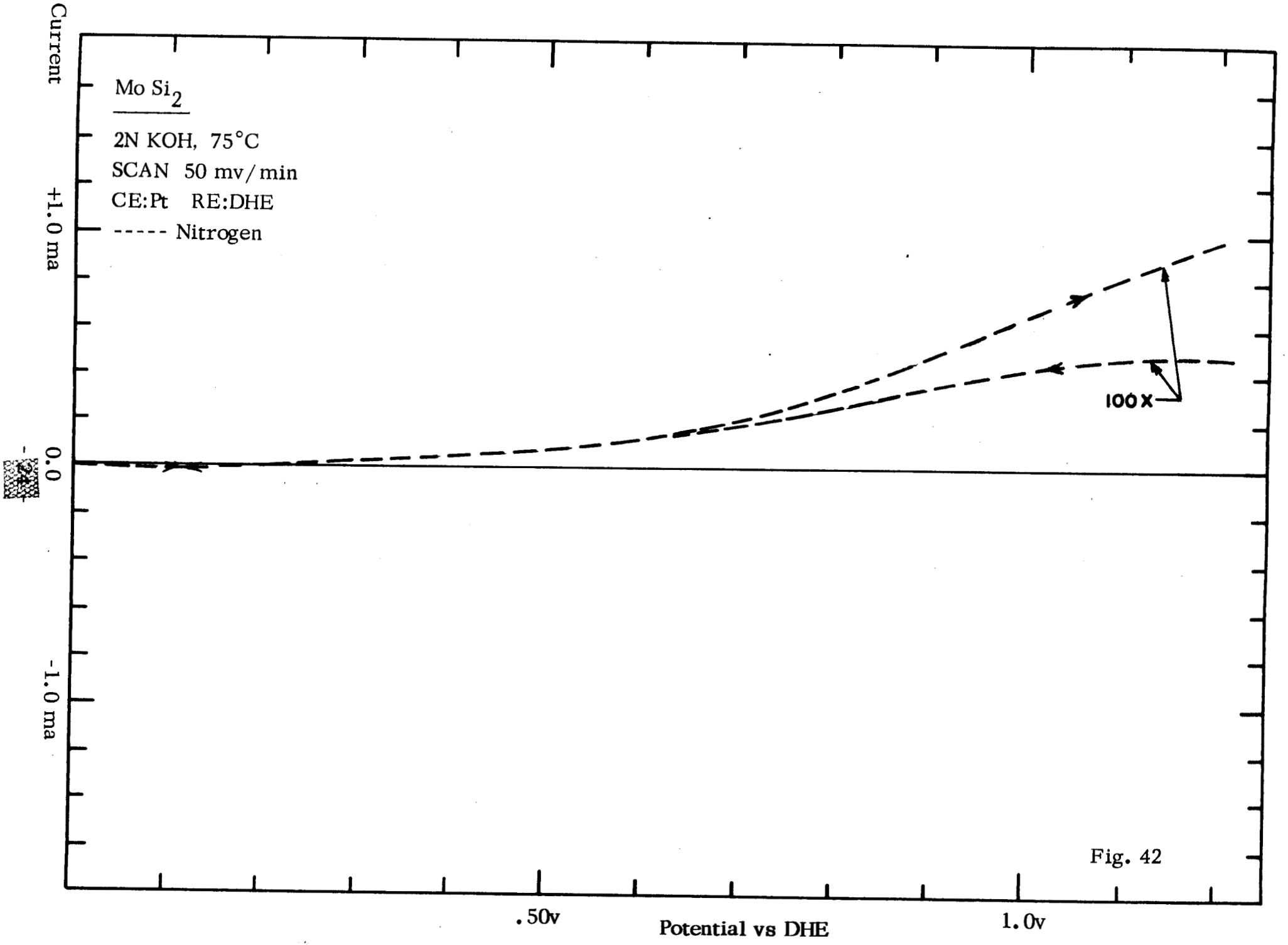
Current
+1.0 ma
0.0
-1.0 ma
Mo Si2
2N KOH, 75°C
SCAN 50 mv/min
CE:Pt RE:DHE
----- Nitrogen
100 X
.50v
Potential vs DHE
1.0v

Fig. 42

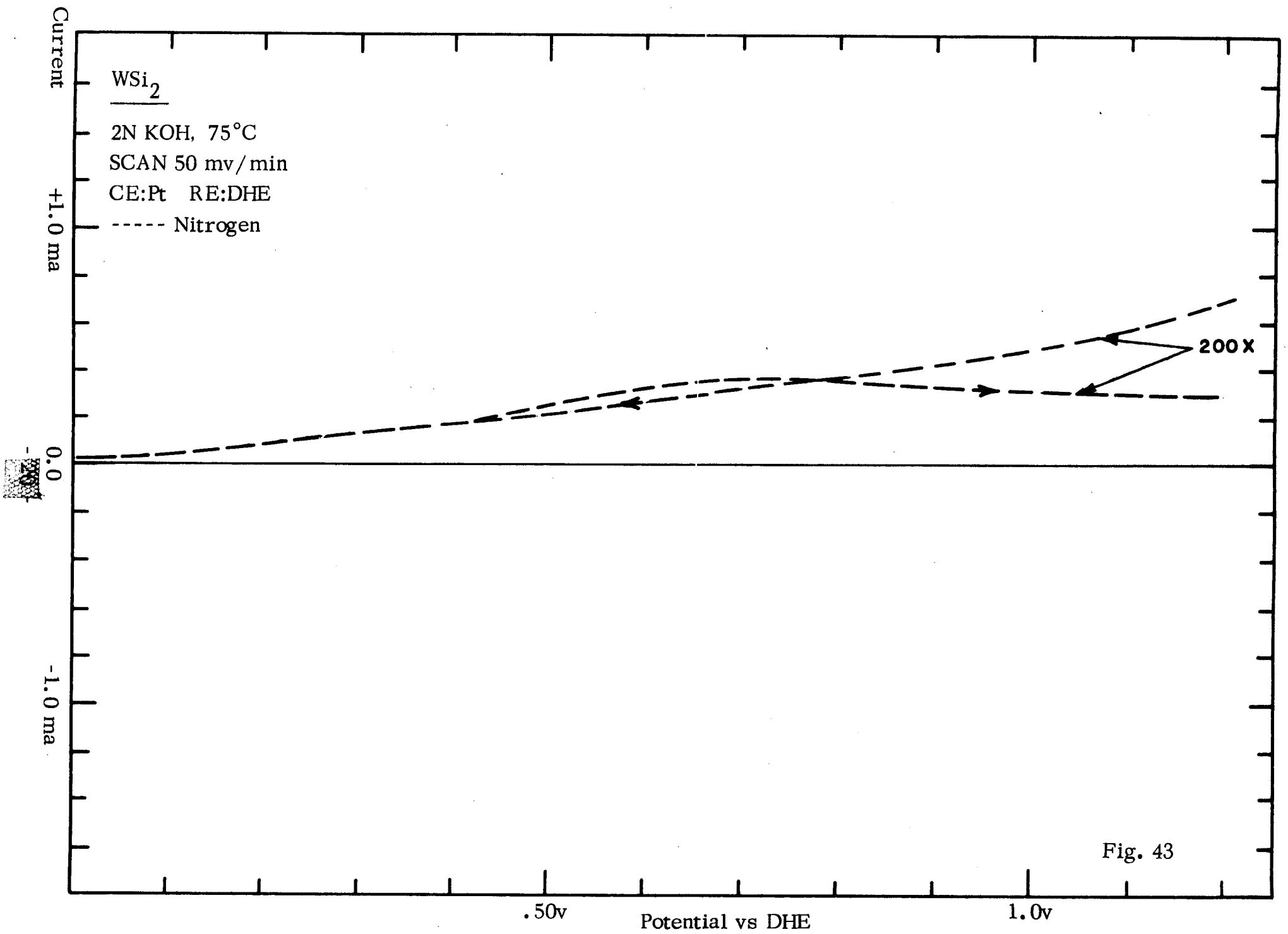
Current
WSi2
2N KOH, 75°C
SCAN 50 mv/min
CE:Pt RE:DHE
----- Nitrogen
+1.0 ma
0.0
-1.0 ma
200X
.50v
Potential vs DHE
1.0v

Fig. 43

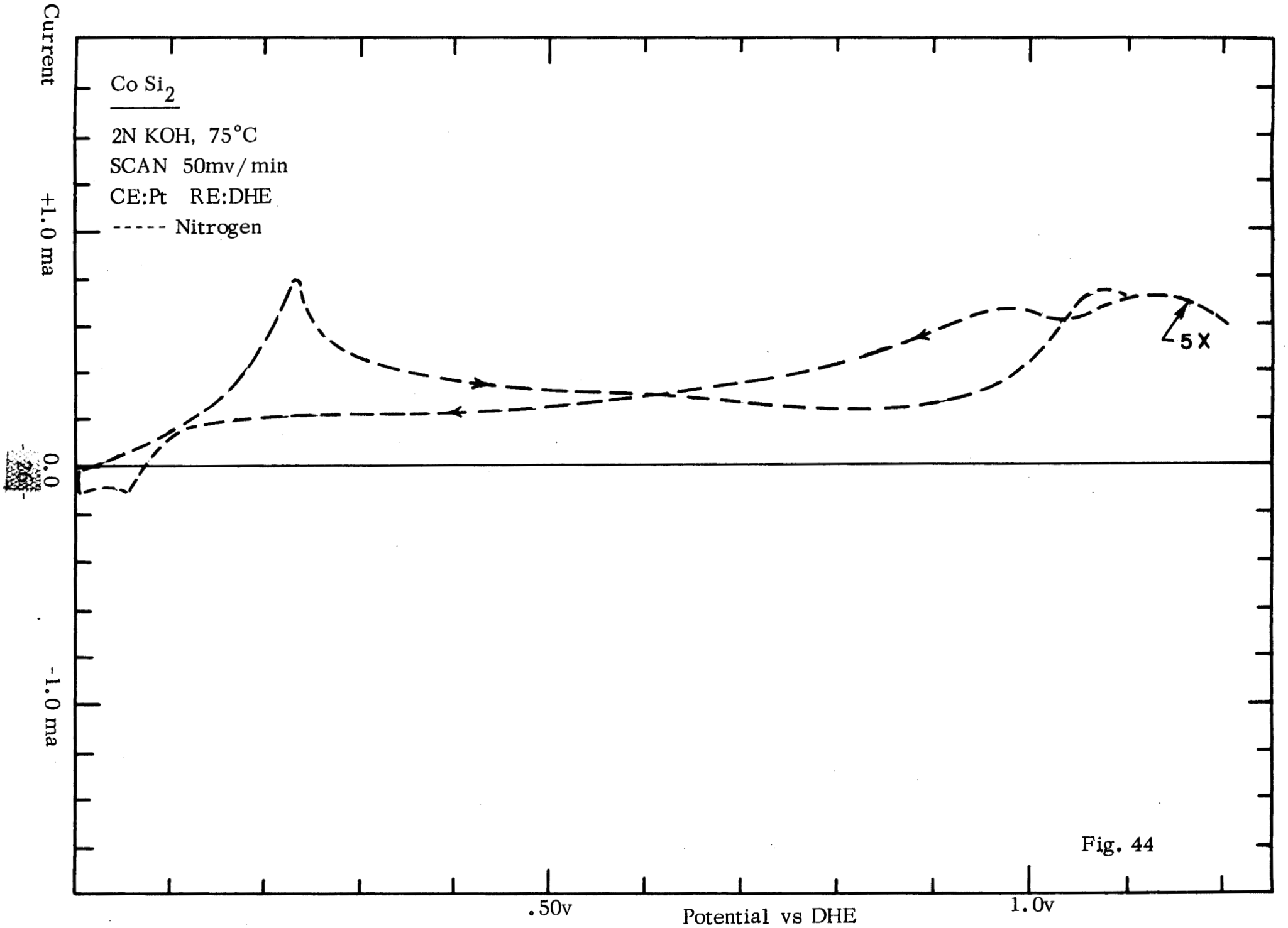
Current
+1.0 ma
0.0
-1.0 ma
Co Si2
2N KOH, 75°C
SCAN 50mv/min
CE:Pt RE:DHE
----- Nitrogen
5X
.50v
Potential vs DHE
1.0v

Fig. 44

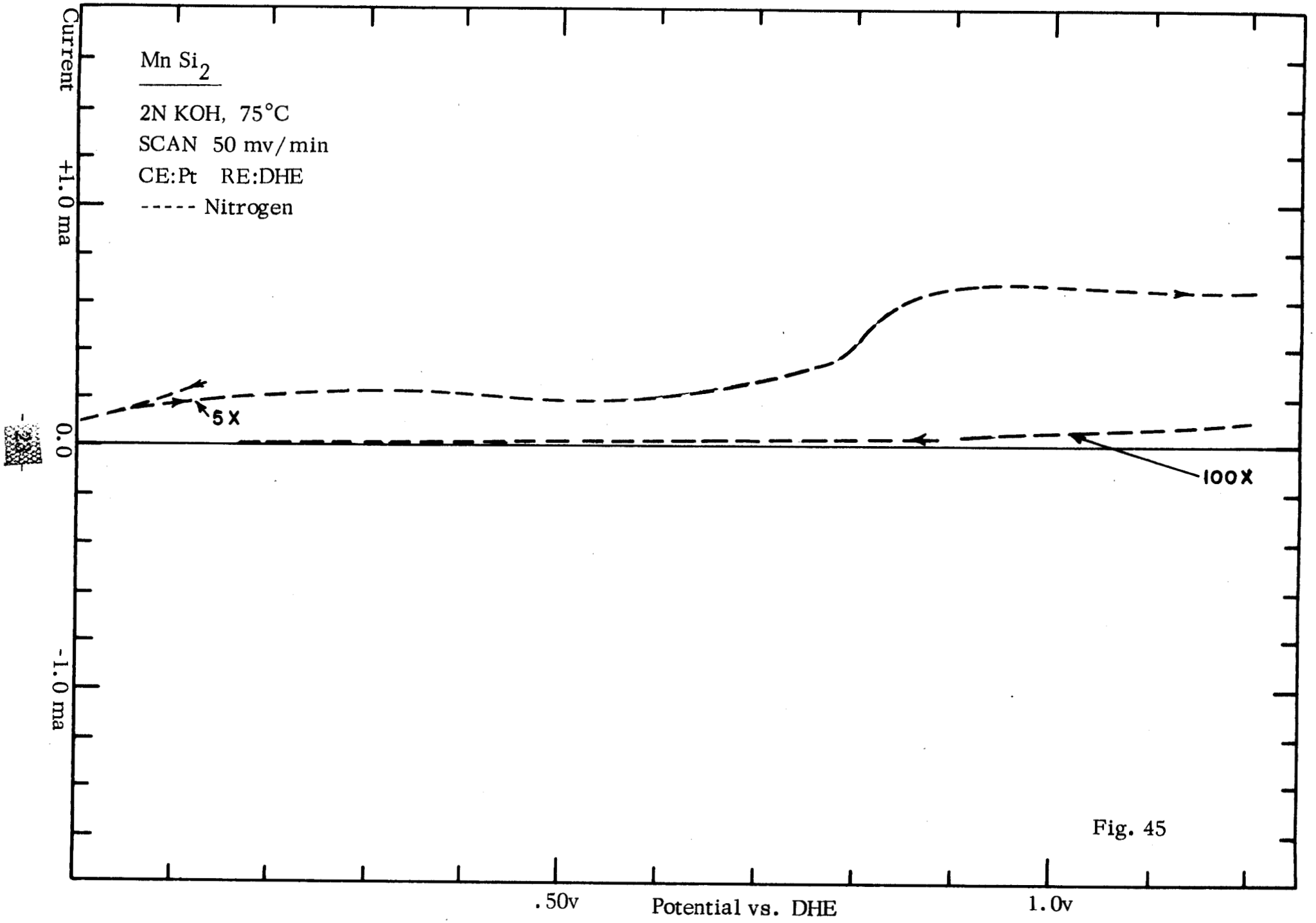
Current
+1.0 ma
0.0
-1.0 ma
Mn Si2
2N KOH, 75°C
SCAN 50 mv/min
CE:Pt RE:DHE
----- Nitrogen
5X
100X
.50v
Potential vs. DHE
1.0v

Fig. 45

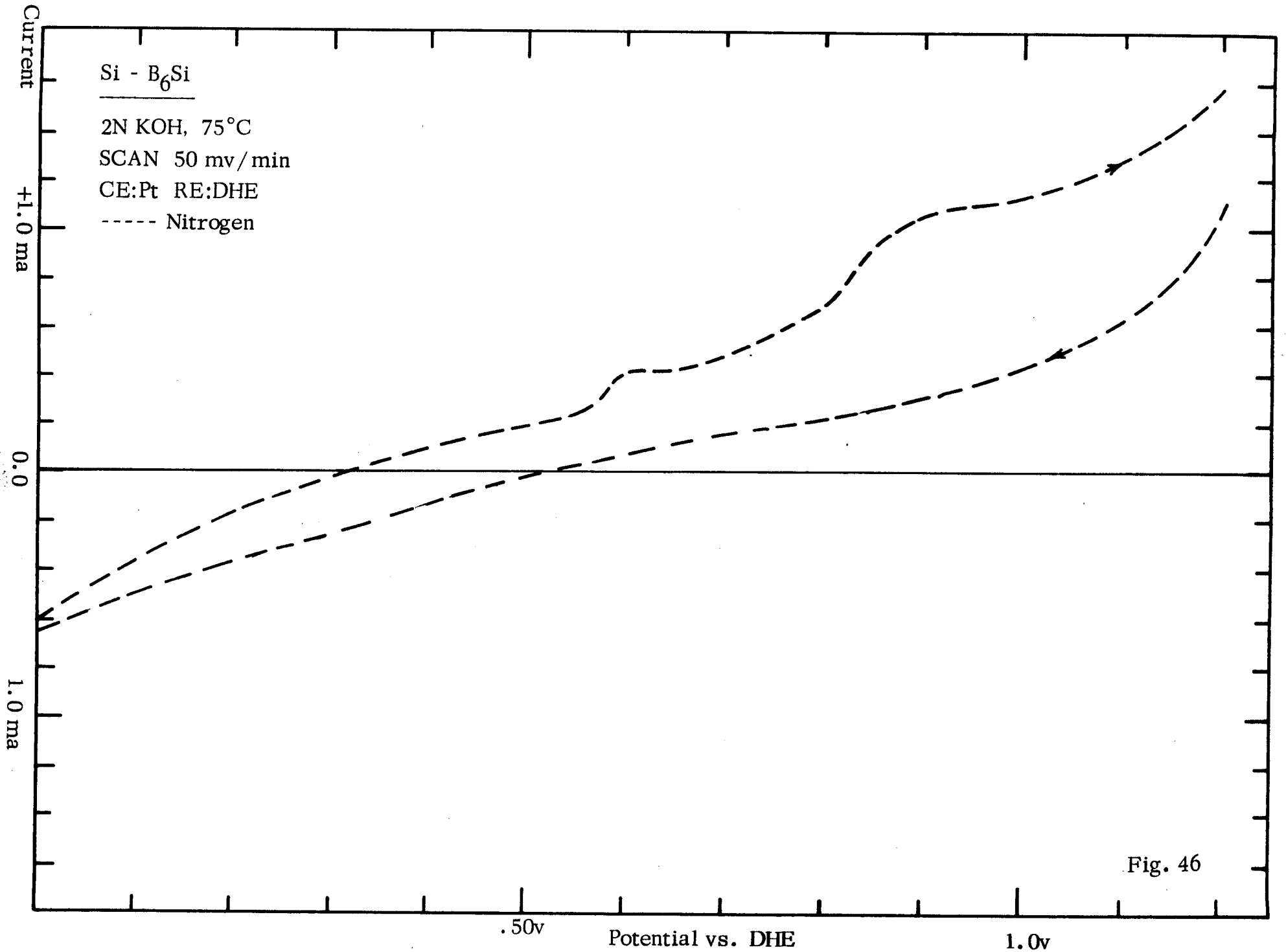
Current
Si - B_6Si
2N KOH, 75°C
SCAN 50 mv/min
CE:Pt RE:DHE
----- Nitrogen
+1.0 ma
0.0
1.0 ma
.50v
Potential vs. DHE
1.0v

Fig. 46

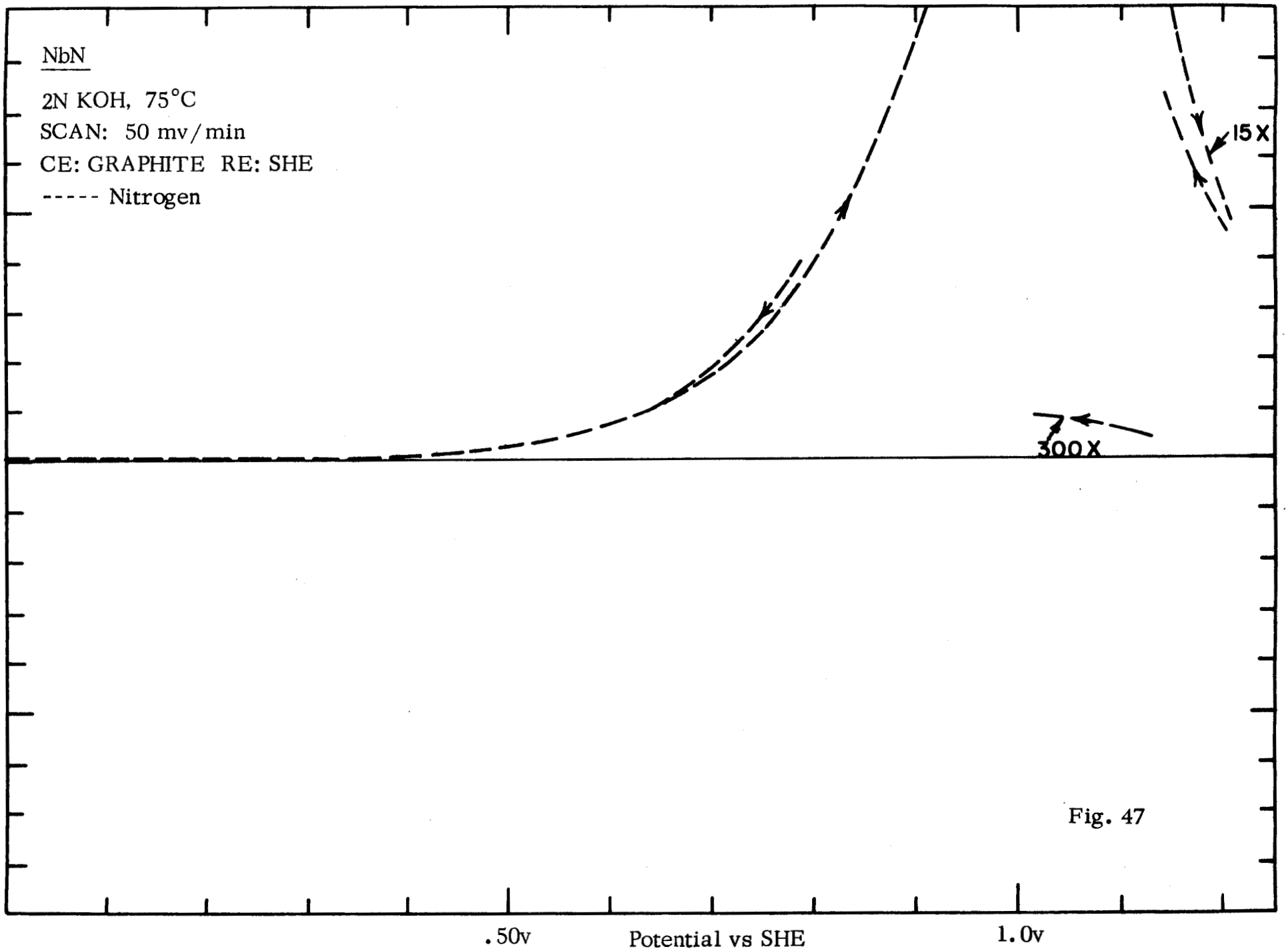
NbN
2N KOH, 75°C
SCAN: 50 mv/min
CE: GRAPHITE RE: SHE
----- Nitrogen
15X
300X
Current
+1.0 ma
0.0
-1.0 ma
.50v
Potential vs SHE
1.0v

Fig. 47

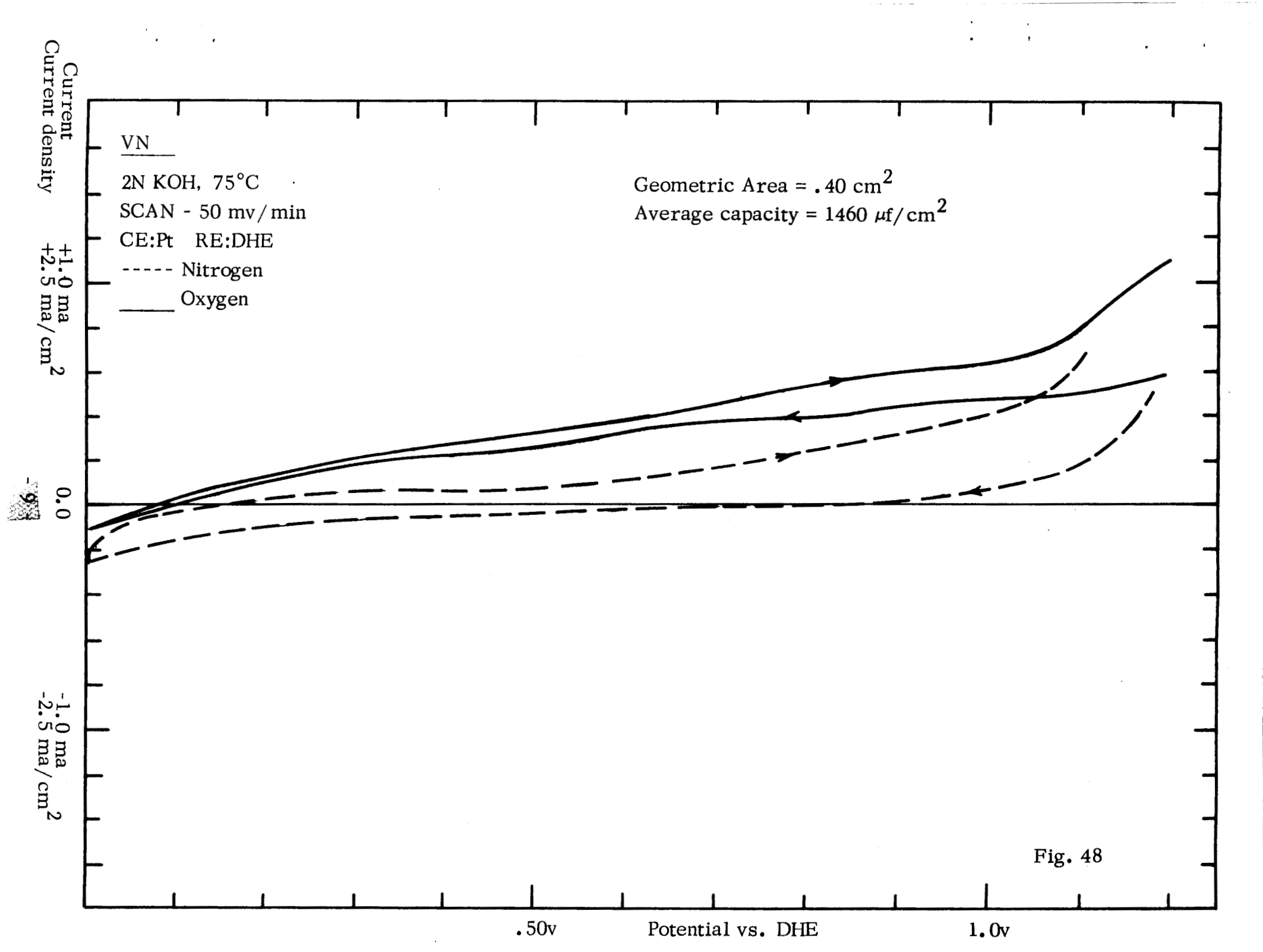
VN
2N KOH, 75°C
SCAN - 50 mv/min
CE:Pt RE:DHE
----- Nitrogen
_____ Oxygen
Geometric Area = .40 cm2
Average capacity = 1460 μf/cm2
Current density
+1.0 ma
+2.5 ma/cm2
0.0
-1.0 ma
-2.5 ma/cm2
.50v
Potential vs. DHE
1.0v

Fig. 48

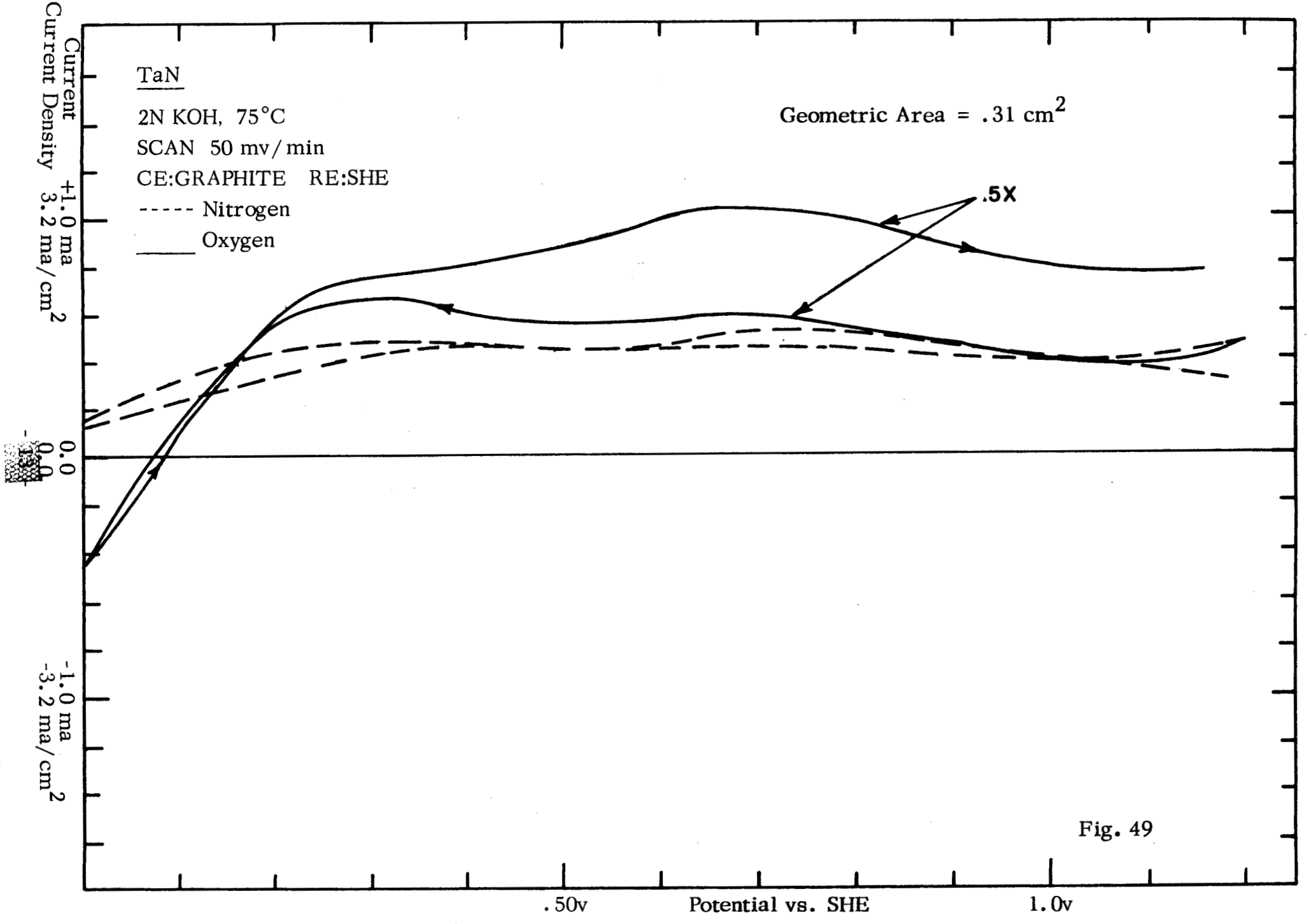
TaN
2N KOH, 75°C
SCAN 50 mv/min
CE:GRAPHITE RE:SHE
----- Nitrogen
_____ Oxygen
Geometric Area = .31 cm2
.5X
Current Density
Current
+1.0 ma
3.2 ma/cm2
0.0
0.0
-1.0 ma
-3.2 ma/cm2
.50v
Potential vs. SHE
1.0v

Fig. 49

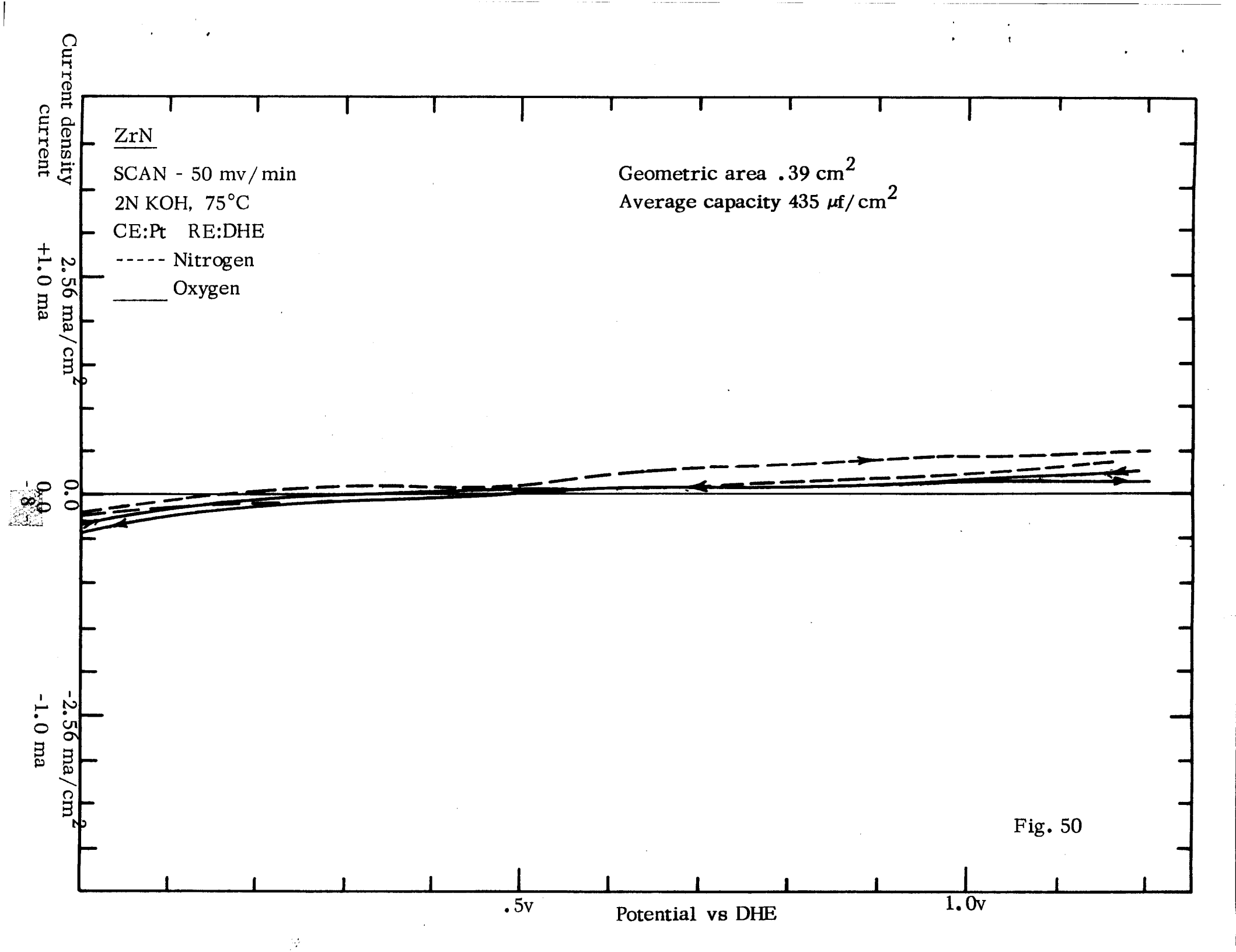
Current density
current
ZrN
SCAN - 50 mv/min
2N KOH, 75°C
CE:Pt RE:DHE
----- Nitrogen
_____ Oxygen
Geometric area .39 cm2
Average capacity 435 μf/cm2
+1.0 ma
2.56 ma/cm2
0.0
0.0
-8
-2.56 ma/cm2
-1.0 ma
.5v
Potential vs DHE
1.0v

Fig. 50

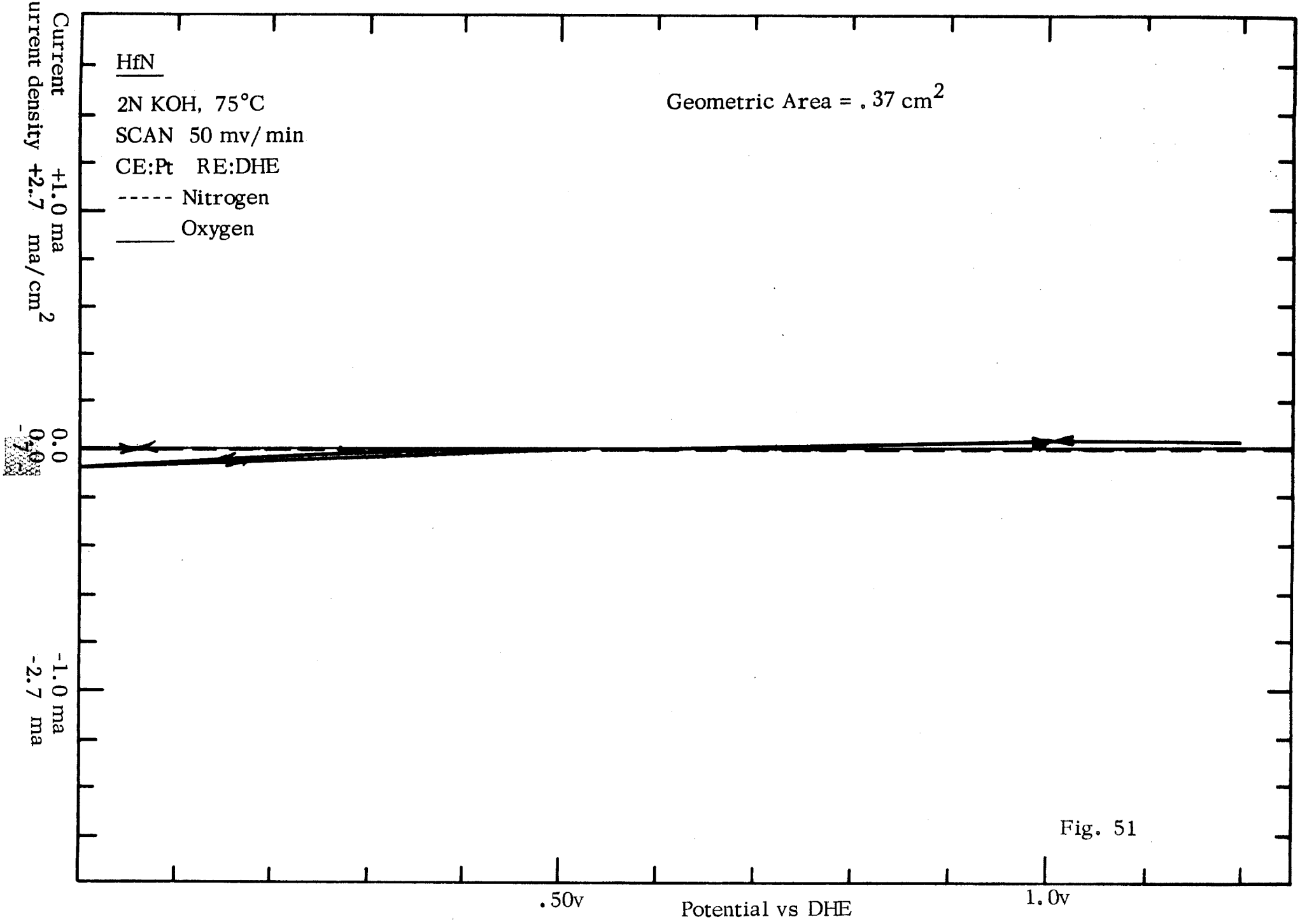
HfN
2N KOH, 75°C
SCAN 50 mv/min
CE:Pt RE:DHE
----- Nitrogen
_____ Oxygen
Geometric Area = .37 cm2
Current
Current density +2.7 ma/cm2
+1.0 ma
0.0
-1.0 ma
-2.7 ma
.50v
Potential vs DHE
1.0v

Fig. 51

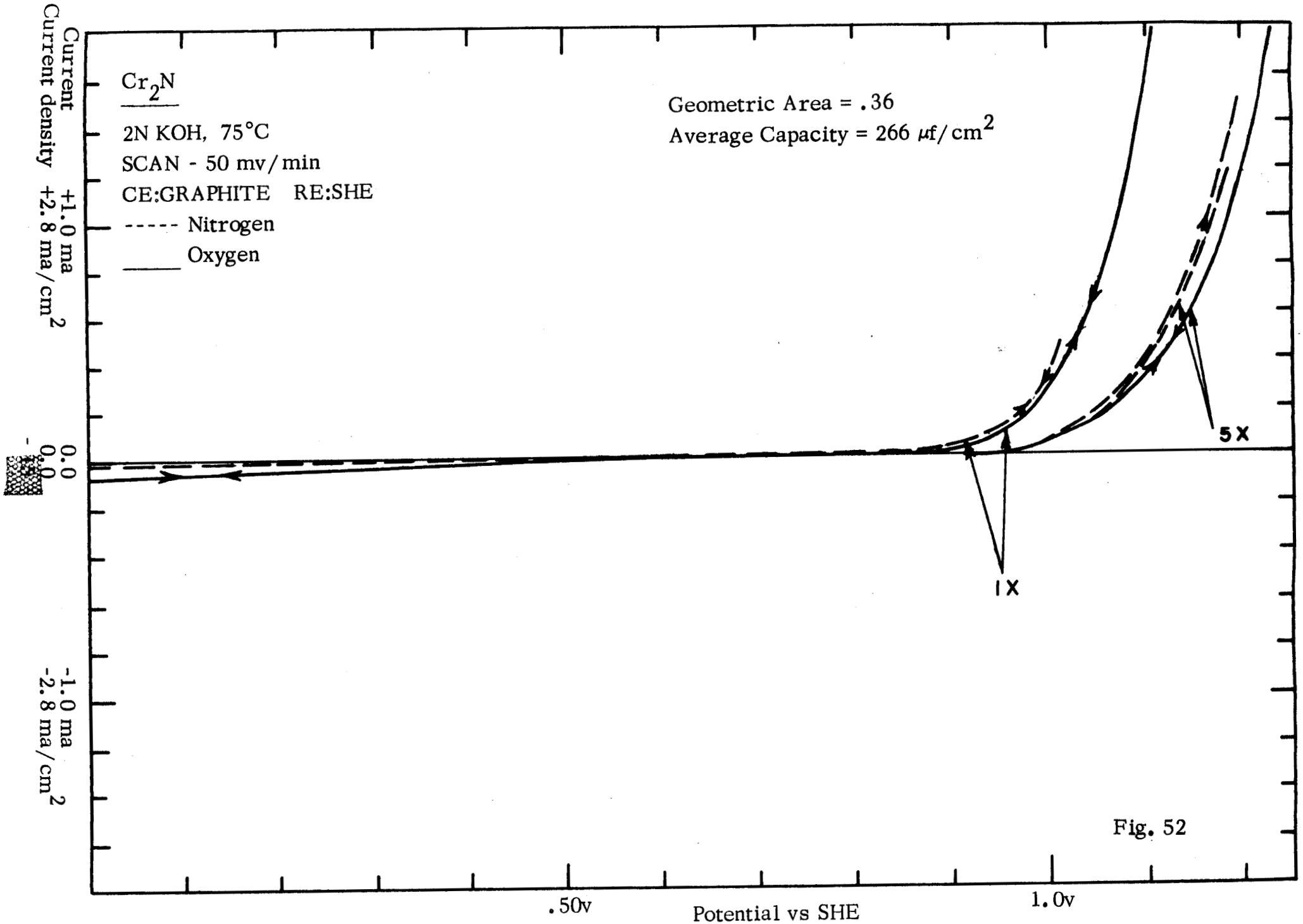
Current
Current density +1.0 ma +2.8 ma/cm2
0.0
0.0
-1.0 ma -2.8 ma/cm2
Cr2N
2N KOH, 75°C
SCAN - 50 mv/min
CE:GRAPHITE RE:SHE
----- Nitrogen
_____ Oxygen
Geometric Area = .36
Average Capacity = 266 μf/cm2
5X
1X
.50v
Potential vs SHE
1.0v

Fig. 52

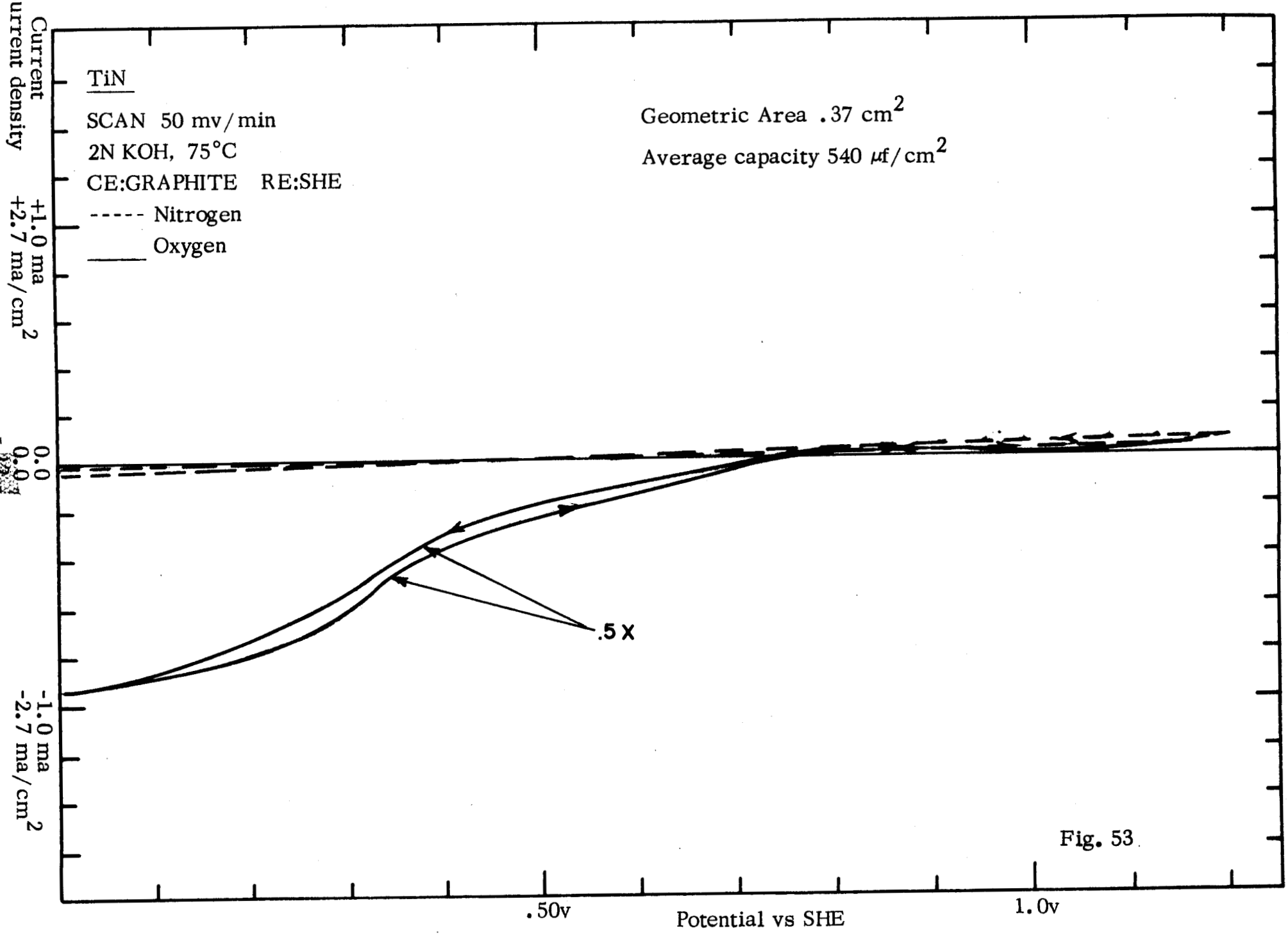
TiN
SCAN 50 mv/min
2N KOH, 75°C
CE:GRAPHITE RE:SHE
----- Nitrogen
_____ Oxygen
Geometric Area .37 cm2
Average capacity 540 μf/cm2
Current
Current density
+1.0 ma
+2.7 ma/cm2
0.0
0.0
-1.0 ma
-2.7 ma/cm2
.5 X
.50v
Potential vs SHE
1.0v

Fig. 53

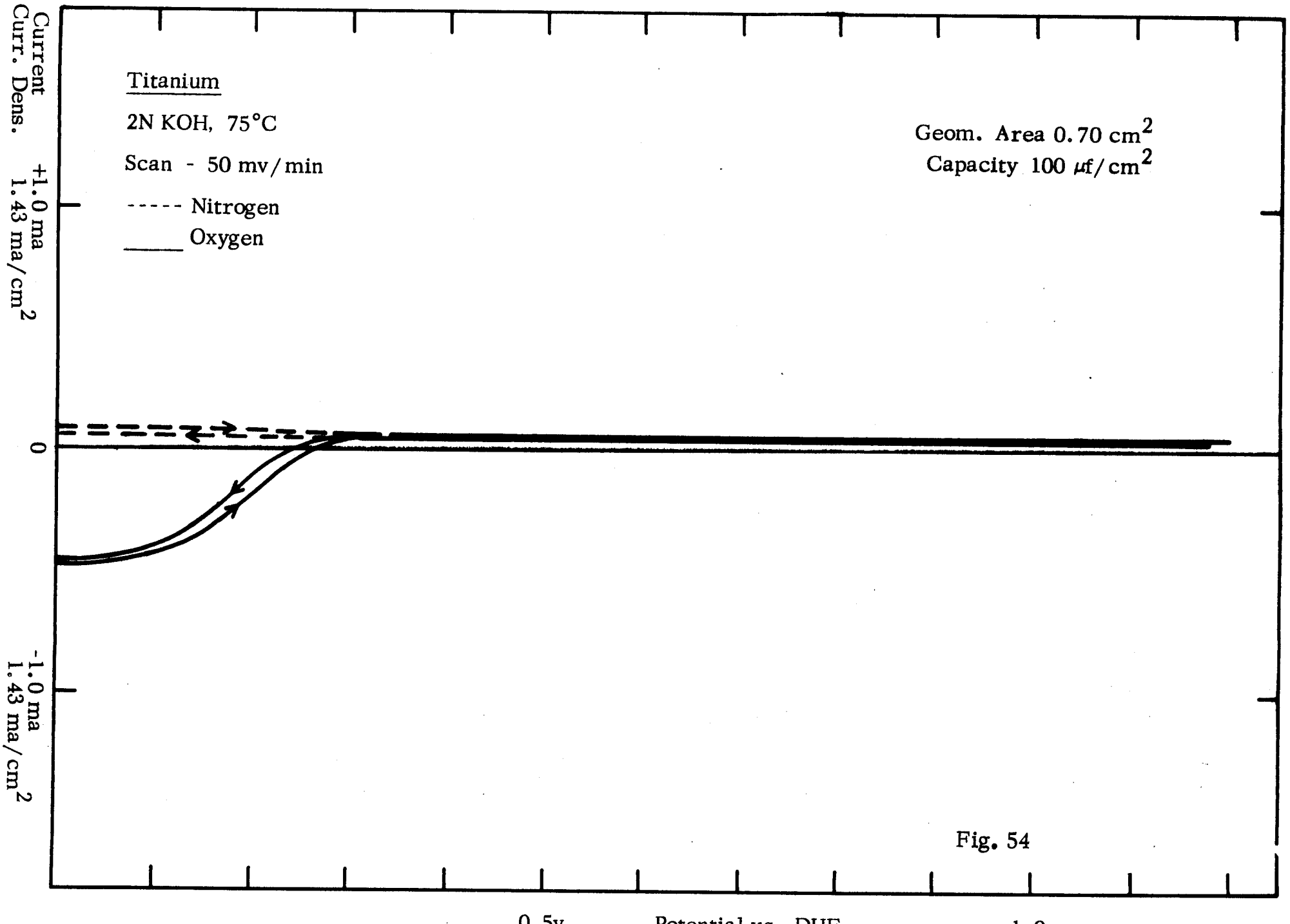
Titanium
2N KOH, 75°C
Scan - 50 mv/min
----- Nitrogen
_____ Oxygen
Geom. Area 0.70 cm2
Capacity 100 μf/cm2
Current
Curr. Dens.
+1.0 ma
1.43 ma/cm2
0
-1.0 ma
1.43 ma/cm2
0.5v
Potential vs. DHE
1.0v

Fig. 54

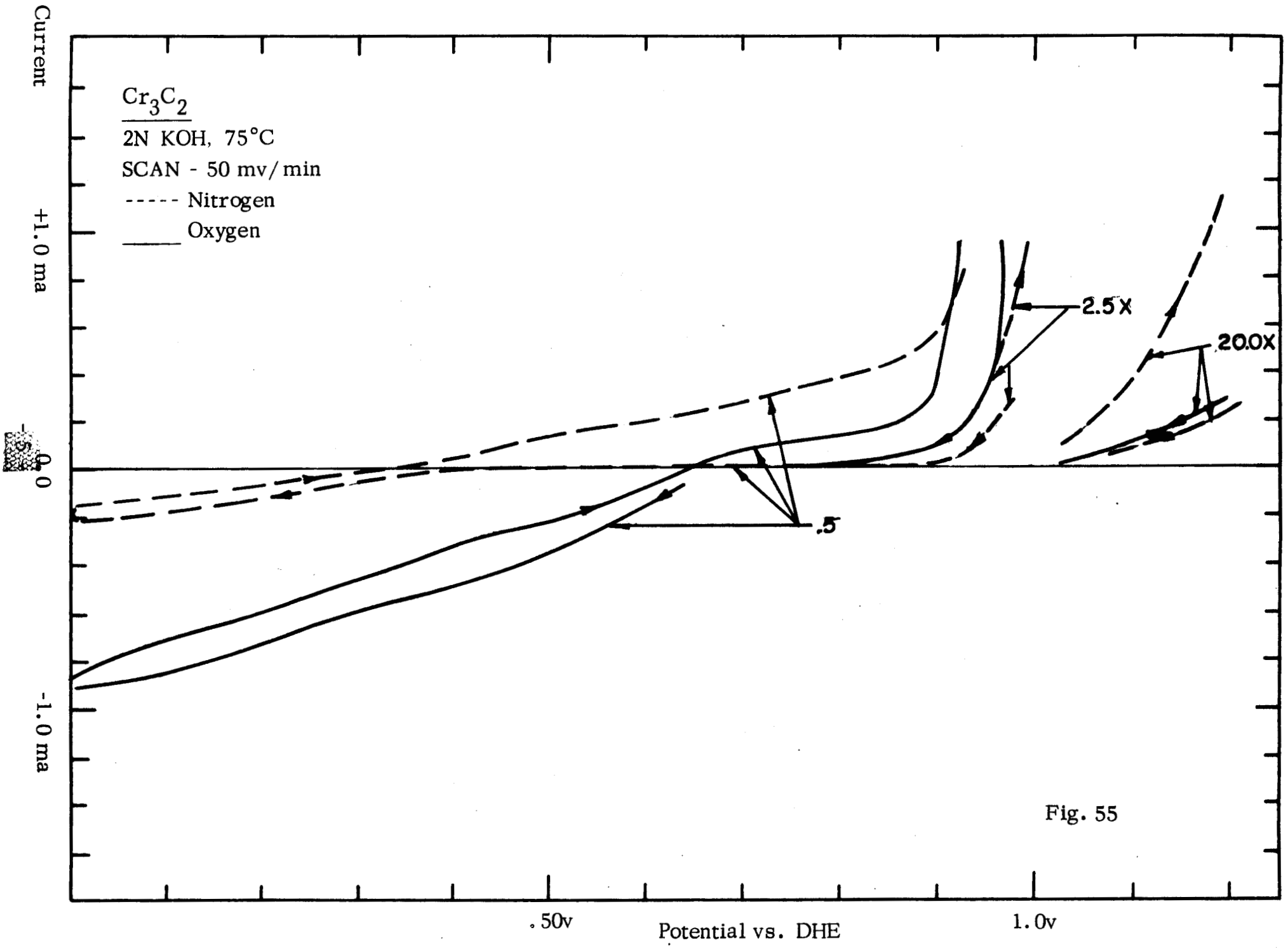
Current
+1.0 ma
0.0
-1.0 ma
Cr_3C_2
2N KOH, 75°C
SCAN - 50 mv/min
----- Nitrogen
_____ Oxygen
2.5X
20.0X
.5
.50v
Potential vs. DHE
1.0v

Fig. 55

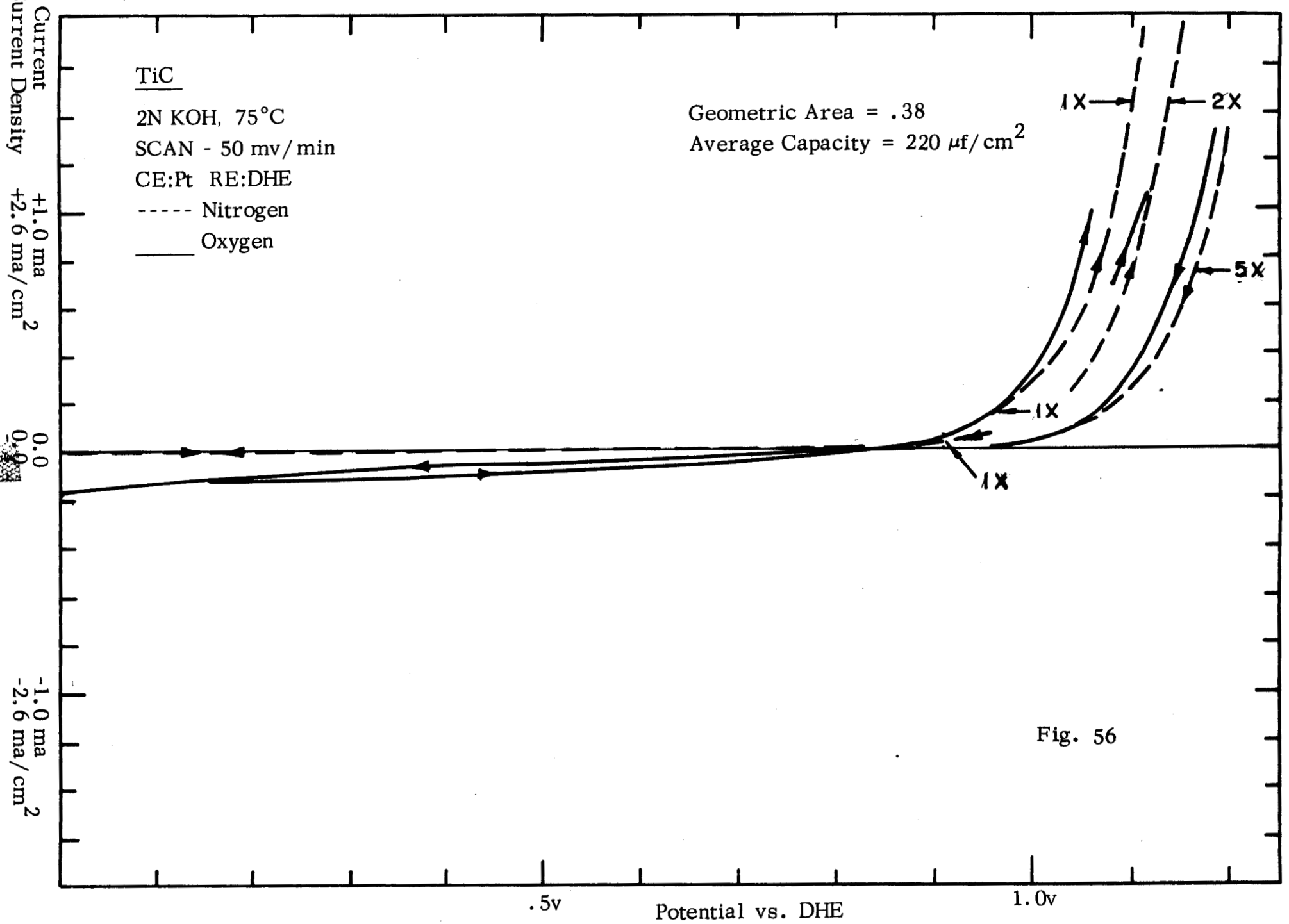
TiC
2N KOH, 75°C
SCAN - 50 mv/min
CE:Pt RE:DHE
----- Nitrogen
_____ Oxygen
Geometric Area = .38
Average Capacity = 220 μf/cm²
1X
2X
5X
1X
1X
Current
Current Density
+1.0 ma
+2.6 ma/cm²
0.0
0.0
-1.0 ma
-2.6 ma/cm²
.5v
Potential vs. DHE
1.0v

Fig. 56

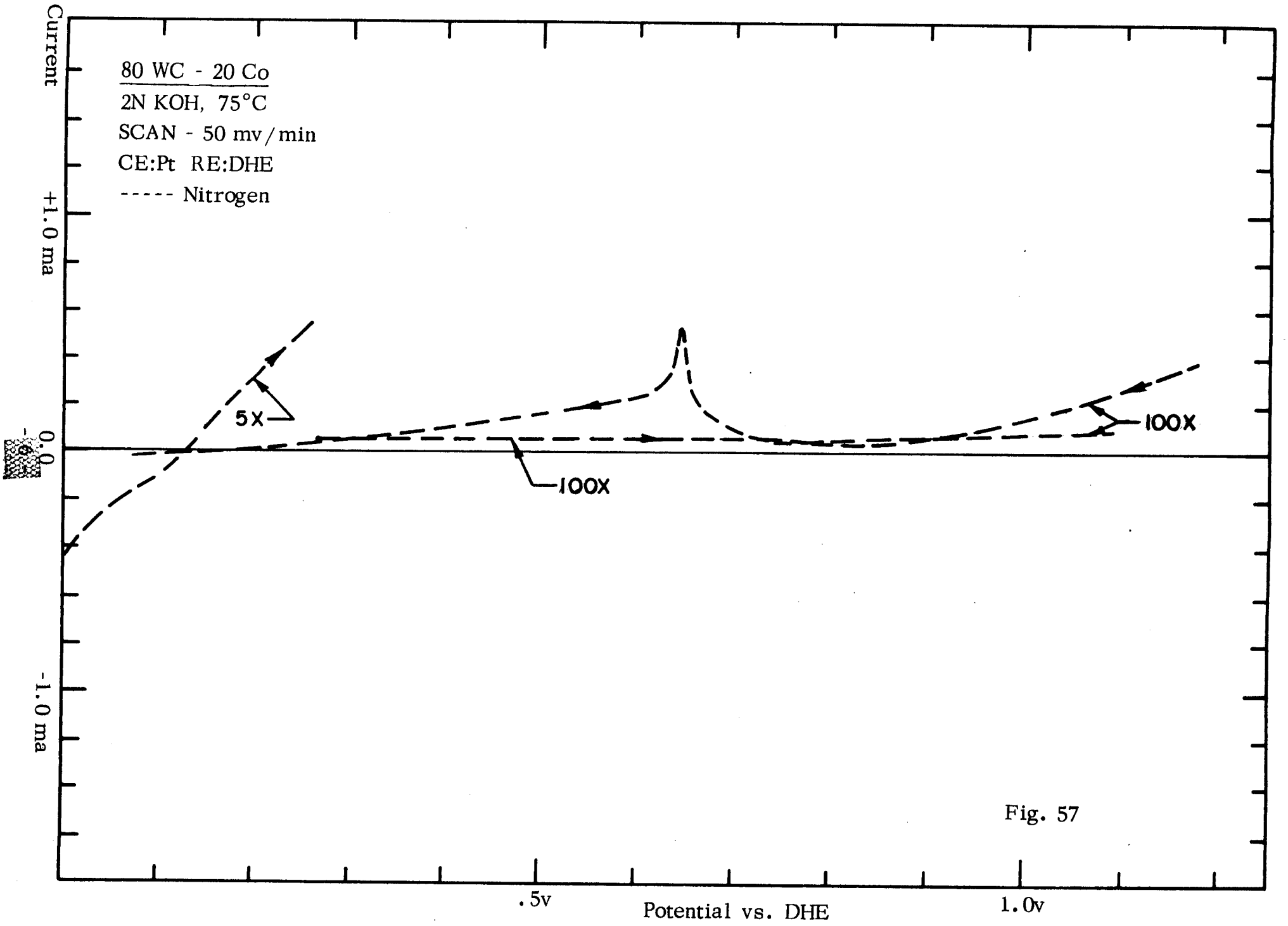
80 WC - 20 Co
2N KOH, 75°C
SCAN - 50 mv/min
CE:Pt RE:DHE
----- Nitrogen
Current
+1.0 ma
0.0
-1.0 ma
5X
100X
100X
.5v
Potential vs. DHE
1.0v

Fig. 57

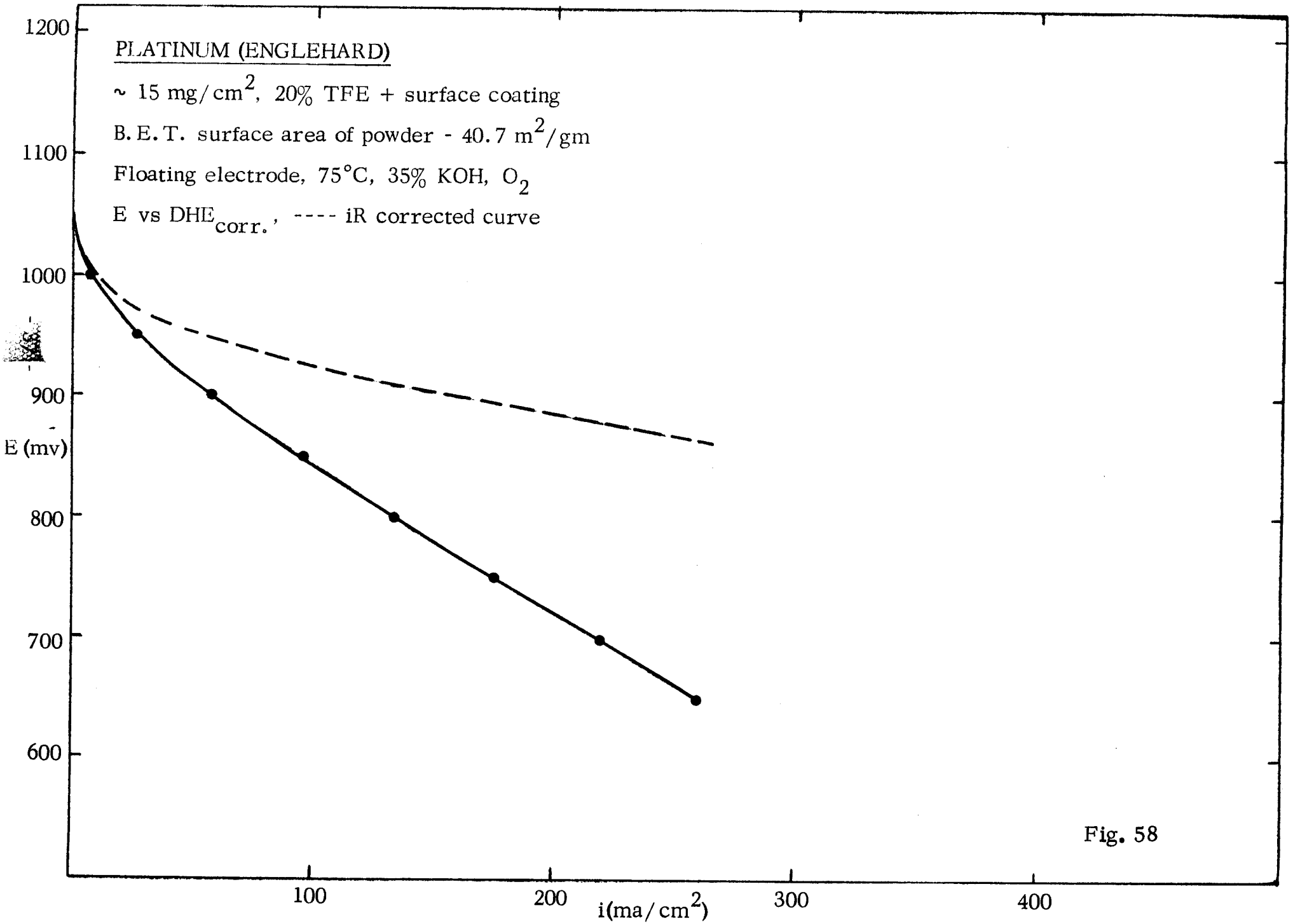
PLATINUM (ENGLEHARD)
~ 15 mg/cm2, 20% TFE + surface coating
B.E.T. surface area of powder - 40.7 m2/gm
Floating electrode, 75°C, 35% KOH, O2
E vs DHEcorr., ---- iR corrected curve
1200
1100
1000
900
800
700
600
E (mv)
100
200
300
400
i(ma/cm2)

Fig. 58

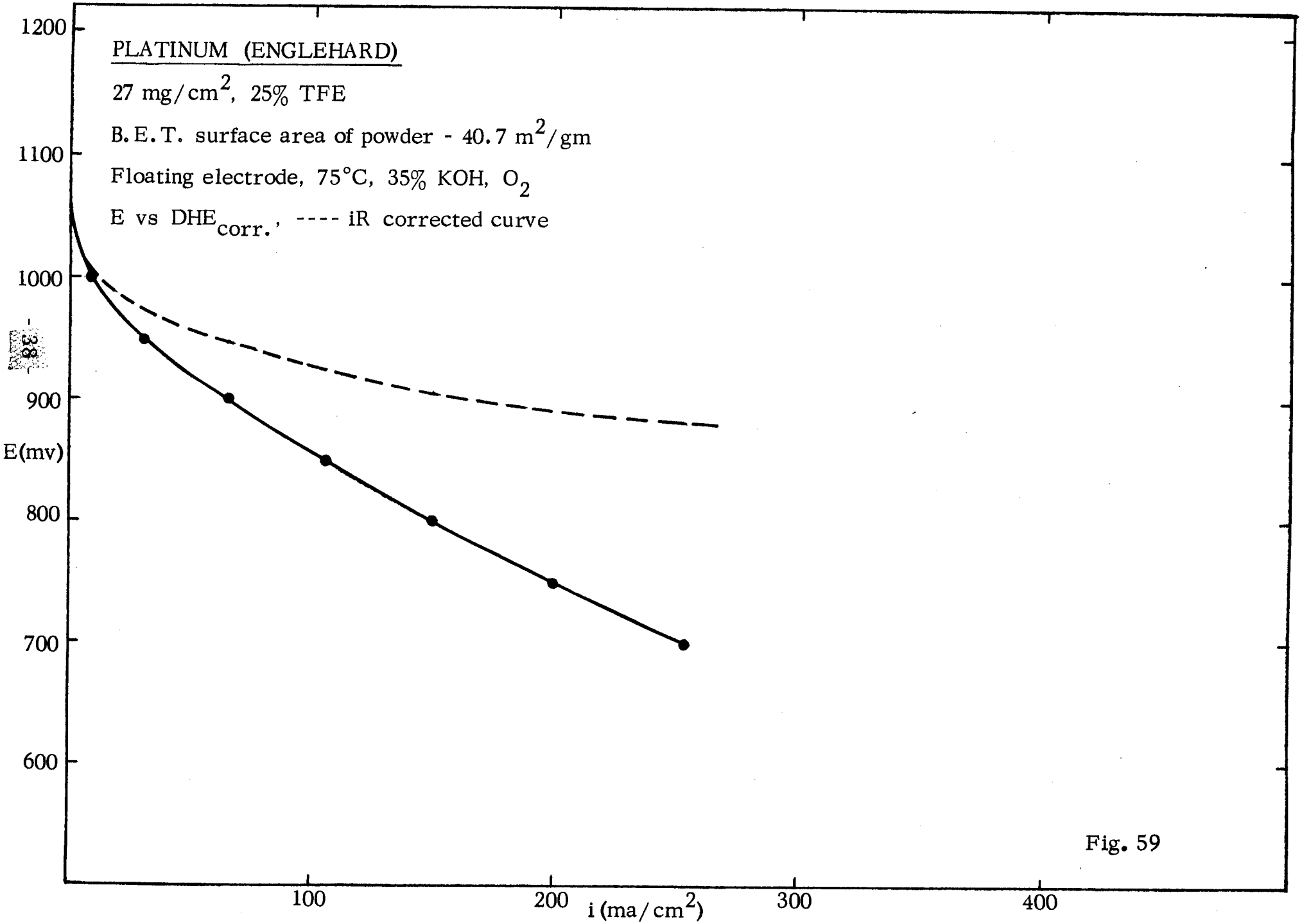
PLATINUM (ENGLEHARD)
27 mg/cm2, 25% TFE
B.E.T. surface area of powder - 40.7 m2/gm
Floating electrode, 75°C, 35% KOH, O2
E vs DHEcorr., ---- iR corrected curve
1200
1100
1000
900
800
700
600
E(mv)
100
200
300
400
i (ma/cm2)

Fig. 59

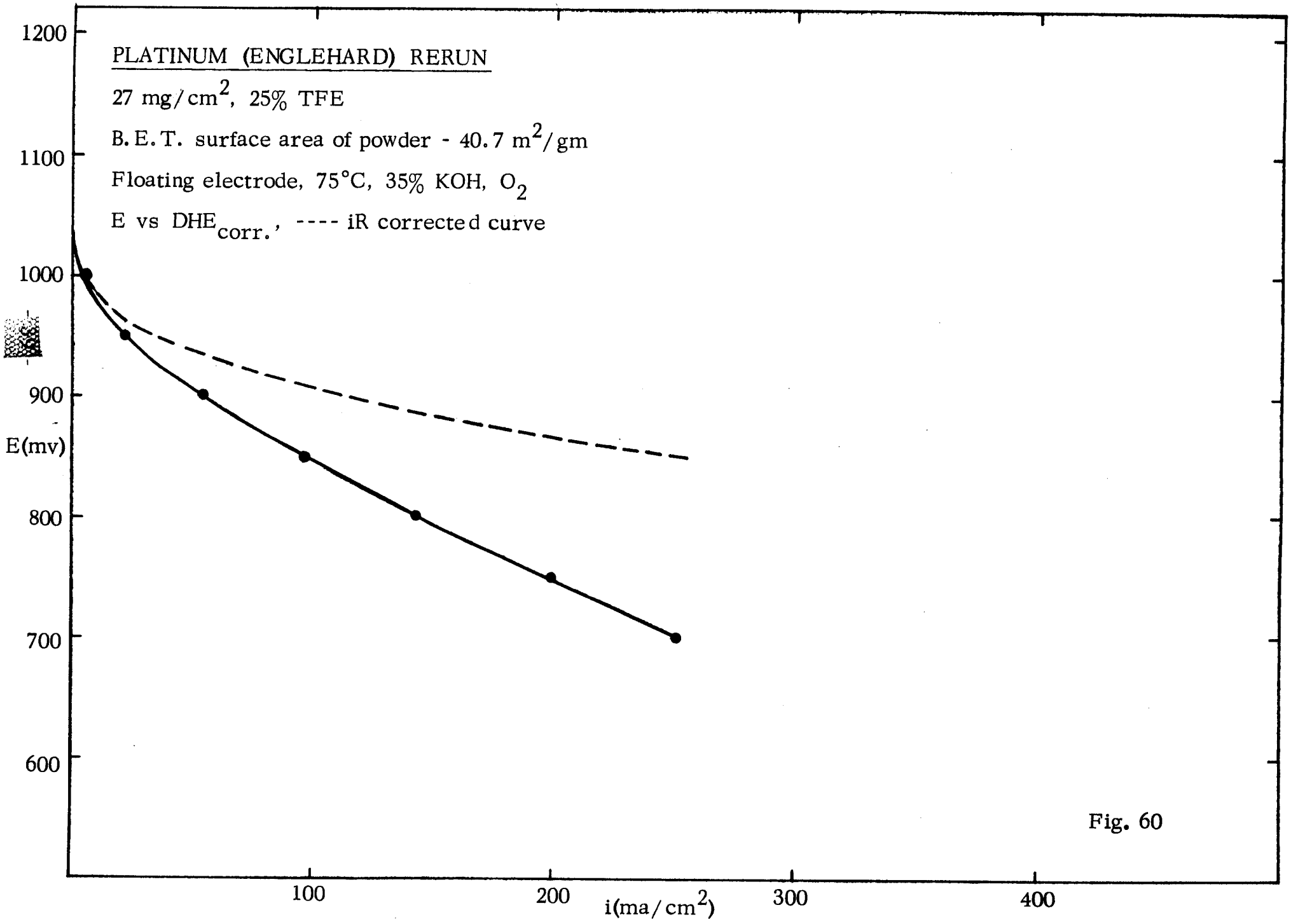
PLATINUM (ENGLEHARD) RERUN
27 mg/cm2, 25% TFE
B.E.T. surface area of powder - 40.7 m2/gm
Floating electrode, 75°C, 35% KOH, O2
E vs DHEcorr., ---- iR corrected curve
1200
1100
1000
900
800
700
600
E(mv)
100
200
300
400
i(ma/cm2)

Fig. 60

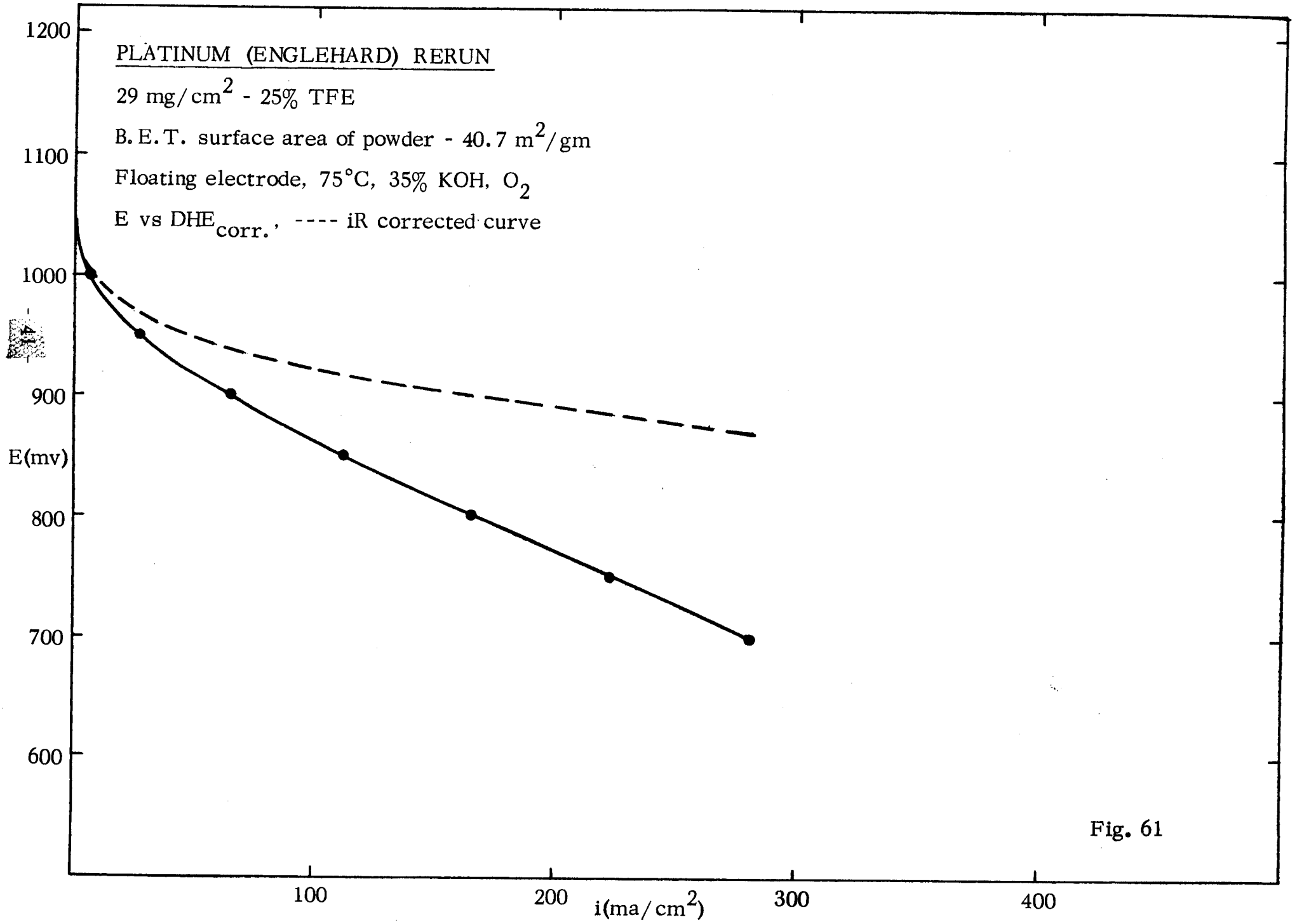
PLATINUM (ENGLEHARD) RERUN
29 mg/cm2 - 25% TFE
B.E.T. surface area of powder - 40.7 m2/gm
Floating electrode, 75°C, 35% KOH, O2
E vs DHEcorr., ---- iR corrected curve
1200
1100
1000
900
800
700
600
E(mv)
100
200
300
400
i(ma/cm2)

Fig. 61

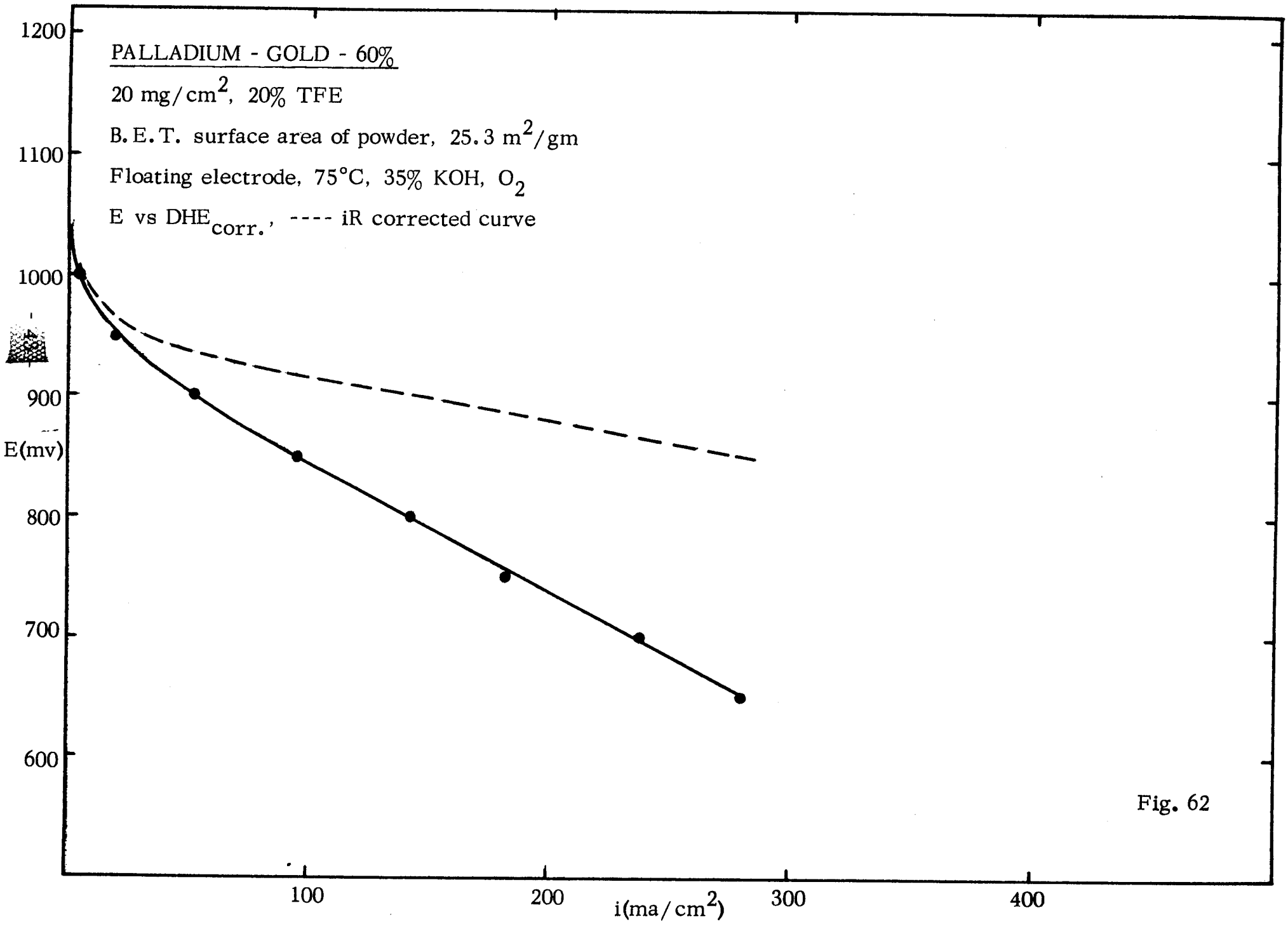
PALLADIUM - GOLD - 60%
20 mg/cm2, 20% TFE
B.E.T. surface area of powder, 25.3 m2/gm
Floating electrode, 75°C, 35% KOH, O2
E vs DHEcorr., ---- iR corrected curve
1200
1100
1000
900
800
700
600
E(mv)
100
200
300
400
i(ma/cm2)

Fig. 62

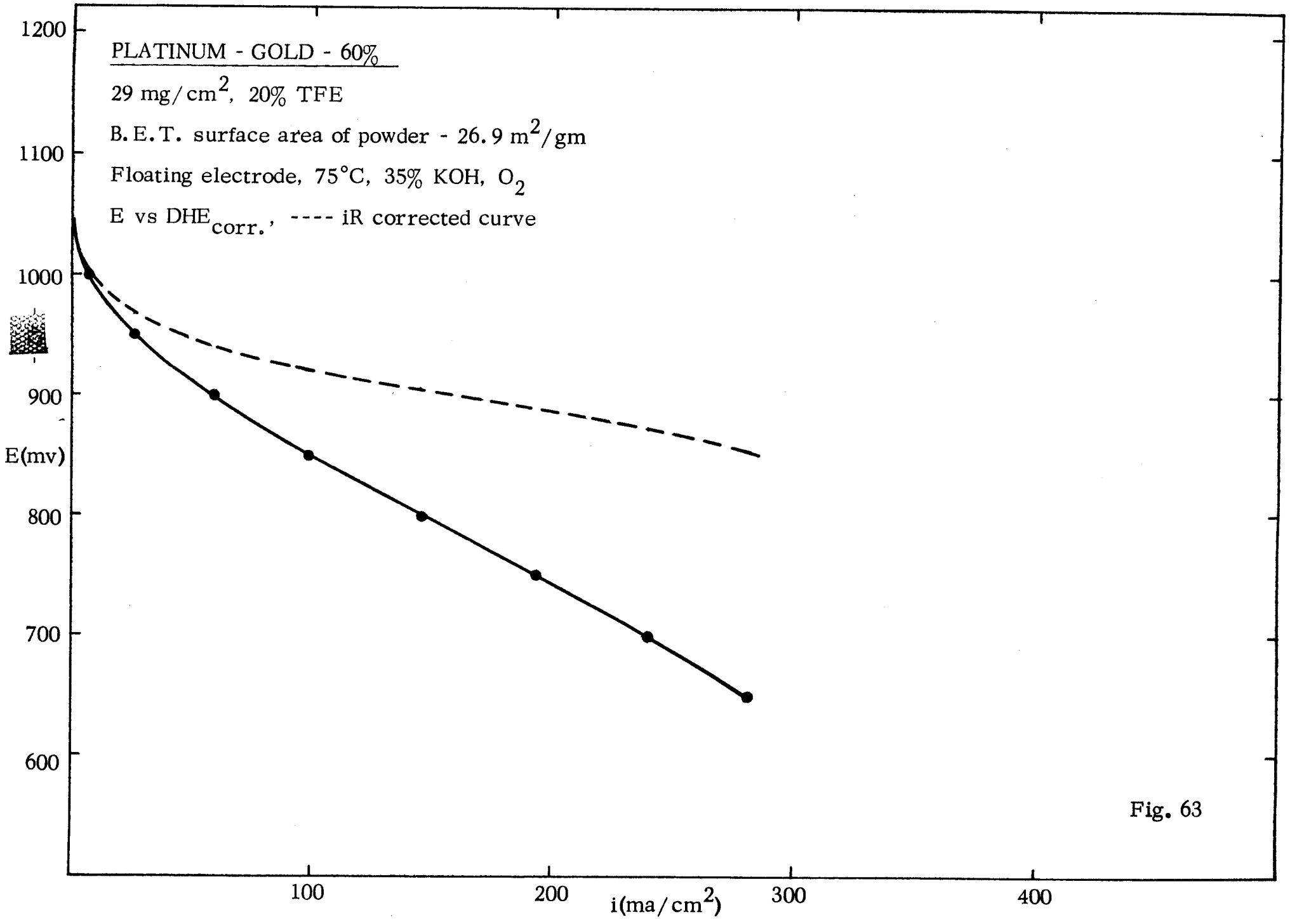
PLATINUM - GOLD - 60%
29 mg/cm2, 20% TFE
B.E.T. surface area of powder - 26.9 m2/gm
Floating electrode, 75°C, 35% KOH, O2
E vs DHEcorr., ---- iR corrected curve
1200
1100
1000
900
800
700
600
E(mv)
100
200
300
400
i(ma/cm2)

Fig. 63

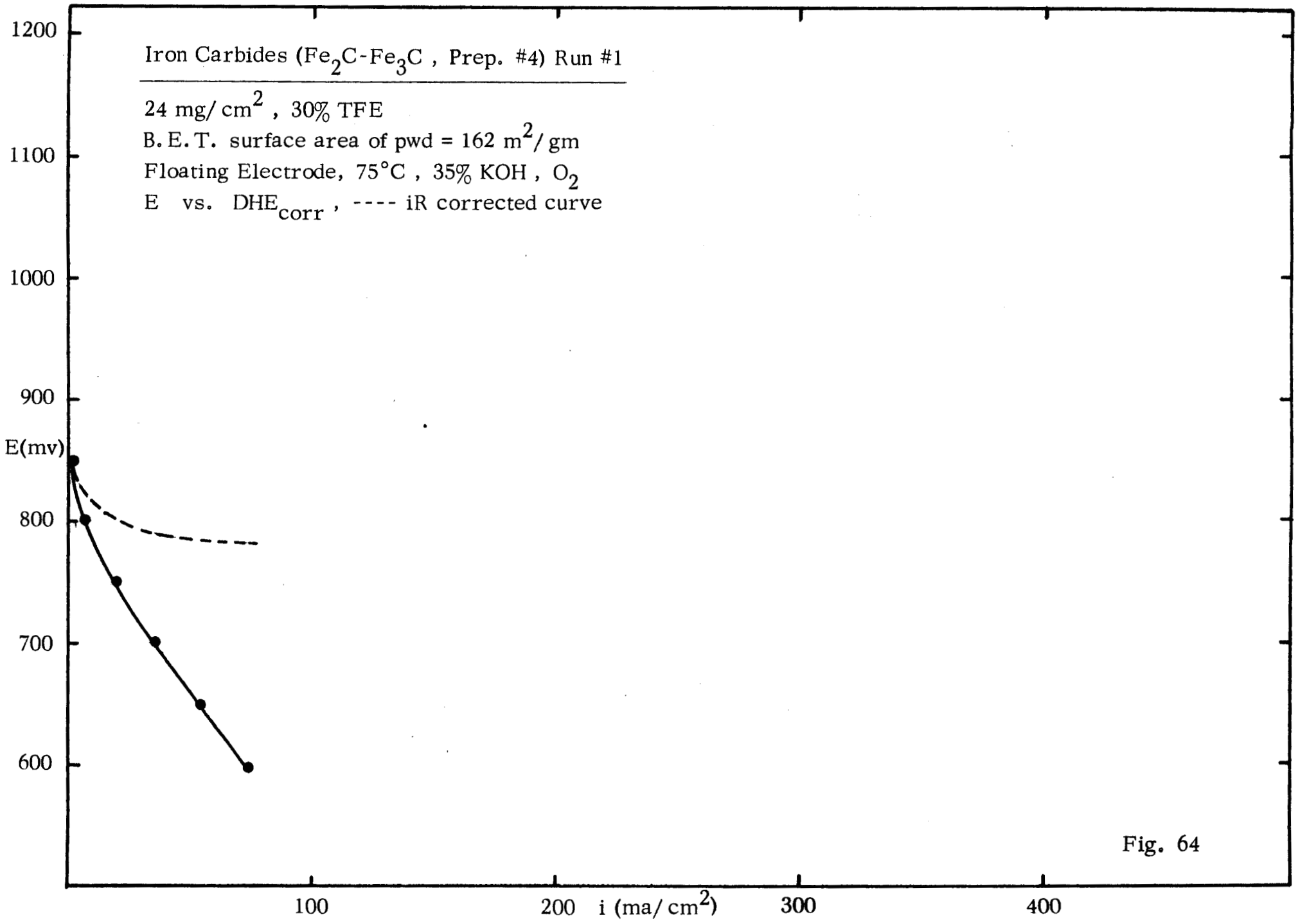
Iron Carbides (Fe_2C-Fe_3C , Prep. #4) Run #1
24 mg/ cm^2 , 30% TFE
B. E. T. surface area of pwd = 162 m^2/ gm
Floating Electrode, 75°C , 35% KOH , O_2
E vs. DHE_{corr} , ---- iR corrected curve
1200
1100
1000
900
800
700
600
E(mv)
100
200
i (ma/ cm^2)
300
400

Fig. 64

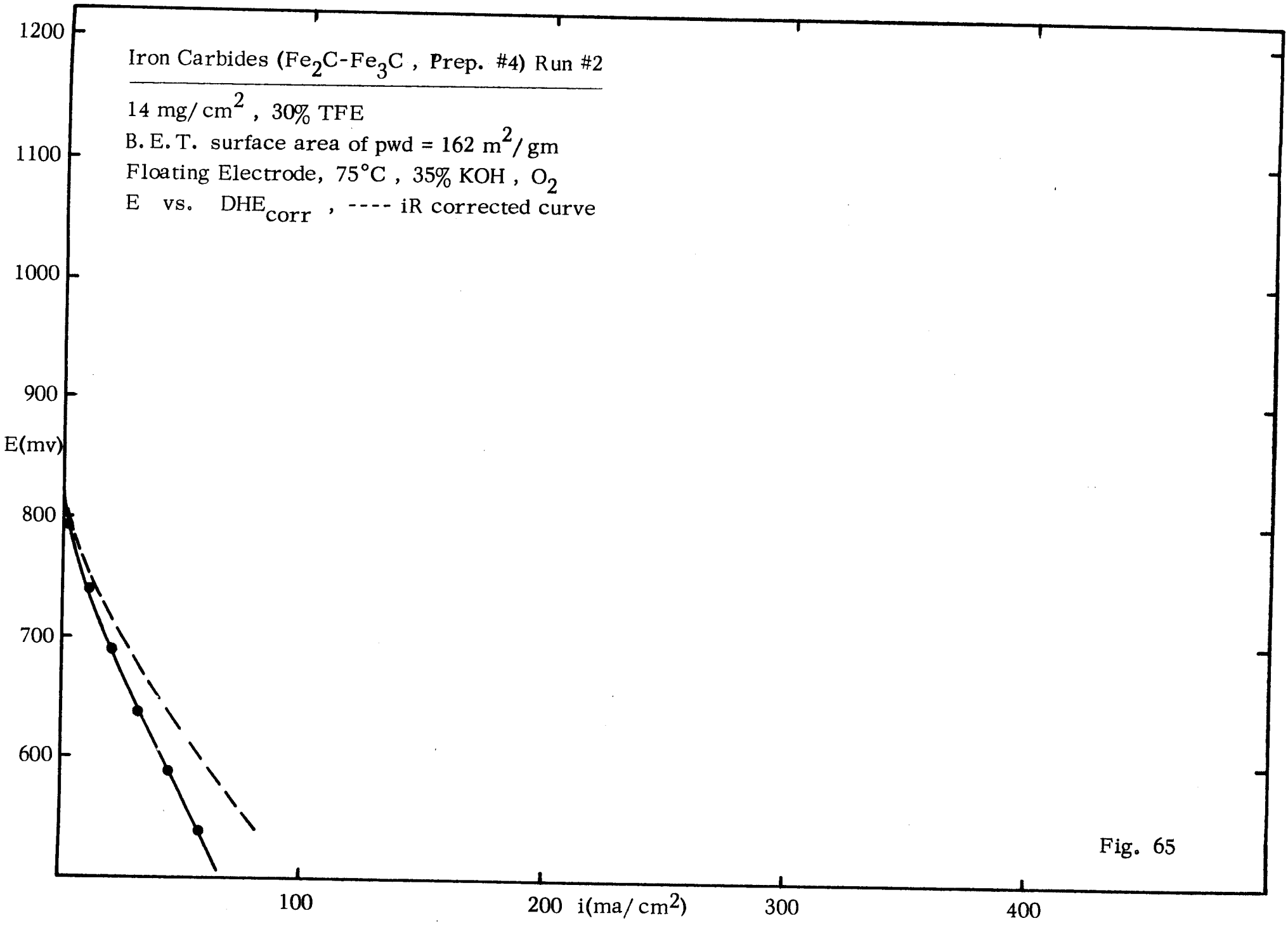
Iron Carbides (Fe_2C-Fe_3C , Prep. #4) Run #2
14 mg/cm^2 , 30% TFE
B. E. T. surface area of pwd = 162 m^2/gm
Floating Electrode, 75°C , 35% KOH , O_2
E vs. DHE_{corr} , ---- iR corrected curve
1200
1100
1000
900
E(mv)
800
700
600
100
200
i(ma/cm^2)
300
400

Fig. 65

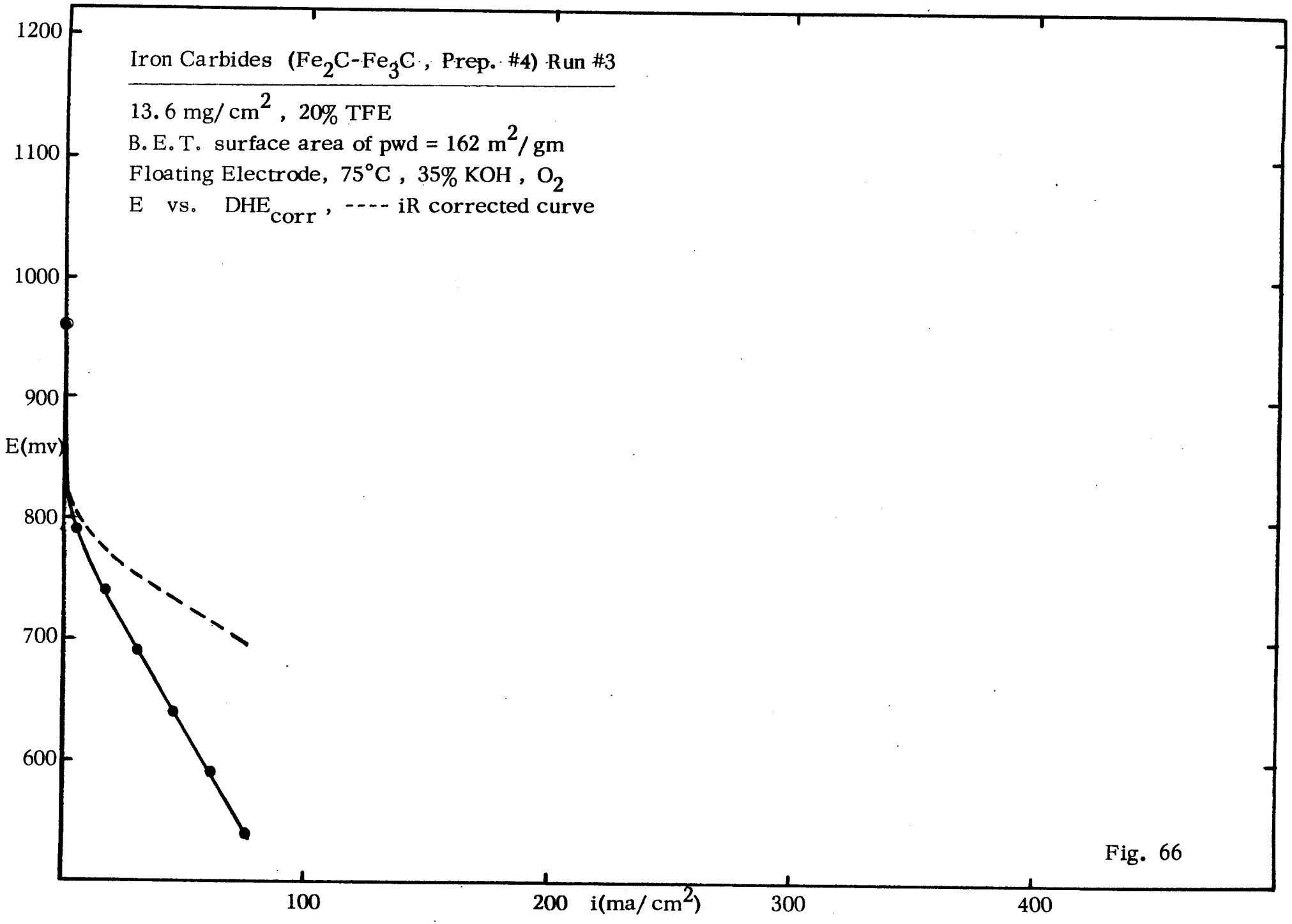
Iron Carbides (Fe_2C-Fe_3C, Prep. #4) Run #3
13.6 mg/cm^2, 20% TFE
B.E.T. surface area of pwd = 162 m^2/gm
Floating Electrode, 75°C, 35% KOH, O_2
E vs. DHE_{corr}, ---- iR corrected curve
1200
1100
1000
900
800
700
600
E(mv)
100
200
i(ma/cm^2)
300
400

Fig. 66

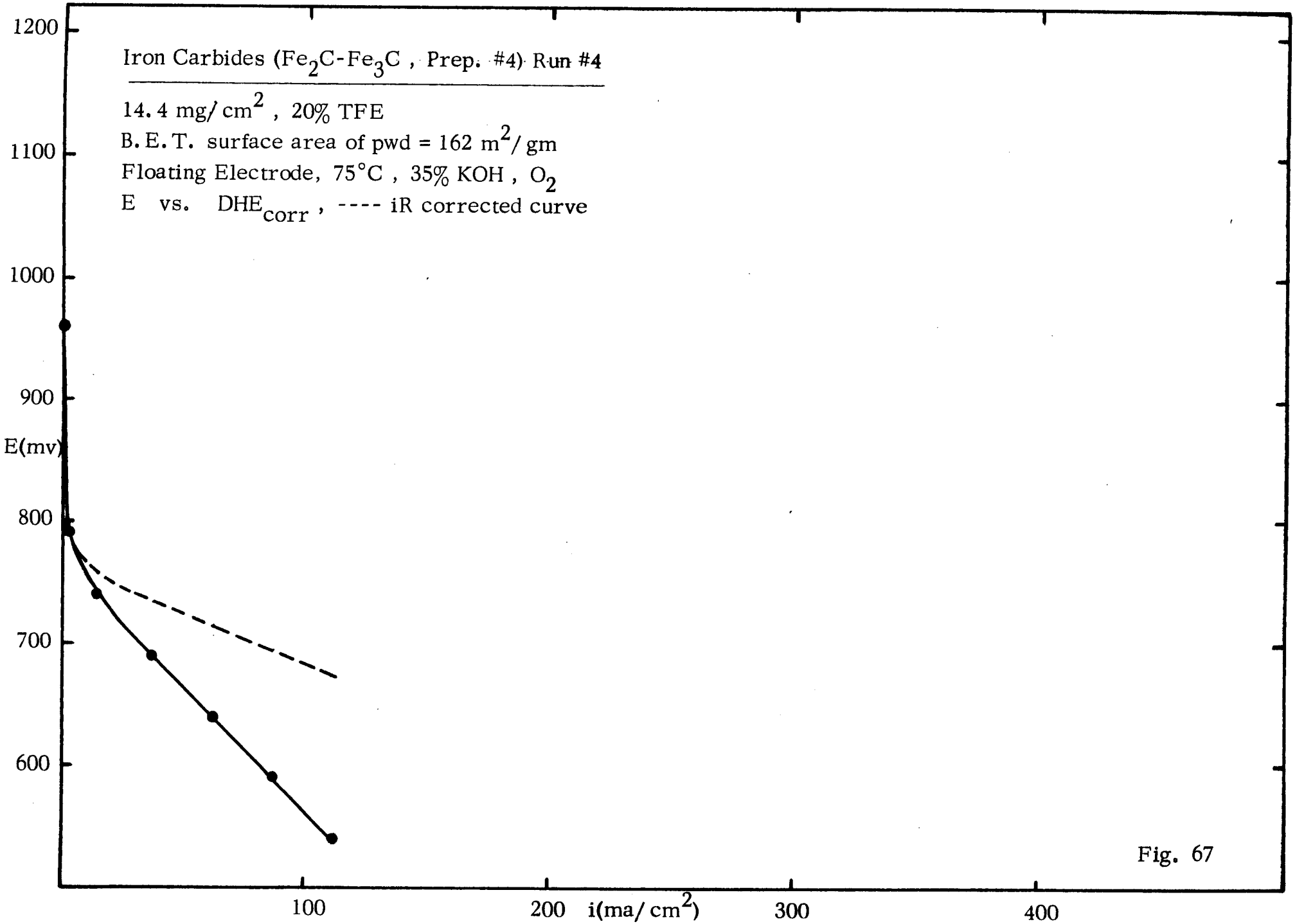
Iron Carbides (Fe_2C-Fe_3C , Prep. #4) Run #4
14.4 mg/cm^2 , 20% TFE
B.E.T. surface area of pwd = 162 m^2/gm
Floating Electrode, 75°C , 35% KOH , O_2
E vs. DHE_{corr} , ---- iR corrected curve
1200
1100
1000
900
E(mv)
800
700
600
100
200
i(ma/cm^2)
300
400

Fig. 67

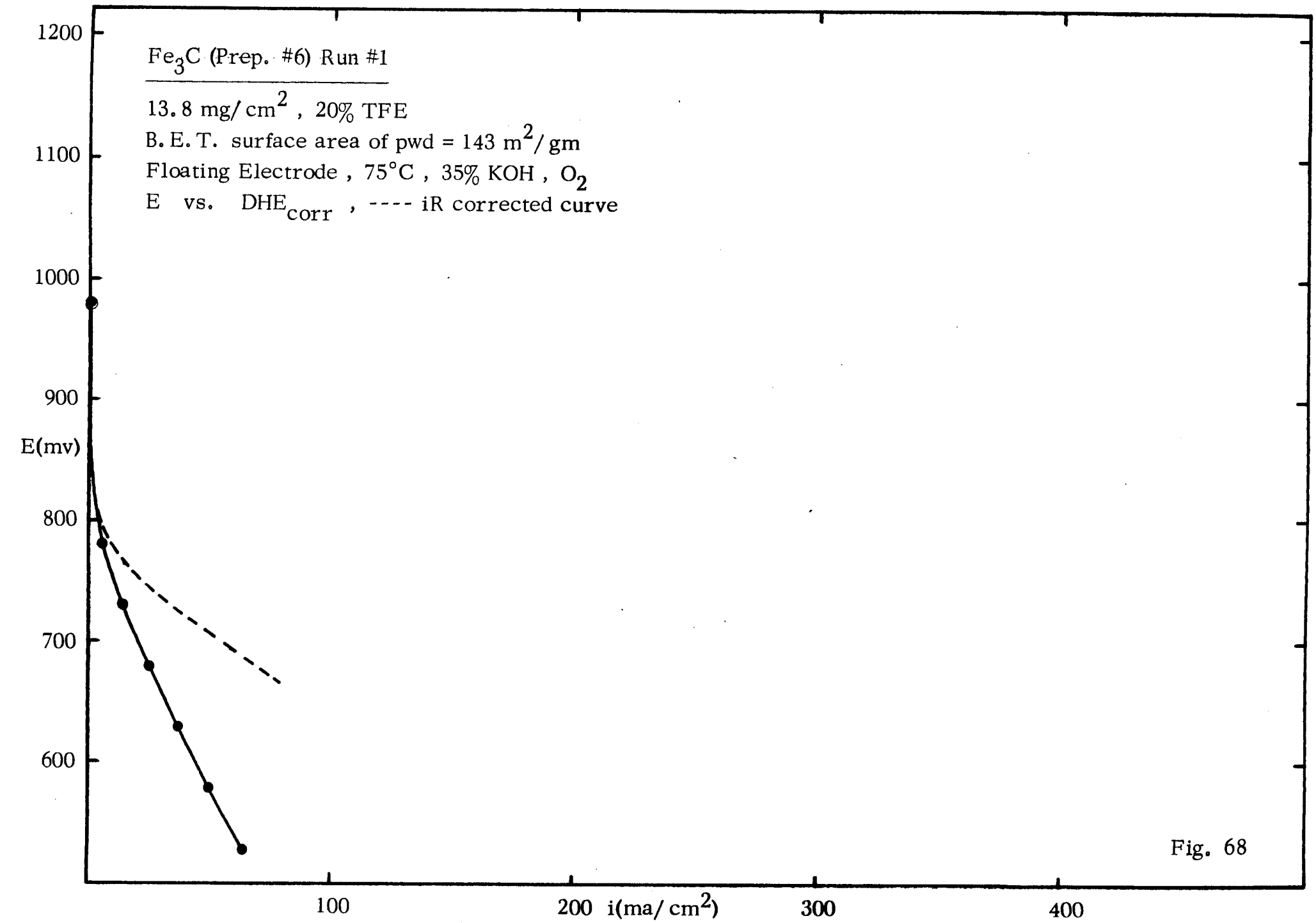
Fe_3C (Prep. #6) Run #1
13.8 mg/cm^2 , 20% TFE
B. E. T. surface area of pwd = 143 m^2/gm
Floating Electrode , 75°C , 35% KOH , O_2
E vs. DHE_{corr} , ---- iR corrected curve
1200
1100
1000
900
E(mv)
800
700
600
100
200
i(ma/cm^2)
300
400

Fig. 68

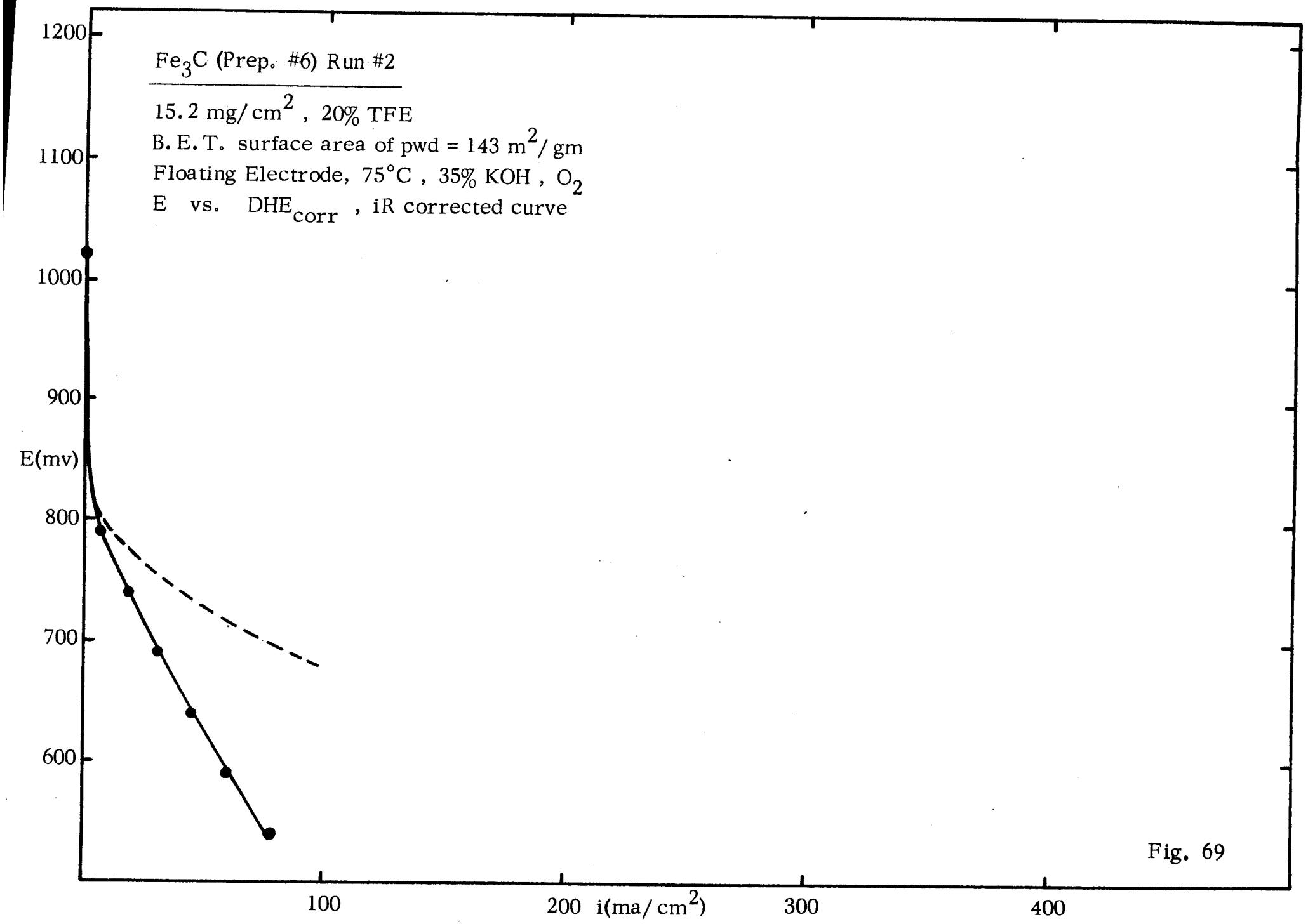
Fe_3C (Prep. #6) Run #2
15.2 mg/cm^2 , 20% TFE
B.E.T. surface area of pwd = 143 m^2/gm
Floating Electrode, 75°C , 35% KOH , O_2
E vs. DHE_{corr} , iR corrected curve
1200
1100
1000
900
800
700
600
E(mv)
100
200
i(ma/cm^2)
300
400

Fig. 69